The inflammatory microenvironment

in a model of inflammatory bowel disease

Von der Naturwissenschaftlichen Fakultät der

Gottfried Wilhelm Leibniz Universität Hannover

zur Erlangung des Grades

Doktorin der Naturwissenschaften (Dr. rer. nat.)

genehmigte Dissertation

von

M.Sc. Sara Ibrahim Al-Ghadban

geboren am 22.01.1980 in Beirut, Libanon

2016

Referent: Prof. Dr. rer. nat. Hassan Y. Naim

Korreferent: Prof. Marwan E. El-Sabban, PhD

Prof. Dr. rer. nat. Georg Herrler

Tag der Promotion: 18.02.2016

Zusammenfassung

Eine chronisch entzündliche Darmerkrankung (CED) ist eine multifaktorielle Erkrankung, welche durch eine chronische, rezidivierende Entzündung und eine gestörte Darmschleimhaut charakterisiert wird. CED ist assoziiert mit einer funktionellen Beeinträchtigung der intestinalen Epithelzellen (IEZ), begleitet durch die Infiltration von Entzündungszellen in die Lamina propria sowie dem Durchbrechen der Basalmembran durch Matrix-Metalloproteasen (MMP). Drei potentielle Mechanismen können die Erkrankung induzieren: (i) Lösliche Mediatoren und extrazelluläre Vesikel, welche durch infiltrierende Entzündungszellen sezerniert werden, (ii) Direkte Adhäsion und Signalmoleküle, welche auf der Oberfläche von Immunzellen exprimiert werden und in Kontakt zu den Epithelzellen stehen, und (iii) Cytoplasmatischer Austausch von spezifischen Signalen zwischen Entzündungszellen und IEZ über *Gap Junction* (GJ)-Kanäle. Die Interaktion zwischen IEZ und Entzündungszellen über GJ ist unter pathologischen Bedingungen, wie bei der CED, nicht genügend erforscht. In dieser Arbeit haben wir die Natur der Interaktion zwischen IEZ und Makrophagen (MΦ) in einem *in vitro* Modell der CED erforscht. Diesbezüglich haben wir die Behandlung der IEZ mit Entzündungsmediatoren aus aktivierten MΦ und deren Ko-Kultivierung mit Entzündungszellen etabliert. Wir haben potentielle Proteine der Zell-Zell-Verbindungen *(junctions)* untersucht, welche an dieser heterozellulären Kommunikation beteiligt sind. In diesem Zusammenhang wurde die Wirkung von Entzündungsmediatoren auf die Expression von ZO-1, E-Cadherin und Connexinen (Cxs) auf dem transkriptionalen, translationalen und funktionalen Level sowie die zelluläre Lokalisation analysiert. Anschließend studierten wir den Transport von Cx26- und Cx43-Dendra2 in Caco-2-Zellen und bestimmten die

Expression dieser Chimären unter normalen und inflammatorischen Bedingungen in IEZs. Wir haben zudem die Lokalisation des *junctional complexes* in Cx43 überexprimierenden Caco-2-Zellen und in humanem Gewebe von CED Patienten untersucht. Unsere Daten zeigen, dass IEZs funktionale homo- und heterozelluläre GJ-Kanäle mit IEZ und MΦ bilden. Die Expression von Cx26 und Cx43 sowie die Enzymaktivität der MMPs sind in IEZ unter Entzündungsbedingungen signifikant hochreguliert, was in einer verstärkten intrazellulären Kommunikation zwischen IEZ und MΦ resultiert. Weiterhin konnten wir zeigen, dass Cx26 und Cx43 an die Plasmamembran transportiert werden und funktionale GJ-Kanäle bilden. Zudem wiesen wir nach, dass Cx43 nach Überexpression in Caco-2-Zellen an der Plasmamembran mit E-Cadherin, ZO-1 und β-Catenin assoziiert ist. Dennoch wird die Expression dieses *junctional complexes* unter Entzündungsbedingungen *in vitro* signifikant reguliert. *In vivo* können wir zeigen, dass die Expression von ZO-1, E-Cadherin, Vimentin und Collagen IV signifikant reduziert ist, wodurch der Verlust des *junctional complexes* in CED-Gewebe und das Durchbrechen der Basalmembran, folglich die Dysfunktion der epithelialen Barriere, bestätigt wird.

Zusammenfassend unterstützen unsere Daten die Vorstellung, dass die parakrine und heterozelluläre Kommunikation zwischen IEZ und MΦs eine entscheidende Rolle in der Regulation der epithelialen Zellfunktion spielt. Diese erfolgt über die Ausbildung eines *junctional complexes* zwischen Entzündungszellen und IEZ, welches zur Dysregulation der intestinalen Epithelbarriere beiträgt.

Stichworte: CED, Intrazelluläre Kommunikation, Connexin

Abstract

Inflammatory bowel disease (IBD) is a multifactorial disease characterized by chronic, relapsing inflammation and mucosal destruction. IBD is associated with functional impairment of intestinal epithelial cells (IECs), concomitant with the infiltration of the lamina propria by inflammatory cells and breaching of the basement membrane by matrix metalloproteinases (MMPs). Three potential mechanisms may contribute to the induction of this state: (i) soluble mediators and extracellular vesicles secreted by infiltrating inflammatory cells, (ii) direct adhesion and signaling molecules expressed on the surface of immune cells in contact with epithelial cells and (iii) cytoplasmic exchange of specific signals between the inflammatory cells and IECs *via* gap junction (GJ) channels. The interaction between IECs and inflammatory cells through GJ under pathological conditions such as IBD is not well elucidated. In this study, we explored the nature of the interaction between IECs and macrophages (MΦ) in an *in vitro* model of IBD established by treating IECs with inflammatory mediators from activated MΦ or their co-culturing with inflammatory cells. We investigated the potential junctional proteins involved in this hetero-cellular communication, and assessed the effect of inflammatory mediators on the expression of ZO-1, E-cadherin, and Connexins (Cxs) at the transcriptional, translational, cellular localization, and functional levels. We then studied the trafficking of Cx26- and Cx43-Dendra2 in Caco-2 cells, and determined the expression of these chimeras under normal and inflammatory conditions in IECs. We also examined the localization of junctional complexes in Cx43 overexpressing Caco-2 cells and in human IBD tissues. Our data demonstrate that IECs establish functional homo- and hetero-cellular GJ channels with IECs and MΦ,

respectively. Cx26 and Cx43 expression and MMPs enzymatic activity are significantly upregulated in IECs under inflammatory conditions, which resulted in enhanced functional IECs-MΦ intercellular communication. Further, we show that Cx26 and Cx43 trafficked to the plasma membrane and formed functional GJ channel. We also demonstrate that Cx43 is associated with E-cadherin, ZO-1, and β-catenin at the plasma membrane in Cx43 overexpressing Caco-2 cells; however, the expression of these junctional complexes is significantly regulated under inflammatory conditions *in vitro*. *In vivo,* we show that ZO-1, E-cadherin, vimentin, and collagen IV expression is significantly decreased, confirming the loss of junctional complexes in IBD tissues and breaching of the basement membrane, hence epithelial barrier dysfunction.

In conclusion, our data support the notion that the combination of paracrine and hetero-cellular communication between IECs and MΦs plays a pivotal role in the regulation of epithelial cell function through the establishment of junctional complexes between inflammatory cells and IECs, which could contribute to the dysregulation of intestinal epithelial barrier.

Keywords: IBD; Intercellular communication; Connexin

Contents

List of figures

Chapter 3 - Results

Chapter 4 - Discussion

List of tables

Chapter 1 - Introduction

Chapter 2 - Materials and Methods

List of abbreviations

AJ   Adherens Junctions

APC   Apical Junctional Complex

ATG   Autophagy Related 16-Like

CD   Crohn's Disease

Cx   Connexin

DSS   Dextran Sulfate Sodium

ECM   Extracellular matrix

ER   Endoplasmic Reticulum

GJ   Gap Junction

IBD   Inflammatory Bowel Disease

IDT   Integrated DNA Technologies

IEC   Intestinal Epithelial Cell

IFN- γ   Interferon-gamma

IL   Interleukin

IL-1RA   Interleukin-1 Receptor Antagonist

IRGM   Immunity-Related GTPase Family M

JAM	Junctional Adhesion Molecule
LPS	Lipopolysaccharide
MΦ	Macrophage
MDR1a	Multidrug Resistance1a
MHC	Major Histocompatibility Complex
MMPs	Matrix Metalloproteinases
NOD2	Nucleotide Oligomerization Domain
NF−κB	Nuclear Factor Kappa B
qPCR	Quantitative PCR
PAMPs	Pathogen Associated Molecular Patterns
Pan	Pannexin
PMA	Phorbol 12-Myristate 13-Acetate
PRRs	Pattern Recognition Receptors
PTPN22	Protein Tyrosine Phosphatase, Non-receptor type 22
SEM	Standard Error of Measurement
SMAD3	Similar to Mothers Against Decapentaplegic 3
TCR	T Cell Receptor

TGF-β	Transforming Growth Factor-β
Th1	T helper 1
TJ	Tight junction
TLR	Toll-like Receptors
TNBS	2,4,6-trinitrobenzenesulfonic acid
TNF-α	Tumor Necrosis Factor-α
UC	Ulcerative Colitis
ZO	Zona Occludens

CHAPTER 1

Introduction

1 Introduction

The human gut comprises the largest surface area of the body, with a mucosal surface of 300–400 m^2. It allows digestion and absorption of nutrients, tolerates dietary and microbial antigens, and protects against pathogenic microorganisms. The mucosal surface regulates the intestinal homoeostasis by maintaining a balance between the external environment and the immune system. Disruption of this homeostasis leads to chronic intestinal inflammation, such as Inflammatory Bowel Disease (IBD).

1.1 The intestinal mucosal barrier

1.1.1 Structure and function

The surface of the intestinal mucosa consists of a continuous sheet of columnar epithelial cells. The epithelial cells prevent the entry of harmful microorganisms while enabling the uptake of nutrients and water. The intestine epithelium is highly organized into crypts and villi, each with definite function. It undergoes a rapid and continuous self-renewal from pluripotent stem cells residing at the base of the crypts. Stem cells differentiate into four intestinal epithelial cell (IEC) types: paneth cells, goblet cells, enterocytes and enteroendocrine cells. Most of the differentiated cells migrate to the tip of the villus; however, the paneth cells reside within the crypt. Paneth cells are terminally differentiated specialized cells that secrete granules containing antimicrobial proteins like defensins, hence having a significant role in host-microbe interactions. Goblet cells are secretory cells that produce highly glycosylated mucins constituting the major components of the mucous layer covering the epithelial surface of the intestine (1). Enterocytes are polarized columnar epithelial cells forming the villi and linked

together by junctional complexes that determine the selective transport of water and electrolytes across the epithelium (Figure 1). Enteroendocrine cells are specialized endocrine cells that secrete a wide range of hormones, which control the physiological functions of the digestive tract (2).
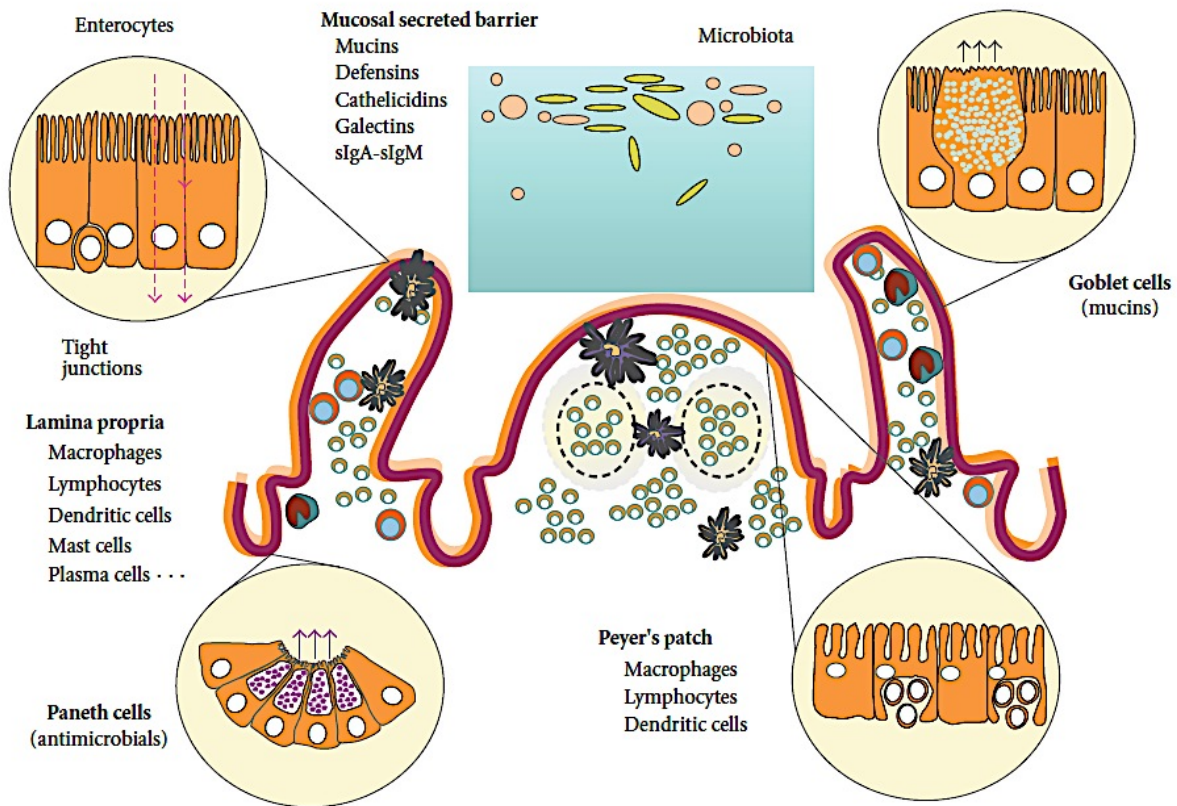
Figure 1: Components of the gut barrier (3).

Microfold cells, M cells, are specialized IECs covering the dome-like structure of the colonic lymphoid follicle. They serve as antigen sampling cells and endocytose a variety of molecules that are rapidly transported to the underlying lymphoid follicles termed the Peyer's patches (3-5). It has been established that IECs play a fundamental role in the maintenance of mucosal

homeostasis through regulating the intestinal barrier. Dysregulation of the mucosal epithelial barrier leads to the initiation and the progression of IBD (6, 7).

1.1.2 Defects in the intestinal epithelial barrier

Alteration in epithelial cell integrity and abnormal mucus secretion are the major determinants of a leaky intestinal barrier.

1.1.2.1 Alterations in epithelial integrity

Polarized epithelial cells lining the intestinal barrier are joined by apical junctional complex (APC) consisting of tight junctions (TJs) and adherens junctions (AJs). APC is regulated under physiological and inflammatory conditions. Studies have shown that alteration in the expression of adherens junction (E- and P-cadherin), and catenins (α- and β-catenin), disrupts the epithelial barrier and increases intestinal permeability. This allows luminal bacteria to enter the lamina propria activating regulatory T cells and triggering a cascade of inflammatory response (8-10). Tight junctions seal the intercellular space between adjacent epithelial cells and regulate the paracellular permeability by allowing the passive selective diffusion of ions, nutrients, and water between cells. They form a boundary within the plasma membrane to limit the exchange of proteins and lipids between the apical and basolateral membrane domains. The TJ family includes three transmembrane proteins: claudins, occludins, and junctional adhesion molecules (JAMs). Claudins are considered the major backbone of the paracellular barrier. Claudin 1, 2, and 4 expression has been shown to be elevated in IBD patients. Alterations in TJ expression and distribution increase the intestinal permeability to pathogens and disrupt the epithelial barrier (11-13).

1.1.2.2 Degradation of the mucus layer

The intestinal mucosal layer is the first line of defense against microbial pathogens. It is formed of a dense inner layer attached to the epithelium and a loose outer layer. The mucosal layer is comprised of water, ions, immunoglobulins, anti-mirobial peptides, and mucin. Mucin is secreted mainly by goblet cells and is composed of glycoproteins, phospholipids, and nucleic acids. MUC2, a gel-forming mucin, is the major constituent of the mucus layer in normal intestine (Figure 2). Studies have shown that alterations of MUC2 and MUC12 expression contribute to the initiation of IBD (14-16).
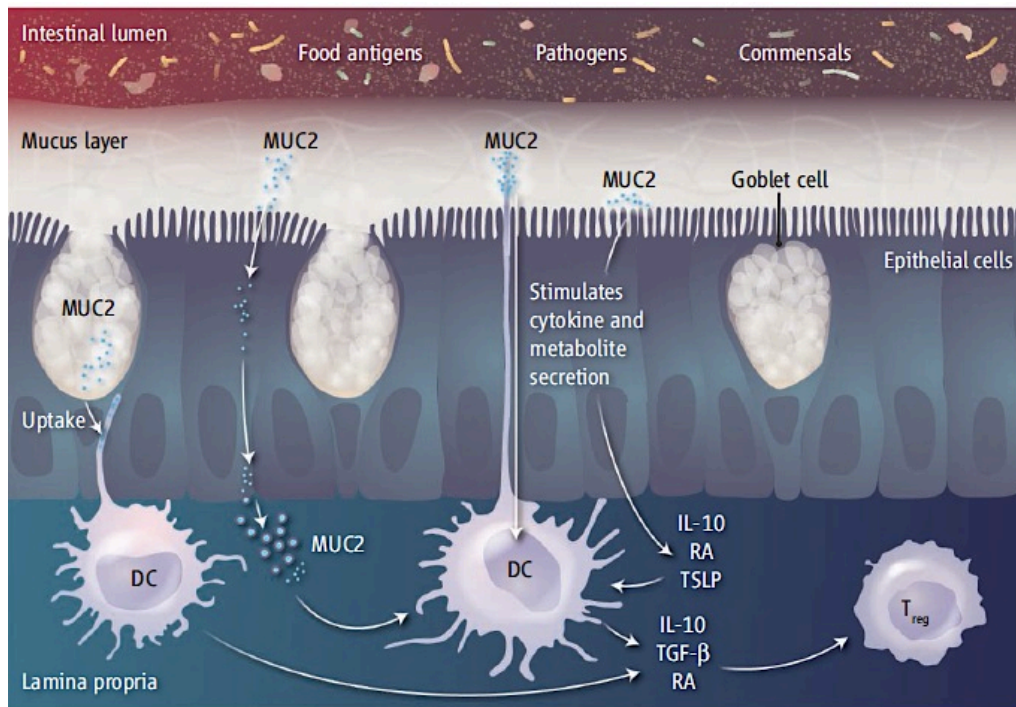
Figure 2: Gut mucus. Dendritic cells (DCs) may be exposed to MUC2 by direct uptake through interactions with goblet cells, or through MUC2-containing vesicles released by epithelial cells. Abbreviations: RA: Retinoic acid, IL-10: interleukin 10, TSLP: Thymic stromal lymphopoietin (17).

1.2 Overview of inflammatory bowel disease

1.2.1 Inflammatory bowel disease

Inflammatory bowel disease is a multifactorial disease determined by the interplay of several factors including genetics, microbes, immune response, and environment. It is characterized by chronic relapsing inflammation and mucosal destruction.

Inflammatory bowel disease encompasses two main classes: Crohn's disease (CD) and ulcerative colitis (UC). They share many clinical and pathological similarities, but have marked differences in their genetic background and underlying immune response. In 10-15% of IBD cases, where the inflammation is limited to the colon, they are indistinguishable and are categorized as 'indeterminate colitis' (18). Crohn's disease is a chronic IBD characterized by mucosal ulceration that can occur through the entire gastrointestinal tract but mostly involves the terminal ileum and the colon. The intestinal wall in CD thickens and becomes narrowed and fibrotic, resulting in chronic, recurrent bowel obstructions and abscess. Clinical features include abdominal pain, perforation, fistula formation, fever, diarrhea, and weight loss (19). Ulcerative colitis involves the rectum and colon and is mostly localized to the mucosa. The crypt architecture of the colon is distorted; it develops tiny open sores, or ulcers, between the crypt bases that produce pus and mucus. Ulcerative colitis is mainly characterized with bloody diarrhea, fecal urgency, passage of mucus and crampy abdominal pain (20).

1.2.2 Pathogenesis of IBD

Defects in the intestinal epithelial barrier and poorly regulated immune response against the normal enteric microbial flora in genetically susceptible patients contribute to the pathogenesis of IBD (21-23).

1.2.2.1 Genetic factors

Genome-wide screening has identified more than 160 distinct susceptibility loci for IBD. IBD1 on chromosome 16 is specific to CD and contains the Nucleotide Oligomerization Domain (NOD2) gene, also referred as Caspase Activation and Recruitment Domain (CARD15). NOD2, the first susceptibility gene in IBD, encodes a cytoplasmic protein, which is expressed in three cell types: macrophages, dendritic cells, and paneth cells. It serves as a pattern recognition receptor for bacterial lipopolysaccharide (LPS) and activates nuclear factor kappa B (NF-κB) (24). A 2-fold risk for CD in NOD2 heterozygotes and a 20-fold risk for CD in NOD2 homozygotes or complex heterozygotes have been demonstrated. However, NOD2 is weakly associated with UC. IBD2 is an extensive UC locus that encompasses a candidate gene, advilin, which might be involved in the morphogenesis of microvilli. IBD3 on chromosome 6 includes the major histocompatibility complex and is mutual to all IBD. Further, mutations in IL23R, ATG16L1, IRGM, TNFSF15, and PTPN22 have been associated with Crohn's disease (25, 26).

1.2.2.2 Immune system dysregulation

Inflammatory bowel disease results from an altered balance between regulatory and inflammatory cytokines. Upon encountering infectious agents, activated macrophages are able to mount a rapid response by secreting inflammatory cytokines that directs the development of

adaptive immunity mediated by T- and B-lymphocytes. In CD, activated T-helper cell (Th1) and Th17 CD4$^+$ T-cells secrete cytokines such as Interleukin-1 (IL-1), Interferon-γ (IFN-γ), Tumor Necrosis Factor-α (TNF-α), IL-2, IL-17/IL-22, and IL-23. In UC, on the other hand, Th2 CD4$^+$ T-cells are characterized by the production of transforming growth factor β (TGF-β), IL-4, IL-5, IL-6, IL-10, and IL-13. Studies have focused on IL-1α and TNF-α as they induce the expression of vascular adhesion molecules. Up regulation of these molecules can recruit leukocytes from the circulation to the site of intestinal mucosal inflammation in CD and UC (27).

1.2.2.3 Environmental trigger in IBD

Many environmental factors have been implicated in the pathogenesis of IBD. These include: smoking, diet, anti-inflammatory drugs (NSAIDs), stress, and microbial factors. Of particular interest, is cigarette smoking, which revealed to have an opposite effect on the two conditions of IBD: protective for UC patients and inductive in CD patients. Further, diet rich in fat, omega-6 fatty acids, refined sugar, and meat has been correlated with the development of IBD whereas high fiber, fruit, and vegetable intake are correlated to decrease the risk of IBD. NSAIDs are associated with an increased risk for CD and UC. These drugs cause neutrophils aggregation and smooth muscle contraction in the intestine leading to mucosal defects and thus increasing the permeability to pathogenic microbes. Finally, microbes have been postulated to play a role in the pathogenesis of IBD (28-30).

1.2.3 Dysregulation of immune response in IBD

In active IBD, the immunological tolerance to luminal antigens mediated by macrophages and dendritic cells is compromised. In the recognition of antigens, the immune system relies on

the presence of highly conserved pathogen associated molecular patterns (PAMPs), found exclusively on pathogenic microbes. Toll-like receptors (TLRs) recognize PAMPs and activate signaling pathways that induce the expression of a variety of immune response genes. Toll-like receptors are pattern recognition receptors (PRRs) expressed by the epithelial cells in the gut mucosa and by the innate immune cells in the lamina propria. Three common features characterize TLRs: a divergent ligand binding extracellular domain with leucine rich repeats (LRRs), a short trans-membrane region and a homologous cytoplasmic toll/IL-1 receptor (TIR) domain essential for the initiation of downstream signaling cascades. A few PAMP-TLR recognition pairs include bacterial lipoprotein (BLP)-TLR1/2, gram-positive peptidoglycan (PNG)-TLR2/6, gram-negative lipopolysaccharide (LPS)-TLR4, and flagellin-TLR5 (31, 32).

TLRs send signals through a conserved transduction pathway through its Toll domain. Signaling intermediates include myeloid differentiation primary response protein 88 (MyD88), interleukin-1 receptor-associated kinase (IRAK), and TNF-receptor associated factor 6 (TRAF6). This leads to the activation of NF-κB pathways resulting in the production of pro-inflammatory cytokines, chemokines, and adhesion molecules (33). In human colon, IECs express high levels of TLR3, TLR5 and low levels of TLR2 and TLR4. TLR2 and TLR4 are located at the cell surface and are responsive to LPS stimulation. In IBD, the expression of TLR3 is down regulated in IECs in active CD but not in UC, and TLR4 is strongly up regulated in both UC and CD with no change in the expression of TLR2 and TLR5 (32). Recently, studies reported the expression of TLR9 in the human gut at the apical surface and intracellularly in epithelial cells, and showed that mutation in its gene is linked to IBD, particularly CD (34). However, other studies reported that TLR9 has a critical role in the maintenance of intestinal homeostasis (35). Localization of TLR expression to

the apical or basolateral membranes modulates the TLR-induced inflammatory response. TLR signaling in the intestine is limited by the presence of inhibitors. Tollip is an inhibitor that binds to IRAK; it is highly expressed by the normal intestinal epithelial cells. Tollip expression is increased by the increase response of LPS to PAMPs. Other inhibitors that control inflammtion in healthy gut include single-immunoglobulin interleukin-1 receptor-related (SIGIRR) and peroxisome proliferator-activated receptor gamma (PPAR-γ). Inappropriate TLR signaling contributes to the loss of tolerance to the normal flora in IBD (36).

1.2.4 Animal model in IBD

Animal models of the intestinal inflammation provide useful tool for studying IBD. Various murine models of IBD have been investigated. These can be classified into five groups: genetic knockouts (genes: TCR-α, IL-2, IL-10, Mdr1a) and transgenic models (Human Antigen leukocyte (HLA-B27) and Signal Transducer and Activator of Transcription protein (Stat4)), adoptive transfer models, spontaneous colitis models, and chemically induced models (DSS and TNBS). Most of these models demonstrate Th1/Th2 intestinal inflammation sharing several immunological features with CD and UC (37-39).

1.3 Influence of altered microenvironment on epithelial cells in IBD

1.3.1 Indirect cell-to-cell interaction

1.3.1.1 Soluble mediators

Inflammatory cytokines are soluble mediators secreted by activated macrophages and dendritic cells. They play a crucial role in the regulation of IBD, by altering tight junction activity and intercellular communication. Pro-inflammatory cytokines (IL-1, IL-6, IL-8, IL-12, and TNF-α)

bind to specific receptors and initiate signaling events leading to inflammatory response. IL-1 exits in two forms IL-1α and IL-1β which bind to two different receptors (type I and II) on the target cells. IL-1 expression increases tremendously in the mucosa of IBD patients; their effect is regulated by IL-1 receptor antagonist (IL1-ra). TNF-α shares similar pro-inflammatory activities with IL-1. However, there are two soluble receptors that inhibit the binding of TNF-α to its cellular receptors reducing its biological effects. In contrast to IL-1, data about TNF-α in IBD are contradictory. Some patients showed an increase in the levels of TNF-α in the inflamed mucosa whereas others showed no change. TNF-α stimulates the production of IL-6 and IL-8 whose levels have been shown to be elevated in IBD patients. IL-8 secretion induces the expression of chemokine that leads to the recruitment of activated neutrophils to the inflammatory site. In the same context, immunoregulatory cytokines (IL-2, IFN- γ and IL-4) have been reported to decrease in IBD (40, 41).

Further, the secreted pro-inflammatory cytokines stimulate intestinal epithelial cells, infiltrating leukocytes and macrophages to release matrix metalloproteinases (MMPs), degrading the extracellular matrix. Several studies have shown the up regulation of MMPs proteolytic activity in the inflamed epithelium of IBD patients (MMP-1, -2, -3, -7, -9, -10, -12, and -13); however, MMPs are no longer regarded as mere proteolytic enzymes but as a potential therapeutic target for IBD (94).

1.3.1.2 Exosomes cargo mediators

Exosomes are vesicles, 50-100 nm in diameter, secreted by a multitude of cell types. They are now recognized as a novel mode of targeted intercellular communication. IECs,

macrophages, dendritic cells, and B- and T- lymphocytes secrete exosomes that exert biological functions. IECs exosomes are enriched in MHC class I and class II molecules, tetraspan molecules (CD37, CD53, CD63, CD81, and CD82), and co-stimulatory molecule (CD86). Macrophages contain PAMPs; and once stimulated with LPS, they secrete exosomes that activate TLR-dependent inflammatory response.

Exosomes from dendritic cells contain MFG-E8, Mac-1, CD9 Annexin II, Gi2a, and HSC73 and are shown to activate CD81 T-lymphocytes and to provoke tumor regression *in vivo*. B-lymphocyte exosomes stimulate CD41 T-lymphocytes *in vitro*, and transfer MHC class II–peptide complexes to follicular dendritic cells in germinal centers (Figure 3). Exosomes are now regarded as regulators for the immune system (42-46).
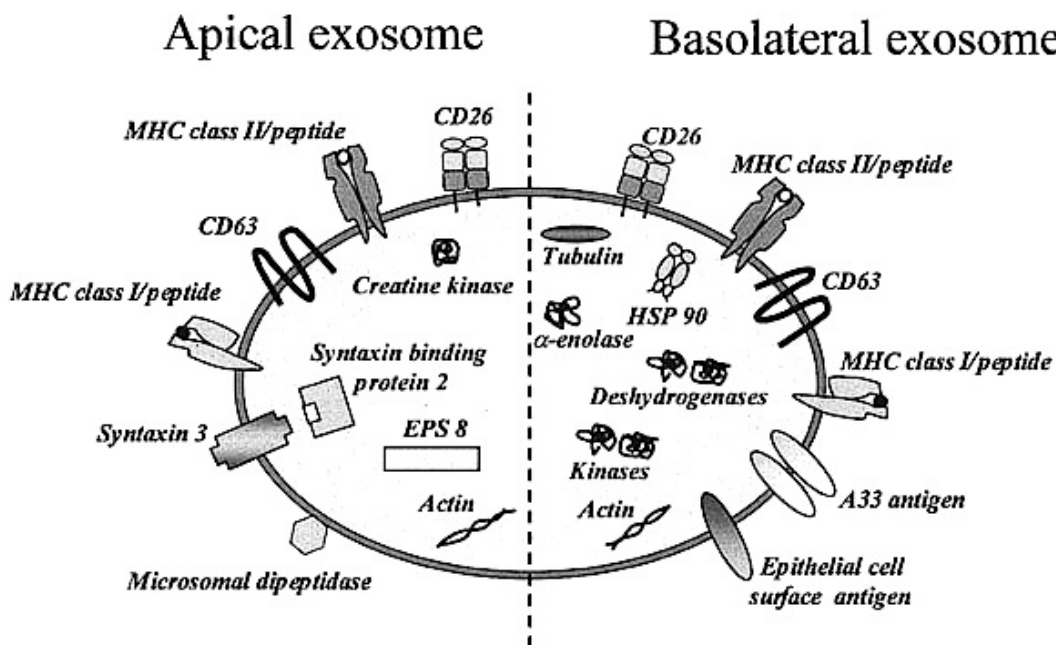
Figure 3: Model for the molecular structure of epithelial-derived exosomes (42).

1.3.2 Direct cell-to-cell interaction

Cell-cell interactions have been widely reported to contribute to the pathogenesis and perpetuation of IBD. These interactions involve both cell adhesion and communication.

1.3.2.1 Cell-cell adhesion

Inflammatory bowel disease is characterized by leukocyte infiltration into the mucosa of the colon. Integrins, selectins, and immunoglobins (Ig) facilitate leukocyte rolling, adhesion, and trans-endothelial migration to the site of infection. $\alpha4\beta7$, $\alpha4\beta1$, and CD18 integrins mediate the binding of leukocytes to their complementary ligands on activated endothelial cells. Studies performed on biopsies from actively inflamed mucosa revealed up regulation of E- and P-selectins, mucosal addressin cell adhesion molecule (MAdCAM-1) and intercellular adhesion molecule 1 (ICAM-1) expression. Vascular cell adhesion molecule 1 (VCAM-1) expression, with no basal level in normal colon tissues, is up regulated in IBD tissues. Targeting adhesion molecules involved in leukocyte-endothelial cell interaction is the novel research focus for IBD treatment (47-49).

1.3.2.2 Cell-cell communication

Cell-cell communication involves tight junction, gap junction, adherens junction, desmosomes, and pannexins. Autocrine, paracrine, and juxtacrine signaling mediate this intercellular communication. Notch signaling pathway, the most studied of juxtacrine signaling, has been shown to be activated in IECs in IBD patients and has a crucial role in the maintenance of intestinal homeostasis (4, 50). Recently, pannexins (Panx) have been implicated in inflammation. A study conducted by Diezmos *et al.* revealed a role of Panx1 in the pathogenesis

of IBD (51, 52). Further, the release of cytokines has been associated with the disruption of intercellular communication between cells (41, 53, 54).

1.4 Overview of Gap Junctions

Gap junctions (GJ) are clusters of intercellular plasma membrane channels, which serve as conduits for intercellular communication that allow passage of ions and low molecular weight metabolites (less than 2kDa) between the cytosol of two adjacent cells. Gap junctions are composed of members of highly homologous family of proteins known collectively as connexins (Cxs). Different connexins can selectively interact with each other to form GJ channels, which differ in their content and spatial arrangement of connexin subunits and hence permeability of the channels.

1.4.1 The Connexin Family

1.4.1.1 Connexin nomenclature

Connexins are named according either to their predicted molecular weight from the cDNA sequence of the connexin (Cx43, originally identified in the heart is the ~ 43 kDa protein and Cx32, originally identified in liver is the ~ 32 kDa protein); or to the sequence similarities and the length of the cytoplasmic domain of connexins, classifying them into α, β, γ, δ, ε subgroups and designated as GJ (for example: GJA1 for the first identified connexin of the α-group, Cx43; GJB1 for the first identified connexin gene of the β-group, Cx32) (Table 1) (55, 56).

Table 1: Expression of connexins in human tissues (modified from reference 56).

Human gap junction protein (connexin) genes			
Approved symbol	Synonyms	Chromosome	Major expressed organ or cell types
GJA1	Cx43	6q22-q23	Ubiquitous, cardiac, lens, skeleton
GJA3	Cx46	13q12.11	Lens, bone
GJA4	Cx37	1p35.1	Endothelium, granulosa cells, lung, skin
GJA5	Cx40	1q21.1	Cardiac atrium and conduction system, endothelium
GJA8	Cx50	1q21.1	Lens
GJA9	Cx59, Cx58	1p34	Ear, retina, testis, skeletal muscle
GJA10	Cx62	6q15-q16	Retinal horizontal cells
GJB1	Cx32	Xq13.1	Hepatocytes, secretory acinar cells, Schwann cells
GJB2	Cx26	13q11-q12	Cochlea, placenta, hepatocytes, skin, pancreas, kidney, intestine
GJB3	Cx31	1p34	Cochlea, placenta, skin
GJB4	Cx30.3	1p35-p34	Skin, kidney
GJB5	Cx31.1	1p34.3	Skin, placenta
GJB6	Cx30	13q12	Skin, ear, intestine, astrocytes, kidney, mammary gland
GJB7	Cx25	6q15	Placenta
GJC1	Cx45	17q21.31	Myofibroblasts, colon, heart, neurons, retina, glomeruli, Bone
GJC2	Cx47, Cx46.6	1q41-q42	Oligodendrocyte, spinal cord, lymphatics
GJC3	Cx30.2	7q22.1	Brain, spinal cord, Schwann cells
GJD2	Cx36	15q13.1	Neurons, pancreatic cells
GJD3	Cx31.9, Cx30.2	17q21.1	Vascular smooth muscle cells; Cardiac tissue
GJD4	Cx40.1	10p11.22	Pancreas, kidney, skeletal muscle, liver, placenta, heart
GJE1	Cx23	6q24.1	Ear

1.4.1.2 Connexin gene structure

The human genome comprises 21 confirmed connexin genes that are temporally and spatially distributed throughout the body. Connexin gene is made of two exons (Ex1, Ex2) separated by an intron, and 3'- and 5'- untranslated region (UTR). The entire coding sequence is uninterrupted in Ex2; however, Cx45 contains three exons with the coding region located in

Ex3. Other connexins, like Cx36 gene has their coding region in Ex1 and Ex2, interrupted by an intron; Cx32 gene is alternatively transcribed by different promoters (Ex1A and Ex1B) resulting in two transcripts, one is functional in liver and pancreas and the other in nerve cells (Figure 4) (57).
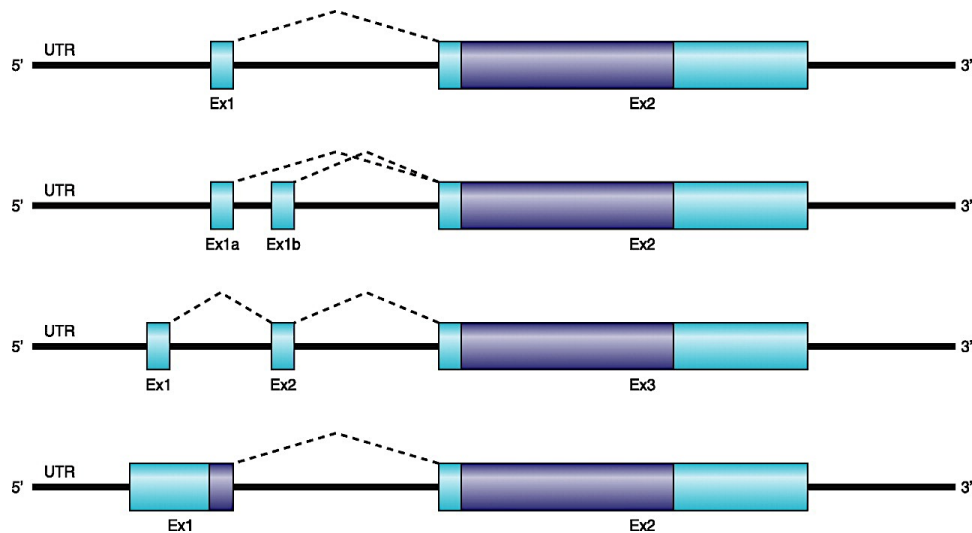
Figure 4: Connexin gene structure (57).

1.4.1.3. Structural domain of the connexin protein

Connexins share a similar structural topology with four hydrophobic regions, spanning the membranes: two extracellular loops (EL1 and EL2) involved in initiating and stabilizing the interactions between two opposing connexins (structure of six Cxs), intracellular loop (IL) and carboxy (CT)- and amino (NT)-terminal domains localized in the cytosol. The ELs, the trans-membrane (TM) regions and the NT, are highly conserved, while the IL and CT are highly divergent, both in length and in sequence. The NT consists of 22 (for β Cxs) and of 23 (for α Cxs) amino acids, except for Cx36 and Cx47. The NT is crucial for the formation of functional

hemichannels and in GJ channel gating (58). The CT encloses many phosphorylation sites implicated in the regulation of GJ channels and in protein-protein interactions (58-60).

1.4.1.4 Biosynthesis, trafficking, and degradation of connexins

Connexins are co-translationally inserted into the endoplasmic reticulum (ER), oligomerize intracellularly in the ER-Golgi intermediate compartment (ERGIC) into a connexon or hemichannel where they must fold correctly as they traffic from ER to the Golgi (Figure 5). Connexons are packaged and transported by microtubule-assisted vesicle to the membrane where they may remain in a closed hemichannel or they dock with compatible connexons on adjacent cells to form GJ channels (55, 61, 62).

Trafficking and assembly of Cxs, and GJ channel formation and degradation have been widely studied by time-lapse imaging of living cells expressing Cx43 tagged to GFP or to green-to-red photoconvertible fluorescent protein Dendra2. All Cxs traffic to the cell surface *via* the classical ER-Golgi pathway except for Cx26 where studies have shown that it is directly inserted into the plasma membrane bypassing the Golgi apparatus (63-66).

Connexins have a short half-life of 1–5 h. Newly delivered connexons are added to the periphery of pre-formed GJ, while the central "older" gap junction fragment are degraded by internalization of a double-membrane structure called "annular junction" or "connexosomes" into one of the two cells. Internalization and degradation of GJs is mediated by the ubiquitin/proteasomes system, lysosomes, and the autophagic system (67-69). In some cases, the non-ubiquitinated connexons are recycled back to the plasma membrane (70).
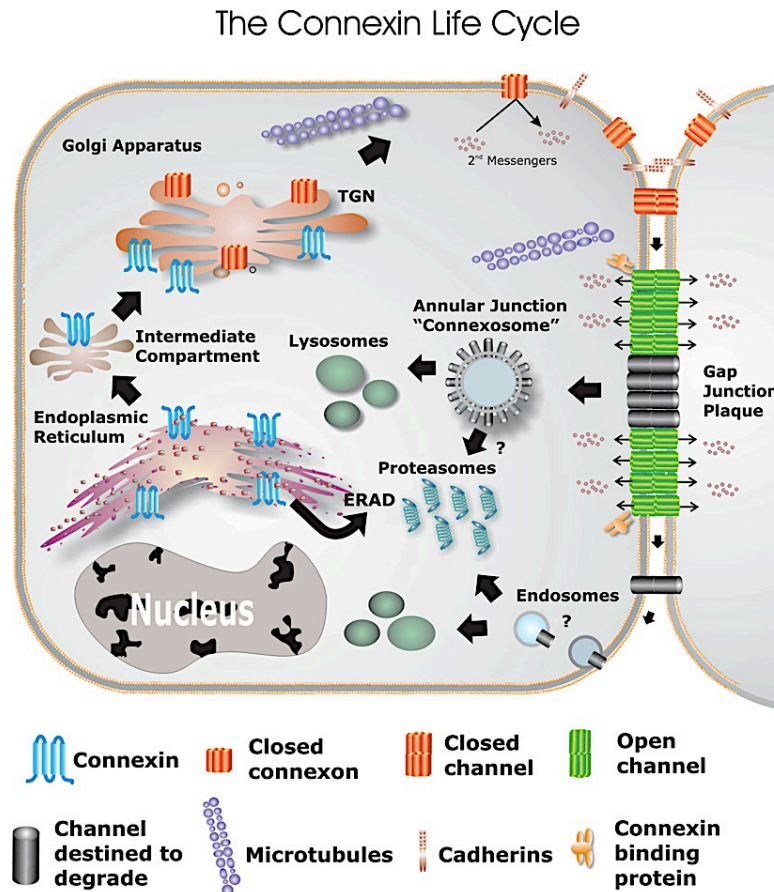
Figure 5: Life cycle of the connexin (71).

1.4.2 Connexin post-translational modifications

Post-translational modifications affect hemichannels, GJ assembly, and Cxs trafficking. These include phosphorylation, hydroxylation, acetylation, disulfide binding, nitrosylation, palmitoylation, and ubiquitination (Figure 6). The most studied of these Cx post-translational modifications is phosphorylation. All Cxs are phosphorylated at multiple sites by multiple kinases present at the C-terminal except Cx26. Connexin 43 phosphorylation has been extensively studied and reviewed (72, 73). Studies have shown that Cx43 is phosphorylated prior to its insertion into the plasma membrane, which is evident by the fact that C-terminal

truncated Cx43 (Δ252) oligomerize and traffic to the membrane and form functional channels. Therefore, phosphorylation is not a critical requirement for Cx trafficking but it is involved in their internalization and degradation (75).
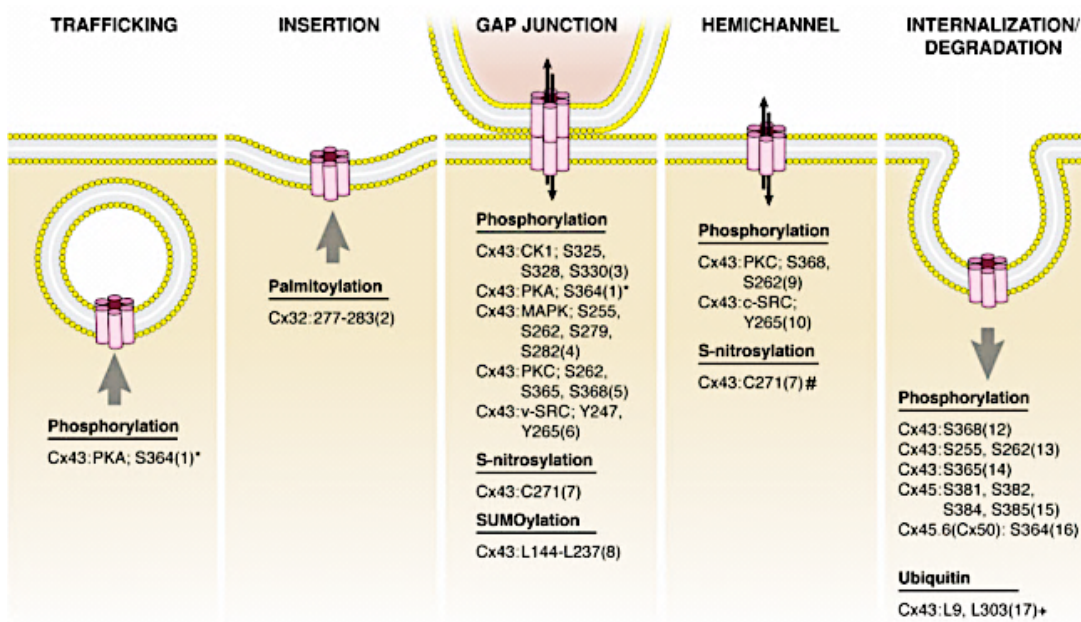
Figure 6: Post-translational modifications throughout the lifespan of connexins. *indicates it was shown indirectly through PKA; # indicates that this cysteine is assumed to be S-nitrosylated in a hemichannel, but has not been directly shown; + indicates that this data is now in dispute according to work by Dunn *et al.,* 2012 (75).

1.4.3 Connexin-interacting proteins

Connexins interact with cytoskeleton structural components such as microtubules and microfilaments, adherens junction proteins such as cadherins, α- and β-catenin, and tight junction proteins such as claudins, occludins and ZO proteins (Figure 7). Studies have shown that Cx43 and Cx45 interact with ZO-1 and ZO-2 through their C-terminal, and the PDZ domain of ZO proteins mediates this interaction. Other reports have shown that Cx26 and Cx32 co-

localize with actin and occludin, and Cx43 with α- and β-catenin (79-81). Connexin also interact

with enzymes such as tyrosine and serine/threonine kinases, phosphatases and caveolin, a

component of lipid rafts (55, 82, 83).
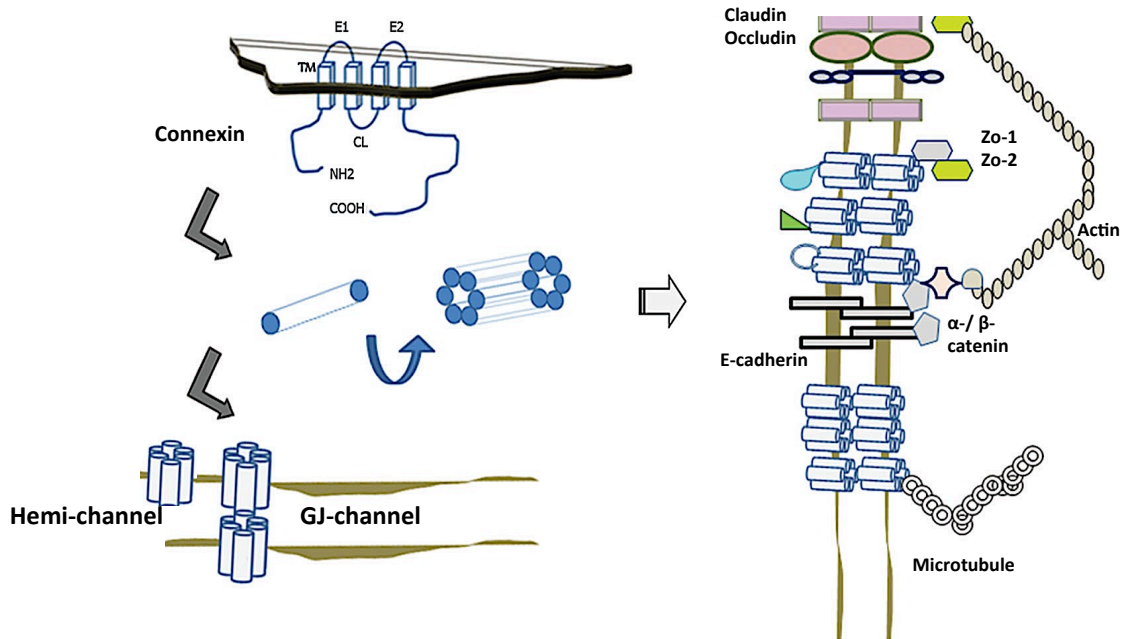
Figure 7: From connexin to gap junction complex. The structure of the connexin protein with its 4 trans membrane (TM) domains, 2 extracellular loops (E1, E2), cytoplasmic loop (CL), and NH_2 and COOH termini. Six connexins (Cx is represented as a cylinder) cluster into a connexon, and two connexons dock together to form a gap junction channel. Gap junctions clustered in plaques and the gap junction complex made up of connexins and their associated proteins (84).

1.4.4 Connexin channel: structure and function

Connexin hemichannels can be either homomeric formed of identical Cx subunits or

heteromeric formed of different Cxs (Figure 9). Hemichannels may remain as a single channel

on the membrane or dock with a hemichannel from opposing cells to form a GJ channel. Cell

adhesion molecules mediate the formation of GJ channel (74). Gap junction channels may be

homotypic, when two identical connexons assemble, or heterotypic, when two dissimilar connexons assemble between the two interacting cells (Figure 8).
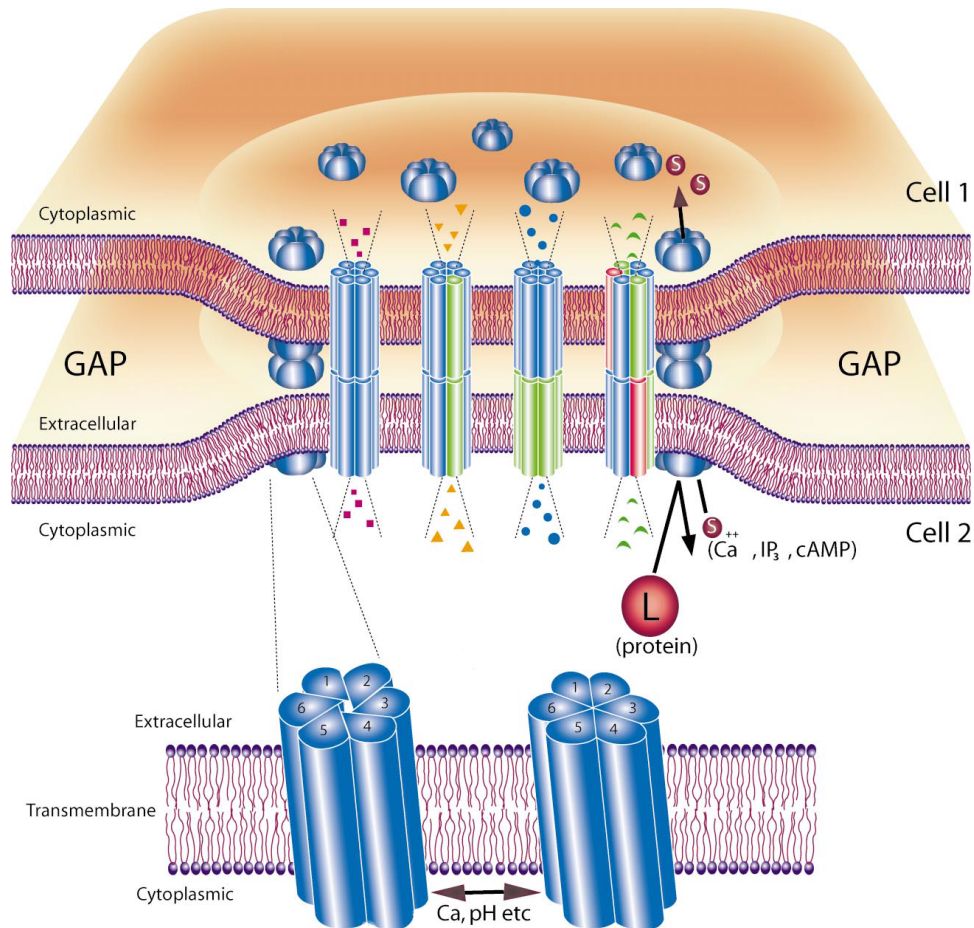
Figure 8: A schematic diagram of a gap junction plaque joining the cytoplasm of two adjacent cells (Cell 1 and Cell 2; top panel). Connexons from two adjacent cells form an intercellular channel that allows the passage of small (s) molecules such as Calcium, IP3, and cAMP, but not large (L) molecules such as proteins, from the cytoplasm of one cell to the other. Depending on the type of connexin (for example black, grey, light grey), the connexon formed could be homomeric or heteromeric and consequently the gap junction could be homotypic or heterotypic, with selective permeability. Each connexon (lower panel) is made of six connexins (1, 2, 3, 4, 5, and 6). Tangential twisting of the connexon mediates gap junction gating that opens (left connexon) or closes (right connexon) the hemichannel. Changes in cytoplasmic pH and calcium ion concentration, among other things, regulate gap junction function (78).

Heterotypic interactions between connexons have been widely investigated. Studies have shown that Cx26 forms channel with either Cx30 or Cx32 but not with Cx43, and Cx43 forms channel with either Cx40 or Cx45. Connexin channels forming interactions are summarized in table 2. Gap junction channels are formed with aqueous pores between the trans-membranes TM2 and TM3 of each participating connexin, mediating the flux of ions, metabolites and signaling molecules between cells and across the plasma membrane (76).

Table 2: Connexin channel forming interactions (59).

Cx26	Cx30	Cx30.3	Cx31	Cx31.1	Cx32	Cx33	Cx36	Cx37	Cx40	Cx43	Cx45	Cx46	Cx50	Cx57	
+	+	−	−	−	+	−	−	−	−	−		+	+	−	Cx26
	+	+			+		+	+	+	+				−	Cx30
		+	−	−	−		−	+	+	+	−			+	Cx30.3
			+	−	−			−	−	−	−			−	Cx31
				−	−			−	−	−	−			−	Cx31.1
					+	−	−	−	−	−	−	+	+	−	Cx32
						−		−		−					Cx33
							+	−	−	−	−			−	Cx36
								+	+	+	+		+		Cx37
									+	+	+	−	−	−	Cx40
										+	+	+	−	+	Cx43
											+			−	Cx45
												+	+	−	Cx46
													+	−	Cx50
														+	Cx57

+, Forms heterotypic channels; −, does not form heterotypic channels, blank = not reported.

Gap junction channels play a crucial role in embryonic growth and cellular development, differentiation, and regeneration. They are well known to be essential for electrical coupling in cardiac tissue, uterus contraction, alveolar differentiation, bone formation, lens growth, and central nervous system (55, 71, 76). Gap junction channels are also implicated in cell signaling and tissue homeostasis. Similar to GJ channel, hemichannels play a crucial role in cell survival, signaling, and development. Most studies have focused on the role of hemichannel in cochlear

homeostasis, ischemic preconditioning in heart and brain, and recently in the intestine, and liver. Voltage, cytoplasmic pH, Ca^{+2}, cAMP, calmodulin (77, 78), protein phosphorylation (72), and cell-cell adhesion molecules regulate both connexin hemichannels and GJ channels (74).

1.4.5 Connexins in tissues and associated diseases

1.4.5.1 Mutations and knockouts

Connexin gene mutations have been associated with a variety of human diseases such as deafness, lens cataract, skin diseases, cardiovascular pathologies, oculodendrodigita dysplasia, Vohwinkel syndrome, and X-linked Charcot-Marie-Tooth neuropathy (Table 3) (71, 85-87). Mutations of connexin-associated proteins have also been documented. Furthermore, mouse models of Cx knockout have been generated to study disease phenotypes and to provide clues into these diseases. A knockout of Cx30 leads to hearing impairment, and that of Cx32 results in liver dysfunction. Cx26, Cx43 and Cx45 knockouts are lethal in early postnatal life due to placental development and congenital cardiac abnormalities, respectively. Interestingly, hearing loss resulted from Cx26 knockout can be restored by knock-in of Cx32 (88, 89).

Table 3: Human connexin genes and major associated human diseases (86).

Human connexin gene/protein	Major associated human diseases	References
GJA1/Cx43	Oculodentodigital dysplasia (ODDD)	Paznekas et al. (2003)
GJA3/Cx46	Cataract	Gong et al. (1997)
GJA4/Cx37	Atherosclerosis	Yamada et al. (2002)
GJA5/Cx40	Atrial fibrillation	Gollob et al. (2006)

GJA8/Cx50	Cataract	White et al. (1998)
GJB1/Cx32	X-linked Charcot-Marie-Tooth disease	Bergoffen et al. (1993)
GJB2/Cx26	Non-syndromic and syndromic deafness	Xia et al. (1998)
	Vohwinkel syndrome	Lee and White, (2009)
	Keratitisichtyosis deafness (KID)	van Geel et al. (2002)
GJB3/Cx31	Non-syndromic and syndromic deafness	Scott and Kelsell (2011)
	Erythrokeratodermia variabilis (EKV)	Richard et al. (1998)
GJB4/Cx30.3	Erythrokeratodermia variabilis (EKV)	Scott et al. (2011)
GJB6/Cx30	Non-syndromic deafness	Scott and Kelsell (2011)
	Hydrotic ectodermal dysplasia	Essenfelder et al. (2004)
GJB7/Cx25	–	–
GJC1/Cx45	–	–
GJC2/Cx47	Pelizaeus–Merzbacher-like disease 1	Bugiani et al. (2006)
	Primary/secondary lymphoedema	Ferrell et al. (2010); Finegold et al. (2012)
GJC3/Cx30.2	–	–
GJD2/Cx36	Myoclonic epilepsy	Hempelmann et al. (2006)
GJD3/Cx31.9	–	–
GJD4/Cx40.1	–	–
GJE1/Cx23	–	–

1.4.5.2 Expression and functional role of connexins in the colonic epithelium

The normal epithelium of the colon expresses the three major connexins: Cx26, Cx32, and Cx43. Kanczuga-Koda *et al.* 2004 showed that all three connexins are expressed between the

epithelial cells in crypts and at the luminal surface (90). Cx26 and Cx43 are expressed in the circular layer of muscularis externa and only Cx43 is expressed in muscularis mucosa. Another study conducted by Sirnes *et al.* 2011 showed that the normal colon tissue expresses six connexin genes including: Cx26, Cx31.2, Cx32, Cx43, Cx45, and Cx59, and their expression at the transcriptional is altered in colorectal carcinomas (91). Dubina *et al.* 2002 showed that mutation in Cx43 but not in Cx32 is involved in the progression of the colon tumor to a malignant state (92). This is supported by report from Kanczuga-Koda *et al.* 2010 that associated progression of colorectal cancer with the gradual loss of functional GJ (93).

1.5 Aim of the study

The aim of this study is to explore the nature of the interaction between human intestinal epithelial cells (IECs) and immune cells (macrophages) in an *in vitro* model of IBD, established by treating IECs with inflammatory mediators or their co-culturing with inflammatory cells. This was accomplished by:

a. Identifying the potential junctional proteins involved in hetero-cellular communication and assessing the effect of inflammatory mediators on their expression at the transcriptional, translational, cellular localization, and functional levels.

b. Studying the trafficking of Cx in Caco-2 cells using traceable photo convertible chimeras (Cx26-Dendra2 and Cx43-Dendra2), and determining the regulation of such chimeras by inflammatory mediators.

c. Examining the association of Cx43 with junctional complexes in Cx43 overexpressing Caco-2 cells to study the junctional barrier between IECs and macrophages.

d. Investigating the expression of junctional proteins and collagen type IV and vimentin in colon tissues.

References

1. Kim YS, Ho SB. Intestinal goblet cells and mucins in health and disease: recent insights and progress. Curr Gastroenterol Rep. 2010 Oct;12(5):319-30.

2. Moran GW, Leslie FC, Levison SE, Worthington J, McLaughlin JT. Enteroendocrine cells: neglected players in gastrointestinal disorders? Therap Adv Gastroenterol. 2008 Jul;1(1):51-60.

3. Clavel T, Haller D. Molecular interactions between bacteria, the epithelium, and the mucosal immune system in the intestinal tract: implications for chronic inflammation. Curr Issues Intest Microbiol. 2007 Sep;8(2):25-43.

4. Okamoto R. Epithelial regeneration in inflammatory bowel diseases. Inflammation and Regeneration. 2011;31(3):275.

5. Peterson LW, Artis D. Intestinal epithelial cells: regulators of barrier function and immune homeostasis. Nat Rev Immunol. 2014 Mar;14(3):141-53.

6. Clayburgh DR, Shen L, Turner JR. A porous defense: the leaky epithelial barrier in intestinal disease. Lab Invest. 2004 Mar;84(3):282-91.

7. Hindryckx P, Laukens D. Intestinal Barrier Dysfunction: The Primary Driver of IBD? In: Inflammatory Bowel Disease - Advances in Pathogenesis and Management. Inflammatory Bowel Disease - Advances in Pathogenesis and Management. DOI: 10.5772/26436.; 2012. p. 23.

8. Dogan A, Wang ZD, Spencer J. E-cadherin expression in intestinal epithelium. J Clin Pathol. 1995 Feb;48(2):143-6.

9. Karayiannakis AJ, Syrigos KN, Efstathiou J, Valizadeh A, Noda M, Playford RJ, et al. Expression of catenins and E-cadherin during epithelial restitution in inflammatory bowel disease. J Pathol. 1998 Aug;185(4):413-8.

10. Laukoetter MG, Bruewer M, Nusrat A. Regulation of the intestinal epithelial barrier by the apical junctional complex. Curr Opin Gastroenterol. 2006 Mar;22(2):85-9.

11. Gonzalez-Mariscal L, Betanzos A, Nava P, Jaramillo BE. Tight junction proteins. Progress in Biophysics and Molecular Biology. 2003;81:1.

12. Balda MS, Matter K. Tight junctions at a glance. Journal of Cell Science. 2008;121:3677.

13. Edelblum KL, Turner JR. The tight junction in inflammatory disease: communication breakdown. Curr Opin Pharmacol. 2009 Dec;9(6):715-20.

14. Johansson ME, Larsson JM, Hansson GC. The two mucus layers of colon are organized by the MUC2 mucin, whereas the outer layer is a legislator of host-microbial interactions. Proc Natl Acad Sci U S A. 2011 Mar 15;108 Suppl 1:4659-65.

15. Kim JJ, Khan WI. Goblet cells and mucins: role in innate defense in enteric infections. Pathogens. 2013 Feb 4;2(1):55-70.

16. Moehle C, Ackermann N, Langmann T, Aslanidis C, Kel A, Kel-Margoulis O, et al. Aberrant intestinal expression and allelic variants of mucin genes associated with inflammatory bowel disease. J Mol Med (Berl). 2006 Dec;84(12):1055-66.

17. Belkaid Y, Grainger J. Immunology. Mucus coat, a dress code for tolerance. Science. 2013 Oct 25;342(6157):432-3.

18. Guindi M, Riddell RH. Indeterminate colitis. J Clin Pathol. 2004 Dec;57(12):1233-44.

19. Abraham C, Cho JH. Inflammatory bowel disease. N Engl J Med. 2009 Nov 19;361(21):2066-78.

20. Danese S, Fiocchi C. Ulcerative colitis. N Engl J Med. 2011 Nov 3;365(18):1713-25.

21. Hanauer SB. Inflammatory bowel disease: epidemiology, pathogenesis, and therapeutic opportunities. Inflamm Bowel Dis. 2006 Jan;12 Suppl 1:S3-9.

22. Baumgart DC, Sandborn WJ. Crohn's disease. Lancet. 2012 Nov 3;380(9853):1590-605.

23. Corridoni D, Arseneau KO, Cominelli F. Inflammatory bowel disease. Immunol Lett. 2014 Oct;161(2):231-5.

24. Bamias G, Nyce MR, De La Rue SA, Cominelli F, American College of Physicians, American Physiological Society. New concepts in the pathophysiology of inflammatory bowel disease. Ann Intern Med. 2005 Dec 20;143(12):895-904.

25. Barrett JC, Hansoul S, Nicolae DL, Cho JH, Duerr RH, Rioux JD, et al. Genome-wide association defines more than 30 distinct susceptibility loci for Crohn's disease. Nat Genet. 2008 Aug;40(8):955-62.

26. Ahern PP, Izcue A, Maloy KJ, Powrie F. The interleukin-23 axis in intestinal inflammation. Immunol Rev. 2008 Dec;226:147-59.

27. Strober W, Fuss IJ. Proinflammatory cytokines in the pathogenesis of inflammatory bowel diseases. Gastroenterology. 2011 May;140(6):1756-67.

28. Lakatos PL. Environmental factors affecting inflammatory bowel disease: have we made progress? Dig Dis. 2009;27(3):215-25.

29. Cabre E, Domenech E. Impact of environmental and dietary factors on the course of inflammatory bowel disease. World J Gastroenterol. 2012 Aug 7;18(29):3814-22.

30. Danese S, Sans M, Fiocchi C. Inflammatory bowel disease: the role of environmental factors. Autoimmun Rev. 2004 Jul;3(5):394-400.

31. Mogensen TH. Pathogen recognition and inflammatory signaling in innate immune defenses. Clin Microbiol Rev. 2009 Apr;22(2):240,73, Table of Contents.

32. Abreu MT. Toll-like receptor signalling in the intestinal epithelium: how bacterial recognition shapes intestinal function. Nat Rev Immunol. 2010 Feb;10(2):131-44.

33. Lawrence T. The nuclear factor NF-kappaB pathway in inflammation. Cold Spring Harb Perspect Biol. 2009 Dec;1(6):a001651.

34. Cario E. Toll-like receptors in inflammatory bowel diseases: a decade later. Inflamm Bowel Dis. 2010 Sep;16(9):1583-97.

35. Rose WA, Sakamoto K, Leifer CA. TLR9 is important for protection against intestinal damage and for intestinal repair. Sci Rep. 2012;2:574.

36. Abreu MT, Fukata M, Arditi M. TLR signaling in the gut in health and disease. J Immunol. 2005 Apr 15;174(8):4453-60.

37. Hoffmann JC, Pawlowski NN, Kuhl AA, Hohne W, Zeitz M. Animal models of inflammatory bowel disease: an overview. Pathobiology. 2002 -2003;70(3):121-30.

38. Goyal N, Rana A, Ahlawat A, Bijjem KR, Kumar P. Animal models of inflammatory bowel disease: a review. Inflammopharmacology. 2014 Aug;22(4):219-33.

39. Low D, Nguyen DD, Mizoguchi E. Animal models of ulcerative colitis and their application in drug research. Drug Des Devel Ther. 2013 Nov 12;7:1341-57.

40. Sanchez-Munoz F, Dominguez-Lopez A, Yamamoto-Furusho JK. Role of cytokines in inflammatory bowel disease. World J Gastroenterol. 2008 Jul 21;14(27):4280-8.

41. Neurath MF. Cytokines in inflammatory bowel disease. Nat Rev Immunol. 2014 May;14(5):329-42.

42. van Niel G, Raposo G, Candalh C, Boussac M, Hershberg R, Cerf-Bensussan N, et al. Intestinal epithelial cells secrete exosome-like vesicles. Gastroenterology. 2001 Aug;121(2):337-49.

43. Van Niel G, Mallegol J, Bevilacqua C, Candalh C, Brugiere S, Tomaskovic-Crook E, et al. Intestinal epithelial exosomes carry MHC class II/peptides able to inform the immune system in mice. Gut. 2003 Dec;52(12):1690-7.

44. Bhatnagar S, Shinagawa K, Castellino FJ, Schorey JS. Exosomes released from macrophages infected with intracellular pathogens stimulate a proinflammatory response in vitro and in vivo. Blood. 2007 Nov 1;110(9):3234-44.

45. Thery C. Exosomes: secreted vesicles and intercellular communications. F1000 Biol Rep. 2011;3:15,15. Epub 2011 Jul 1.

46. Li XB, Zhang ZR, Schluesener HJ, Xu SQ. Role of exosomes in immune regulation. J Cell Mol Med. 2006 Apr-Jun;10(2):364-75.

47. Salmi M, Jalkanen S. Human leukocyte subpopulations from inflamed gut bind to joint vasculature using distinct sets of adhesion molecules. J Immunol. 2001 Apr 1;166(7):4650-7.

48. Rivera-Nieves J, Gorfu G, Ley K. Leukocyte adhesion molecules in animal models of inflammatory bowel disease. Inflamm Bowel Dis. 2008 Dec;14(12):1715-35.

49. Panés J, Peñalva M, Piqué JM. New therapeutic targets in Inflammatory Bowel Disease (IBD): Cell Adhesion Molecules. In: Inmunología. ; 2003. p. 203.

50. Obata Y, Takahashi D, Ebisawa M, Kakiguchi K, Yonemura S, Jinnohara T, et al. Epithelial cell-intrinsic Notch signaling plays an essential role in the maintenance of gut immune homeostasis. J Immunol. 2012 Mar 1;188(5):2427-36.

51. Makarenkova HP, Shestopalov VI. The role of pannexin hemichannels in inflammation and regeneration. Front Physiol. 2014 Feb 25;5:63.

52. Diezmos EF, Sandow SL, Markus I, Shevy Perera D, Lubowski DZ, King DW, et al. Expression and localization of pannexin-1 hemichannels in human colon in health and disease. Neurogastroenterol Motil. 2013 Jun;25(6):e395-405.

53. Strober W, Fuss IJ. Proinflammatory cytokines in the pathogenesis of inflammatory bowel diseases. Gastroenterology. 2011 May;140(6):1756-67.

54. Heinrich M, Oberbach A, Schlichting N, Stolzenburg JU, Neuhaus J. Cytokine effects on gap junction communication and connexin expression in human bladder smooth muscle cells and suburothelial myofibroblasts. PLoS One. 2011;6(6):e20792.

55. Dbouk HA, Mroue RM, El-Sabban ME, Talhouk RS. Connexins: a myriad of functions extending beyond assembly of gap junction channels. Cell Commun Signal. 2009 Mar 12;7:4,811X-7-4.

56. Oyamada M, Takebe K, Oyamada Y. Regulation of connexin expression by transcription factors and epigenetic mechanisms. Biochim Biophys Acta. 2013 Jan;1828(1):118-33.

57. Bosco D, Haefliger JA, Meda P. Connexins: key mediators of endocrine function. Physiol Rev. 2011 Oct;91(4):1393-445.

58. Kyle JW, Minogue PJ, Thomas BC, Domowicz DA, Berthoud VM, Hanck DA, et al. An intact connexin N-terminus is required for function but not gap junction formation. J Cell Sci. 2008 Aug 15;121(Pt 16):2744-50.

59. Harris AL. Emerging issues of connexin channels: biophysics fills the gap. Q Rev Biophys. 2001 Aug;34(3):325-472.

60. Martin PE, Evans WH. Incorporation of connexins into plasma membranes and gap junctions. Cardiovasc Res. 2004 May 1;62(2):378-87.

61. Martin PE, Blundell G, Ahmad S, Errington RJ, Evans WH. Multiple pathways in the trafficking and assembly of connexin 26, 32 and 43 into gap junction intercellular communication channels. J Cell Sci. 2001 Nov;114(Pt 21):3845-55.

62. Musil LS, Goodenough DA. Multisubunit assembly of an integral plasma membrane channel protein, gap junction connexin43, occurs after exit from the ER. Cell. 1993 Sep 24;74(6):1065-77.

63. Gurskaya NG, Verkhusha VV, Shcheglov AS, Staroverov DB, Chepurnykh TV, Fradkov AF, et al. Engineering of a monomeric green-to-red photoactivatable fluorescent protein induced by blue light. Nat Biotechnol. 2006 Apr;24(4):461-5.

64. Chudakov DM, Lukyanov S, Lukyanov KA. Tracking intracellular protein movements using photoswitchable fluorescent proteins PS-CFP2 and Dendra2. Nat Protoc. 2007;2(8):2024-32.

65. Lauf U, Giepmans BN, Lopez P, Braconnot S, Chen SC, Falk MM. Dynamic trafficking and delivery of connexons to the plasma membrane and accretion to gap junctions in living cells. Proc Natl Acad Sci U S A. 2002 Aug 6;99(16):10446-51.

66. Baker SM, Buckheit RW,3rd, Falk MM. Green-to-red photoconvertible fluorescent proteins: tracking cell and protein dynamics on standard wide-field mercury arc-based microscopes. BMC Cell Biol. 2010 Feb 22;11:15,2121-11-15.

67. Bejarano E, Girao H, Yuste A, Patel B, Marques C, Spray DC, et al. Autophagy modulates dynamics of connexins at the plasma membrane in a ubiquitin-dependent manner. Mol Biol Cell. 2012 Jun;23(11):2156-69.

68. Falk MM, Baker SM, Gumpert AM, Segretain D, Buckheit RW,3rd. Gap junction turnover is achieved by the internalization of small endocytic double-membrane vesicles. Mol Biol Cell. 2009 Jul;20(14):3342-52.

69. Thomas T, Jordan K, Laird DW. Role of cytoskeletal elements in the recruitment of Cx43-GFP and Cx26-YFP into gap junctions. Cell Commun Adhes. 2001;8(4-6):231-6.

70. Su V, Lau AF. Connexins: mechanisms regulating protein levels and intercellular communication. FEBS Lett. 2014 Apr 17;588(8):1212-20.

71. Laird DW. Life cycle of connexins in health and disease. Biochem J. 2006 Mar 15;394(Pt 3):527-43.

72. Laird DW. Connexin phosphorylation as a regulatory event linked to gap junction internalization and degradation. Biochim Biophys Acta. 2005 Jun 10;1711(2):172-82.

73. Lampe PD, Lau AF. The effects of connexin phosphorylation on gap junctional communication. Int J Biochem Cell Biol. 2004 Jul;36(7):1171-86.

74. Hervé JC, Bourmeyster N, Sarrouilhe D, Duffy HS. Gap junctional complexes: from partners to functions. Prog Biophys Mol Biol. 2007 May-Jun;94(1-2):29-65.

75. Johnstone SR, Billaud M, Lohman AW, Taddeo EP, Isakson BE. Posttranslational modifications in connexins and pannexins. J Membr Biol. 2012 Jun;245(5-6):319-32.

76. Yeager M. Chapter 2
Gap Junction Channel Structure. In: A. Harris, D. Locke (eds.), Connexins: A Guide ed. Human Press, a part of Springer Science Business Media, LLC 2009; 2009. p. 27.

77. Wei CJ, Xu X, Lo CW. Connexins and cell signaling in development and disease. Annu Rev Cell Dev Biol. 2004;20:811-38.

78. El-Sabban ME, Abi-Mosleh LF, Talhouk RS. Developmental Regulation of Gap Junctions and Their Role in Mammary Epithelial Cell Differentiation. J Mammary Gland Biol Neoplasia. 2003 Oct;8(4):463-73.

79. Giepmans BN, Verlaan I, Hengeveld T, Janssen H, Calafat J, Falk MM, et al. Gap junction protein connexin-43 interacts directly with microtubules. Curr Biol. 2001 Sep 4;11(17):1364-8.

80. Giepmans BN. Gap junctions and connexin-interacting proteins. Cardiovasc Res. 2004 May 1;62(2):233-45.

81. Talhouk RS, Mroue R, Mokalled M, Abi-Mosleh L, Nehme R, Ismail A, et al. ellular interaction enhances recruitment of alpha and beta-catenins and ZO-2 into functional gap-junction complexes and induces gap junction-dependant differentiation of mammary epithelial cells. Exp Cell Res. 2008 Nov 1;314(18):3275-91.

82. Chakraborty S, Mitra S, Falk MM, Caplan SH, Wheelock MJ, Johnson KR, et al. E-cadherin differentially regulates the assembly of Connexin43 and Connexin32 into gap junctions in human squamous carcinoma cells. J Biol Chem. 2010 Apr 2;285(14):10761-76.

83. Schubert AL, Schubert W, Spray DC, Lisanti MP. Connexin family members target to lipid raft domains and interact with caveolin-1. Biochemistry. 2002 May 7;41(18):5754-64.

84. Mroue RM, El-Sabban ME, Talhouk RS. Connexins and the gap in context. Integr Biol (Camb). 2011 Apr;3(4):255-66.

85. Krutovskikh V, Yamasaki H. Connexin gene mutations in human genetic diseases. Mutation Research/Reviews in Mutation Research. 2000 4;462(2–3):197-207.

86. Molica F, Meens MJ, Morel S, Kwak BR. Mutations in cardiovascular connexin genes. Biol Cell. 2014 Sep;106(9):269-93.

87. Kleopa KA, Sargiannidou I. Connexins, gap junctions and peripheral neuropathy. Neurosci Lett. 2014 Oct 24.

88. Xu J, Nicholson BJ. The role of connexins in ear and skin physiology - functional insights from disease-associated mutations. Biochim Biophys Acta. 2013 Jan;1828(1):167-78.

89. Nishii K, Shibata Y, Kobayashi Y. Connexin mutant embryonic stem cells and human diseases. World J Stem Cells. 2014 Nov 26;6(5):571-8.

90. Kanczuga-Koda L, Sulkowski S, Koda M, Sobaniec-Lotowska M, Sulkowska M. Expression of connexins 26, 32 and 43 in the human colon--an immunohistochemical study. Folia Histochem Cytobiol. 2004;42(4):203-7.

91. Sirnes S, Honne H, Ahmed D, Danielsen SA, Rognum TO, Meling GI, et al. DNA methylation analyses of the connexin gene family reveal silencing of GJC1 (Connexin45) by promoter hypermethylation in colorectal cancer. Epigenetics. 2011 May;6(5):602-9.

92. Dubina MV, Iatckii NA, Popov DE, Vasil'ev SV, Krutovskikh VA. Connexin 43, but not connexin 32, is mutated at advanced stages of human sporadic colon cancer. Oncogene. 2002 Jul 25;21(32):4992-6.

93. Kanczuga-Koda L, Koda M, Sulkowski S, Wincewicz A, Zalewski B, Sulkowska M. Gradual loss of functional gap junction within progression of colorectal cancer -- a shift from membranous CX32 and CX43 expression to cytoplasmic pattern during colorectal carcinogenesis. In Vivo. 2010 Jan-Feb;24(1):101-7.

94. O'Sullivan S, Gilmer JF, Medina C. Matrix Metalloproteinases in Inflammatory Bowel Disease: An Update. Mediators of Inflammation. 2015; 2015: 19 pages.

CHAPTER 2

Materials and Methods

2 Materials and Methods

2.1 Materials

Cell culture media, fetal bovine serum (FBS), penicillin and streptomycin, trypsin, mouse anti-D-glyceraldehyde-3-phosphate dehydrogenase (GAPDH) antibody, phorbol 12-myristate 13-acetate (PMA), 18 β-glycyrrhetinic acid (18 β-GA), lipopolysaccharide (LPS), kanamycin, ampicillin, and Triton X-100 were purchased from Sigma (USA). Protein determination kit, N', N'-bis-methylene acrylamide, polyvinylidene difluoride membranes (PVDF), sodium dodecyl sulfate (SDS), glycine, Tris-HCl, TEMED, glycerol, ammonium persulfate, gelatin, and iQ SYBR GreenSupermix were from BioRad Laboratories (USA). NF-κBp65, β-catenin and α-tubulin antibodies, western blotting luminol reagents and IgG horseradish peroxidase conjugated secondary antibodies were purchased from Santa Cruz Biotechnology (USA). Connexin 26, Cx43, and ZO-1 antibodies, Calcein-AM, goat anti-rabbit IgG conjugated Texas red, goat anti-rabbit IgG Alexa 488 and Prolong Anti-fade were from Life technologies (USA). COX-2 antibody was from Cayman chemical company (USA). E-cadherin antibody was from Cell Signaling Technology (USA). Collagen IV and Vimentin were from abcam (UK). Protease and phosphatase inhibitors were from ROCHE (Switzerland). Restriction enzymes, T4 DNA ligase and gel band purification kit were purchased from MBI Fermentas (Canada). Endofree maxi plasmid purification kit was purchased from Qiagen (Germany). 2β-mercaptoethanol, agarose and ethidium bromide were from Amresco (USA). pDendra2-N plasmid and Dendra2 antibody were from Evrogen (Russia). Glass bottom culture dishes (Confocal dishes) were from MatTek Corporation (USA). LB agar and LB broth were from Difco Laboratories (USA). Normal goat serum (NGS) was from

Chemicon (USA). Phusion Flash High-Fidelity PCR Master Mix and Revertaid 1st strand cDNA synthesis kit from Thermo Fisher Scientific (USA), Nucleospin RNA II kit from Macherey-Nagel (Germany), and Coomassie Brilliant Blue R-250 stain from Affymetrix (USA).

2.2 Methods

2.2.1 Cell lines and culture conditions

In this study, we used human intestinal epithelial cell lines (IECs): Caco-2 and HT-29, which are two colorectal adenocarcinoma cell lines widely used as models of intestinal transport and pathology, including inflammation. We also used a human non-adherent, monocytic cell line (THP-1), a human embryonic kidney cell line (293T), and a communication deficient cell line (HeLa). THP-1 cells were used under two conditions: in suspension or activated with 50 ng/ml PMA for 24 h and with 1 µg/ml of LPS for additional 4 h to be utilized as adherent cells in the hetero-cellular communication assay. 293T and HeLa cells were used for production of viral particles and for viral titration, respectively. Cells were maintained in RPMI 1640 (HT-29, THP-1), and DMEM AQ (Caco-2, 293T, HeLa). All media were supplemented with 10% FBS, 100 U/ml penicillin G and 100 µg/ml streptomycin. All cells were cultured at 37 °C in a humidified incubator with 5% CO_2 atmosphere.

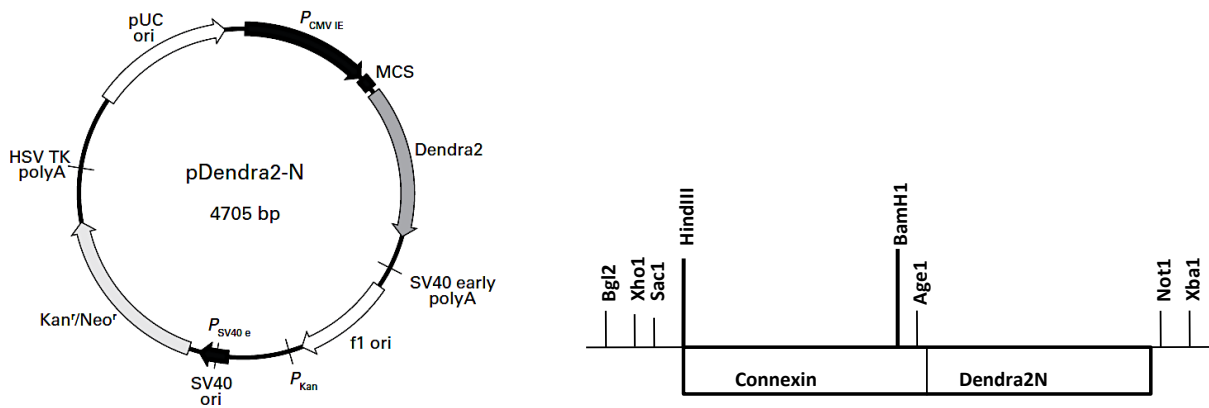### 2.2.2 Construction of Cxs-Dendra2 plasmids

Cx26-Dendra2 and Cx43-Dendra2 chimeras were constructed by cloning Cxs into the multiple cloning site (MCS) of pDendra2-N plasmid. Dendra2 is a monomeric green to red photoconvertible fluorescent protein. Dendra2 was ligated to the C-terminal of the Cxs using Hind III and BamH1 restriction enzymes (Figure 1). Primers for PCR and for sequence analysis

were designed using the Integrated DNA Technologies (IDT) software and summarized in table

1. cDNA covering the complete reading frame of Cx26 and Cx43 were synthesized from 1 μg of

total cellular RNA and amplified by Phusion Flash High-Fidelity PCR Master Mix. The PCR

program consists of 95 °C for 3 min, followed by 35 cycles of 95 °C for 10 sec, 65 °C for 30 sec,

and 72 °C for 1 min and a final extension at 72 °C for 5 min. PCR products were separated by

electrophoresis on 1% agarose gel, and visualized with ethidium bromide staining. PCR

fragments corresponding to Cx26-cDNA (780bp), Cx43-cDNA (1171bp), and pDendra2N

(4700bp) were excised, purified, and digested with restriction enzymes. A ligation reaction

containing three molar (3M) excess of the purified Cxs-cDNA to pDendra2-N was allowed to

proceed for 20 min at room temperature (RT) using T4 DNA ligase. Aliquots of the ligation

reaction were transformed into DH5α competent bacteria using heat shock method, spread on

agar plates and grown overnight. Colonies were picked from plates into 5ml LB-Kanamycin

media and grown at 170 rpm at 37 °C overnight. Bacterial pellets were spun down and re-

suspended in 50ml fresh LB-Kanamycin media and grown until the optical density (A 500)

reached 0.5. The cells were spun down and the pellet was extracted by maxi plasmid

purification kit. Positive colonies were identified by restriction enzymes analysis. New

constructs within the plasmid were confirmed by sequencing (Applied Biosystems 3500 Genetic

Analyzer, USA).

Table 1: Primers used to construct and sequence Cx-Dendra2 plasmids.

Primer	Sequence
For PCR	
Forward-Cx26-Hind III	5'- cat aag ctt ccg cca tgg att ggg gca cgc tg-3'
Reverse-Cx26-BamHI	5'- cag gga tcc cga act ggc ttt ttt gac ttc cca g -3'
Forward-Cx43-Hind III	5'- cat aag ctt ccg cca tgg gtg act gga gcg -3'
Reverse-Cx43-BamHI	5'- cgc gga tcc atg atc tcc agg tca tca ggc -3'
For Sequencing	
Forward-Cx-MCS	5'- gta ggc gtg tac ggt ggg ag-3'
Reverse-Dendra2	5'- ctc gcc ctc gat cac gaa g-3'
Midregion-Cx43	5'- ggc tca atg tgt tct atg tga tgc -3'

Figure 1: Cxs-Dendra2 plasmid design.

2.2.3 Construction of Cxs-Dendra2 lentiviral vectors

For efficient delivery of Cxs-Dendra2 chimeric protein into IECs (Caco-2 and HT-29), we generated lentiviral vectors by cloning Cxs, N-terminally tagged with Dendra2, into the transfer

vector pCSCW under the control of the CMV promoter. pCSCW lentiviral vectors was a generous gift from Dr. Bakhos Tannous laboratory at the Massachusetts General Hospital (Boston, USA). NheI and XhoI were used to insert Cxs-Dendra2 in pCSCW vector (Figure 2). Primers were designed using IDT software and summarized in table 2. Cx26-Dendra2 (1480bp) and Cx43-Dendra2 (1871bp) cDNAs were amplified, purified, and ligated to the pCSCW vector. The ligation reaction was transformed into DH5α competent bacteria using heat shock method, spread on agar plates and grown overnight. As previously mentioned colonies were picked from plates into 5ml LB-Ampicillin media and grown overnight. Bacterial pellets were spun and re-suspended in 50ml fresh LB-Ampicillin media and grown until A 500 reached 0.5. The cells were spun down and the pellet was extracted by maxi plasmid purification kit. The plasmids were then sequenced and used for transduction.

Table 2: Primers used to construct and sequence CSCW-CxDendra2 Lentiviral vectors.

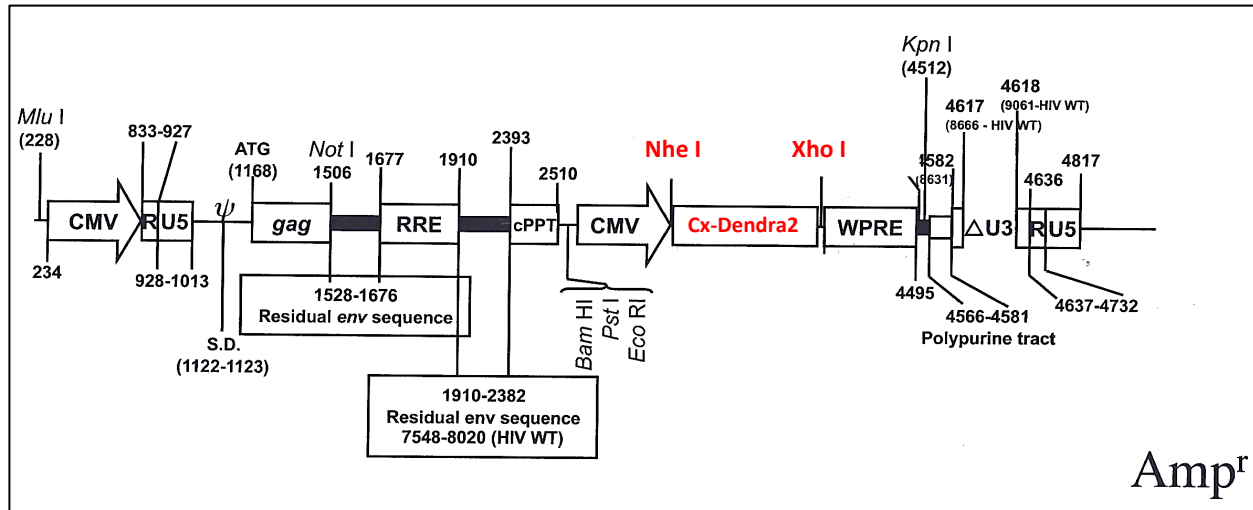| Primer	Sequence
For PCR	
Forward-Cx43-NheI	5'-cat gct agc ccg cca tgg gtg act gga gcg cc-3'
Forward-Cx26-NheI	5'-cat gct agc ccg cca tgg att ggg gca cgc tg-3'
Reverse-Dendra2-XhoI	5'-gc ctc gag tta cca cac ctg gct gggc-3'
For Sequencing	
Forward-CMV	5'-cac caa aat caa cgg gac tt-3'
Reverse-Dendra2	5'-gc ctc gag tta cca cac ctg gct gggc-3'

Figure 2: CSCW-CxsDendra2 lentiviral vector design.

2.2.3.1 Virus production

293T cells were transfected with three lentiviral plasmids: pCMVDR8.91 (containing gag/pol), pVSVG2 (containing the envelope gene VSV-G) and pCSCW-CxsDendra2 using calcium phosphate. The cell supernatants containing the lentiviral particles were collected 48-72 h post transfection, filtered and frozen at -80 °C. To determine the viral titer, HeLa cells were transduced with the produced lentiviral particles and the number of fluorescent cells was quantified by flow cytometry. The titer was extrapolated from the percentage of fluorescent cells, which correlates directly to the number of transducing viral units present in the supernatant used (tu/ml).

2.2.3.2 Transduction of IECs with lentiviral vectors

A total of $2x10^6$ viral particles were used to transduce $2x10^5$ IECs. Transductions were performed in transduction medium (Opti-MEM medium containing lentiviral particles) and 2 h

later complete medium was added. Forty-eight hour later, the efficiency of transduction was determined by flow cytometry. Highly transduced cells producing the Cx-Dendra2 fusion proteins were used for biochemical studies.

2.2.4 Fluorescence-Activated Cell Sorting (FACS)

Forty-eight hours post-transduction of Caco-2 cells with Cx43Dendra Lentiviral vectors, cells were detached by trypsinization, collected by centrifugation at 100g, and the pellet was resuspended in complete media. Cells were sorted using FACS Aria SORP cell sorter (BD Biosciences) in the single cell mode. Dendra2 positive cells were selected based on forward scatter and fluorescence excluding cellular debris and doublets. Highly positive Dendra2 cells were collected in 15ml conical tubes containing complete media. After sorting, the cells were analyzed by flow cytometry for purity of population. A negative control of non-fluorescent cells was used to determine the background fluorescence.

2.2.5 Connexin trafficking and photo conversion

Caco-2 cells, seeded on confocal dishes, were transduced with Cxs-Dendra2 vectors for 48 h. Dendra2 is a green-to-red photo switchable fluorescent protein. Selected Cxs-Dendra2 proteins accumulated at the ER region were irreversibly photoconverted to red using a 405 nm laser. Live video microscopy was used to follow up the intracellular trafficking of the Cxs from the ER to the plasma membrane. Cells were imaged directly after photoconversion in both the green (488 nm) and red channels (561 nm) using a laser-scanning confocal microscope (LSM 710, Carl Zeiss, Germany). Images were captured after photo conversion using X63 oil-immersion objective lens.

2.2.6 Fluorescence recovery after photobleaching (FRAP)

HT-29 cells, seeded on confocal dishes until confluent, were labeled with 1 µM calcein-AM for 1 h. Pre-bleach images were taken. A specific cell was photobleached at 10% 488 nm laser power for 5 iterations at 10 sec interval. Images were collected at 5 sec interval for a total of 5 min. Fluorescence intensity of the bleached cells was quantified and normalized to that of control cells.

2.2.7 Dye transfer assay

IECs were seeded in 6-well plates at a density of 2.5×10^3 per cm^2 for 24 h. IECs were labeled with 1 µM calcein-AM for 1 h (HT-29) and 3 µM calcein-AM for 2 h (Caco-2), washed and incubated with serum-free medium for 30-60 min to allow the intracellular esterase to convert non-fluorescent calcein-AM to a green-fluorescent calcein. The cells were washed again to remove unbound calcein-AM in the media. Labeled IECs were co-cultured with either unlabeled IECs or unlabeled THP-1 cells for predetermined time intervals. Non-adherent cells were then removed, and adherent cells were washed with 1X phosphate buffered saline (PBS) , detached by trypsinization and re-suspended in PBS containing 2% formaldehyde to be analyzed by flow cytometry. Alternatively, co-cultures in suspension: THP-1: THP-1 and IECs: THP-1 were directly fixed in PBS containing 2% formaldehyde. Mean fluorescence intensity (MFI) of both the labeled and the unlabeled populations were determined by forward scatter-fluorescence quadrant analysis of dot plots. Quadrant boundaries were set for each experiment based on fluorescence of unlabeled and calcein-labeled control samples. To confirm that calcein dye transfer was due to gap junction formation, cells were co-cultured in the presence of 100 µM of gap junction inhibitor, 18β-GA.
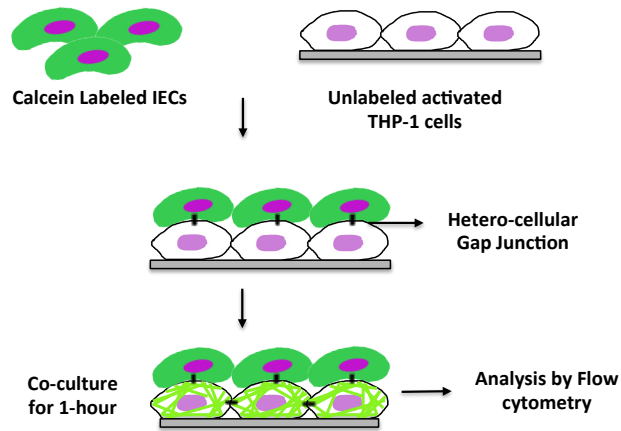
Figure 3: Schematic representation of dye transfer assay.

2.2.8 Quantitative PCR

Total RNA was extracted from cell lines using Nucleospin RNA II kit as per the manufacturer's instructions. 1 µg of total RNA was reverse transcribed to cDNA using Revertaid 1st strand cDNA synthesis kit. Quantitative PCR (qPCR) was performed using the iQ SYBR GreenSupermix in a CFX96 system (Bio-Rad Laboratories, USA). QPCR products were amplified using primers that recognize Cxs, TLRs, MMPs and GAPDH. The primers used in this study are summarized in table 3. PCR parameters consist of a pre-cycle of 95 °C for 3 min followed by 40 cycles consisting of 95 °C for 10 sec, 52 °C - 62 °C for 30 sec, and 72 °C for 30 sec. A final extension at 72 °C for 5 min was then followed by a melting curve, starting at 55 °C with the temperature gradually increased in steps of 0.5 °C to 95 °C. The fluorescence threshold cycle value (Ct) was obtained for each gene and normalized to their corresponding GAPDH in the same sample. The comparative cycle threshold (ΔΔCt) method was used to describe the change in expression of the target gene to the corresponding control group, set to 1. All experiments were carried out in duplicates and independently performed three times

Table 3: Quantitative PCR primers.

Genes	Primers Sequences	Annealing temperature (^{o}C)	Amplicon size (bp)
Cx26	F: CCTCCCGACGCAGAGCAA R: CAGACAAAGTCGGCCTGCTCA	62	175
Cx32	F: GCTCCCCAAGGTGTGAATG R: GCACCATGATTCTGAAGATGAAGAT	58	100
Cx43	F: CTTCACTACTTTTAAGCAAAAGAG R: TCCCTCCAGCAGTTGAG	52	81
Cx45	F: GGAAGATGGGCTCATGAAAA R: GCAAAGGCCTGTAACACCAT	56	200
TLR2	F: GGCTTCTCTGTCTTGTGACC R: GGGCTTGAACCAGGAAGACG	58	271
TLR4	F: CCGCTTCCTGGTCTTATCAT R: TCTGCTGCAACTCATTTCAT	58	128
MMP-9	F: TTGACAGCGACAAGAAGTGG R: GCCATTCACGTCGTCCTTAT	55	158
E-cadherin	F: CAGAAAGTTTTCCACCAAAG R: AAATGTGAGCAATTCTGCTT	58	87
ZO-1	F: CAGCCGGTCACGATCTCCT R: GTGATGGACGACACCAGCG	58	275
GAPDH	F: TGGTGCTCAGTGTAGCCCAG R: GGACCTGACCTGCCGTCTAG	52-62	91

2.2.9 Western blot

Cells were washed with PBS and scraped at 4 °C in lysis buffer (0.5M Tris-HCl buffer, pH 6.8; 2% SDS; 20% glycerol; phosphatase and protease inhibitors). The samples were loaded onto 8-12% SDS-polyacrylamide gel, subjected to electrophoresis, and transferred to PVDF membrane. Following transfer, membranes were blocked with 5% skimmed milk and 0.05% Tween 20 in PBS (TPBS). Primary antibodies were then added for 3 h at RT or overnight at 4 °C. Blots were developed using horseradish peroxidase-conjugated secondary antibody and enhanced chemiluminescence detection kit. Positive and negative controls were performed to evaluate

the specificity of the antibodies used. The intensity of bands, in the linear range of intensity, was quantified using ImageJ software (U. S. National Institutes of Health, USA).

2.2.10 Gelatin zymography

50 µg of IECs proteins extracted from the cells or from the conditioned media of the cells were loaded into a stacking gel with 10% polyacrylamide resolving gel-containing gelatin. 2.5% FBS was used as a positive control to detect pro- and active MMP-2 and MMP-9 enzymatic activities at 72 and 92 kDa, respectively. The gel was washed twice with a wash buffer (water with 2.5% Triton X-100) for 30 min and incubated overnight in a substrate buffer (1M Tris-HCl, pH 8; 0.07% $CaCl_2$ and 0.02% sodium azide) at 37 °C. The gel was then stained with 0.5% Coomassie Brilliant Blue R-250 stain for 1 h followed by a de-staining step using a de-staining buffer (30% ethanol, 10% acetic acid and 60% water) and visualized by Ultra-violet trans illuminator (UPV company, UK); clear bands on a blue background indicate enzymatic activity. Bands were quantified using ImageJ software.

2.2.11 Immunofluorescence of cells

IECs, untransduced or transduced with either Cx26-Dendra2 or Cx43-Dendra2, were cultured on coverslips, fixed with ice-cold methanol and stored at -20 °C. Cells were then washed 3X with PBS, and blocked with 5% NGS in PBS for 1 h in a humidified chamber. Cells were incubated with primary antibody for Cx26, Cx43, E-cadherin, β-catenin and ZO-1 antibodies for 2 h at RT, followed by washing and incubation with IgG-conjugated secondary antibody (Texas red: 1 µg/ml) for 1 h. The cells were then incubated with DAPI (1 µg/ml) for 10

min to stain their nuclei, washed 3X with PBS, mounted on slides using Prolong Anti-fade kit and observed by confocal microscopy.

2.2.12 Immunofluorescence of paraffin-embedded tissues

Tissue sections were obtained from normal and IBD patients. All patients identifiers were kept confidential and no use of identities were utilized in this study. Tissues, 5-μm thick, were immunostained for Cx26, Cx43 E-cadherin, ZO-1, collagen IV and vimentin expression. Sections were heated to 50 °C for 40 min; washed 3X with xylol, and hydrated in a gradient series of alcohol to water. Antigen retrieval was performed by incubating sections in sodium citrate buffer (pH 6.0) and incubated at 100 °C for 40 min. They were allowed to cool for 15 min and then washed 2X with deionized H_2O. The sections were blocked with 5% NGS in PBS for 1 h in a humidified chamber. Sections were incubated with Cx26 and Cx43 antibodies overnight at 4 °C, followed by washing and incubation with IgG-conjugated secondary antibody (Alexa 488: 1 μg/ml) for 1 h. The sections were then washed 2X with PBS, mounted with Prolong Anti-fade, and observed by confocal microscopy.

2.2.13 Exosomes isolation

Exosomes were isolated from cultured supernatants of THP-1 and activated THP-1 cells by differential centrifugations. Briefly, cells seeded at ratio of 3×10^5 per cm^2 for three days. They were then incubated with serum-free media for additional 72 h. After incubation, the supernatants were centrifuged at 300 g for 10 min, 2,000 g for 20 min and 10,000 g for 30 min to remove residual cells and debris. The supernatants were filtered through 0.22-μm filter.

Exosomes were pelleted by ultracentrifugation at 100,000 g for 70 min (Thermo Scientific Sorvall, USA) followed by washing with 1XPBS. Exosomes in PBS were concentrated by micro-ultracentrifugation at 100,000 g for 70 min in an S120-AT2 rotor (Thermo Scientific Sorvall, USA) and re-suspended in 50 µl of 1XPBS. Exosomes were characterized by Scanning Electron Microscope (Tescan Mira 3 MLU, Czech Republic) and Western Blot for exosome markers.

2.2.14 Statistics

Statistical significance was determined by the unpaired Student's t-test. P value is indicated by asterisk or asterisks in the figures: *, ** denotes P <0.05 and P <0.01, respectively. Error bar represents SEM of 3 independent experiments.

CHAPTER 3

Results

3. Results

3.1 Expression of connexins in human colon tissue

In the human colon tissue, Kanczuga-Koda *et al.* 2004 showed the expression the three major connexins: Cx26, Cx32, and Cx43. In our study, we screened for Cx26 and Cx43 expression by immunofluorescence in paraffin embedded tissue sections from normal human intestine. We show that Cx26 and Cx43 are expressed in the epithelial columnar cells in normal colon tissue. Their expression was observed on the membranes of adjacent cells of the crypt (Figure 1B-C). In the colonic mucosa, Cx26 and Cx43 expression was detected at the apical and basolateral surfaces of the epithelial columnar cells (Figure 1E-F).
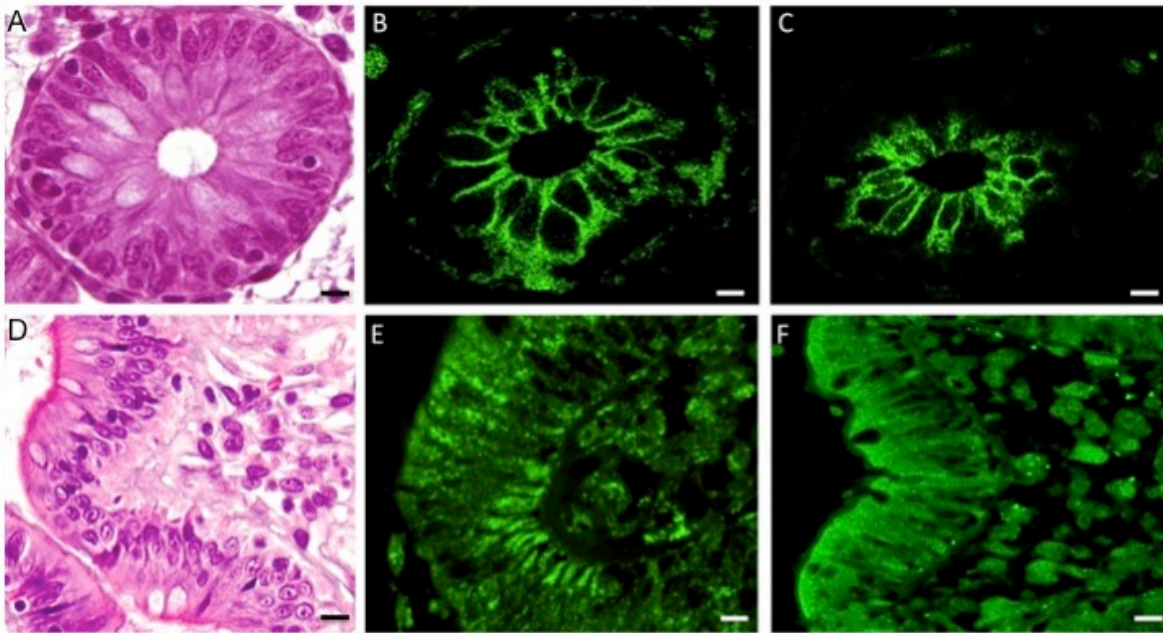

Figure 1: Connexin expression in normal human colon tissue. (A, D) H and E stain of normal tissue. Expression patterns of Cx26 (B, E) and Cx43 (C, F) protein in the crypt (A-C, scale bar 5 μm) and in the epithelium of colonic mucosa (D-F, scale bar = 10 μm).

3.2 Expression and functional analysis of connexins in cultured intestinal epithelial cells

3.2.1 Connexin profiling

In order to determine which Cxs are involved in the coupling between human IECs, screening for the different Cxs at the transcriptional, translational, and cellular localization levels was performed. Connexin expression was assessed in two human intestinal epithelial cell lines: Caco-2 and HT-29. The two cell lines express different levels of Cx26 and Cx43 (Figure 2). Caco-2 cells expressed lower level of Cx26 transcript but similar level of Cx43 transcript as compared to HT-29 cells (Figure 2A). This data is further supported by western blot analysis showing the expression levels of Cxs in Caco-2 cells and HT-29 cells (Figure 2C, D). At the cellular localization level, using immunofluorescence microscopy, we observed the expression and localization of Cx26 and Cx43 in HT-29 cells. However, we could not detect any Cx expression in Caco-2 cells (Figure 2B).
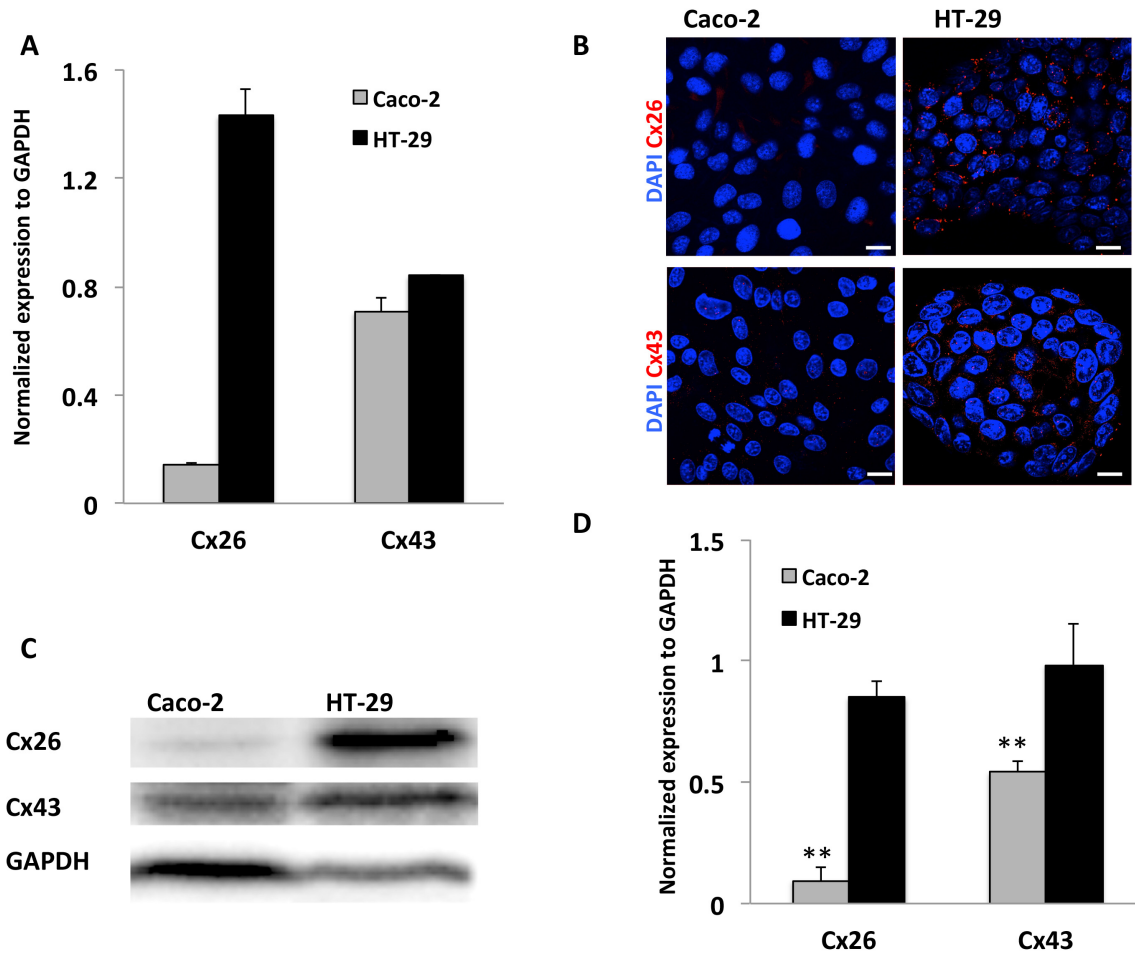
Figure 2: Expression of connexins in IECs. (A) Histogram representing the normalized expression of Cx26 and Cx43 to GAPDH as assessed by qPCR. (B) Cellular localization of Cx, scale bar = 10 μm. (C) Representative western blot of Cx26 and Cx43 expression in IECs. (D) Densitometry analysis of western blots of Cx expression normalized to GAPDH in IECs.

3.2.2 Homo-cellular dye coupling between IECs

Dye transfer and Fluorescence Recovery After Photobleaching (FRAP) assays were conducted to determine the formation of functional homo-cellular gap junction between IECs. Calcein-labeled IECs were co-cultured with unlabeled IECs at 1:1, 1:2, and 2:1 ratio for predetermined time points.

Dye transfer between IECs was evaluated by flow cytometry and mean fluorescence intensity (MFI) was quantified. We observed a shift in fluorescence intensity in unlabeled IECs of both Caco-2 (Figure 3A) and HT-29 cells (Figure 3B). Dye transfer was optimally observed when IEC were co-cultured at a ratio of 2:1 (labeled: unlabeled) for Caco-2 cells and a 1:1 ratio for HT-29 cells. Addition of 100 μM of gap junction–inhibitor, 18 β-GA, reduced the fluorescence of unlabeled IECs confirming that dye transfer occurred through gap junctions (Figure 3A, B).
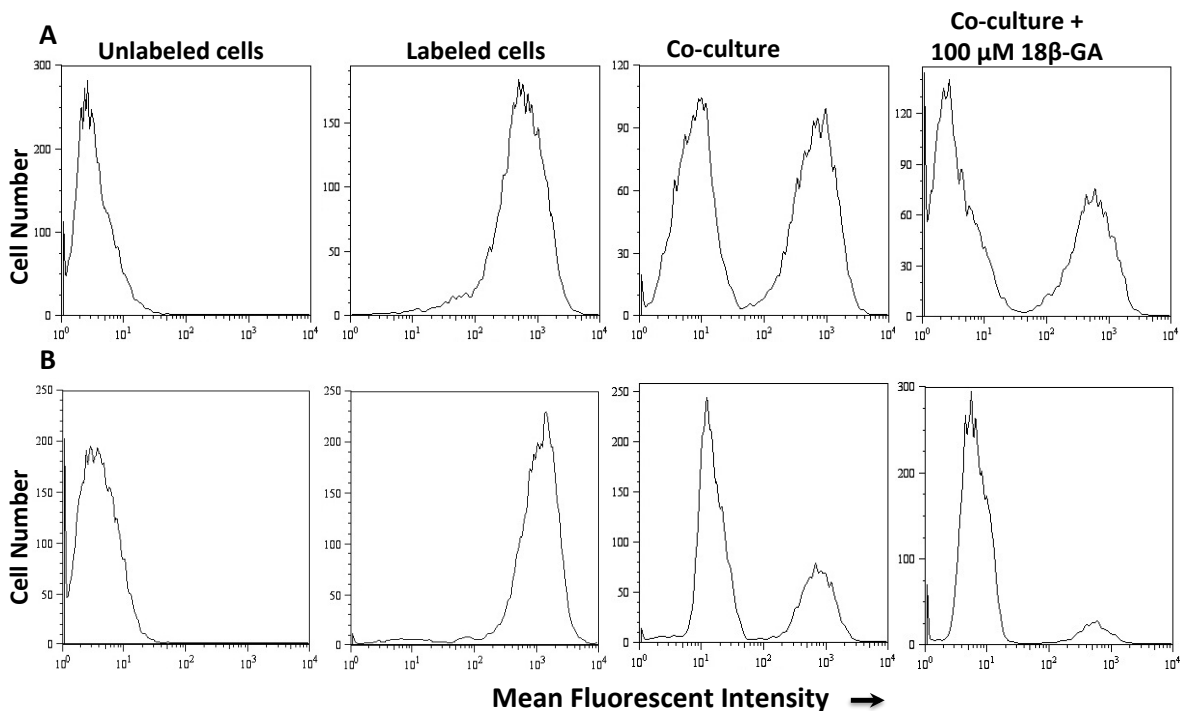

Figure 3: Homo-cellular gap junctional intercellular communication between (A) Caco-2 and (B) HT-29 cells using dye transfer assay. A representative flow cytometry graph where the shift in MFI is shown following co-culture of unlabeled IECs with calcein-labeled IECs; inhibition of this communication is achieved using 100 μM of 18 β-GA.

To further confirm the functionality of connexins in IECs, Fluorescence Recovery After Photobleaching (FRAP) assay was conducted on HT-29 cells. A single cell within the calcein-loaded monolayer was bleached using 488 laser and recovery of fluorescence was recorded immediately after photobleaching for up to 5 min (Figure 4B, C). The target cell recovered up to 50% of it's initial fluorescence intensity within the first 3 min, and almost 100% after 8 min with no significant loss of fluorescence intensity in neighboring cells (reference cells). Pretreating cells with 100 µM of 18 β-GA prevented fluorescence recovery further demonstrating the specificity of the assay and the functionality of the homo- cellular GJ between IECs (Figure 4F, G).
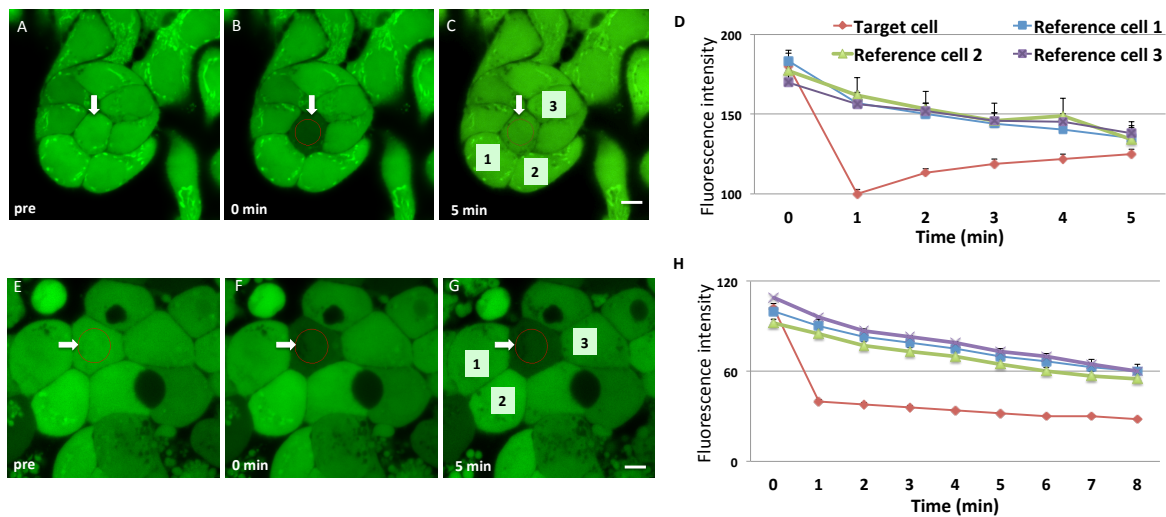

Figure 4: Fluorescence Recovery After Photobleaching of HT-29 cells. (A, E) The white arrow indicates the target cell before bleaching. (B, F) Immediately after bleaching the target cell. (C, G) FRAP of the bleached cell after 5 min. Scale bar = 5 µm. Images captured at a 63x/1.46 Oil Plan-Apochromatic objective. (D, H) Histogram analysis of fluorescent intensity of target cell relative to reference cells of untreated cells (A-C) and treated cells with 100 µM of 18 β-GA (E-G).

3.3 Expression and functional analysis of connexins in the monocyte/macrophage-like (THP-1) cell line

Connexin expression was assessed in the monocytes/macrophages THP-1 cell line at the transcriptional, translational, and functional levels. Our data showed that THP-1 cells expressed Cx26 and Cx43 transcript (Figure 5A) and protein (Figure 5B). Activation of THP-1 cells by PMA and LPS increased the expression of connexins at the transcriptional level but not at the translational level (Figure 5A, B). Functionality of the connexins expressed in THP-1 cells was further assessed by the transfer of calcein dye from unlabeled to labeled THP-1 cells in a co-culture system (Figure 5C).
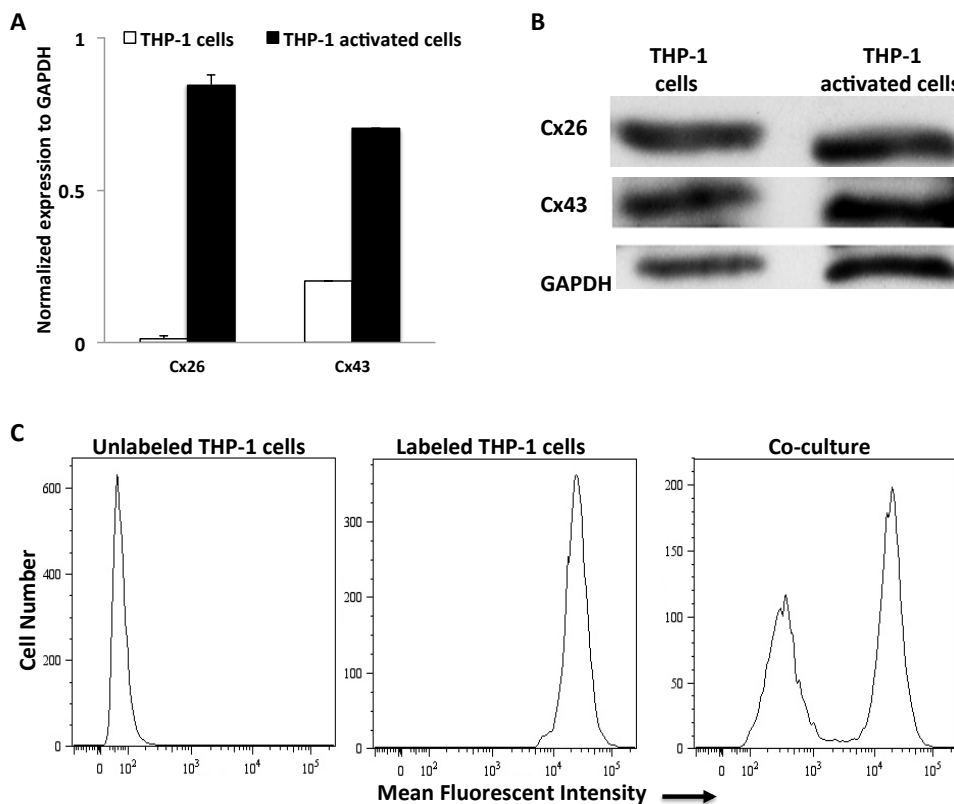

Figure 5: Expression of Cxs in THP-1 cells. (A) Histogram representing the expression of connexins in THP-1 cells normalized to GAPDH assessed by qPCR. (B) A representative western blot showing Cx26 and Cx43 expression. (C) Homo-cellular gap junctional intercellular communication established between THP-1 cells.

3.4 Hetero-cellular communication between IECs and THP-1 cells

3.4.1 Activation of THP-1 cells

To study the interaction between IECs and macrophages, we established an *in vitro* model for IBD using activated THP-1 cells. LPS significantly up regulates TLR2 expression in activated cells THP-1 cells by 4-fold, and TLR4 by 2-fold as assessed by real-time PCR (Figure 6A). To further document the activation of THP-1 cells, the levels of NF-κB p65 (Figure 6C) and COX-2 protein (Figure 6D) levels were determined by western blot. A 5.5- and 10- fold increase in NF-κB p65 and COX-2 protein expression was detected in activated cells, respectively (Figure 6B).
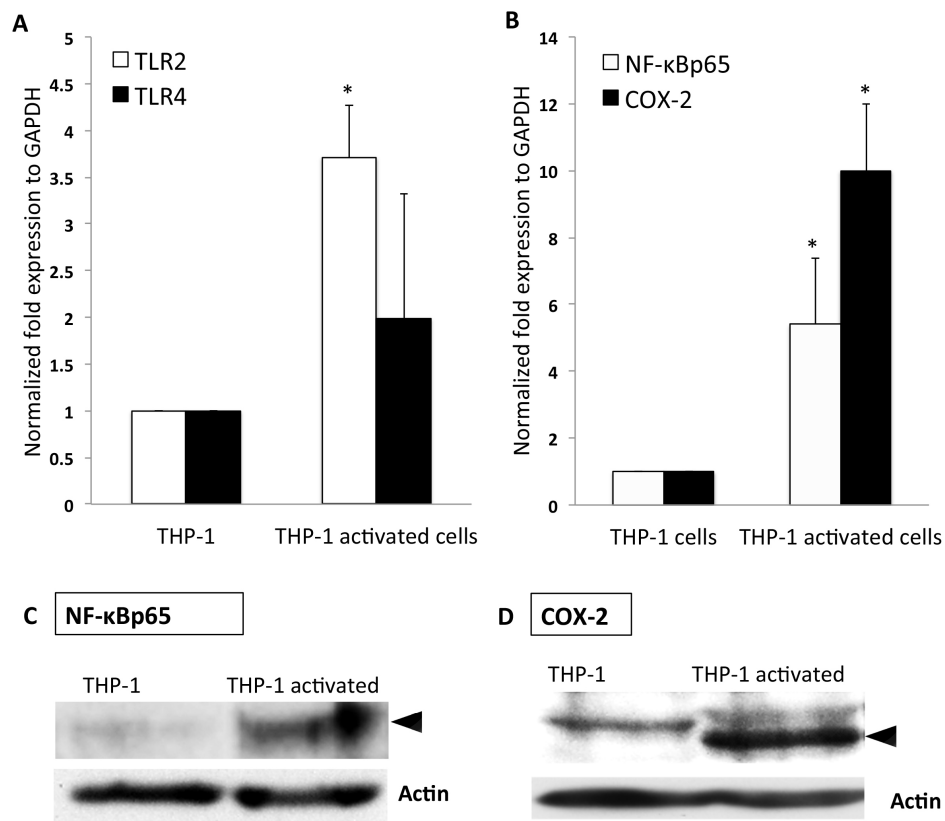

Figure 6: Expression of TLRs, NF-κB p65, and COX-2 monocytes/macrophages THP-1 cell lines. (A) Expression of TLR2 and TLR4 assessed by qPCR. Histogram representing the normalized expression to GAPDH. (B) Densitometry analysis of western blots of NF-κB p65 and COX-2 expression normalized to β-actin in THP-1 cells. (C, D) Representative images of Western blots of NF-κB p65 and COX-2, respectively.

We also investigated the expression of matrix metalloproteinases (MMPs) at the transcriptional level and their zymogenic activity in THP-1 cells. A 2.5-fold and a 20-fold increase in expression of MMP-2 and MMP-9 was detected in activated THP-1 cells, respectively (Figure 7A). The increase in MMP-9 expression at the transcriptional level was accompanied by an increase in its enzymatic activity assessed by gelatin zymography (Figure 7C).
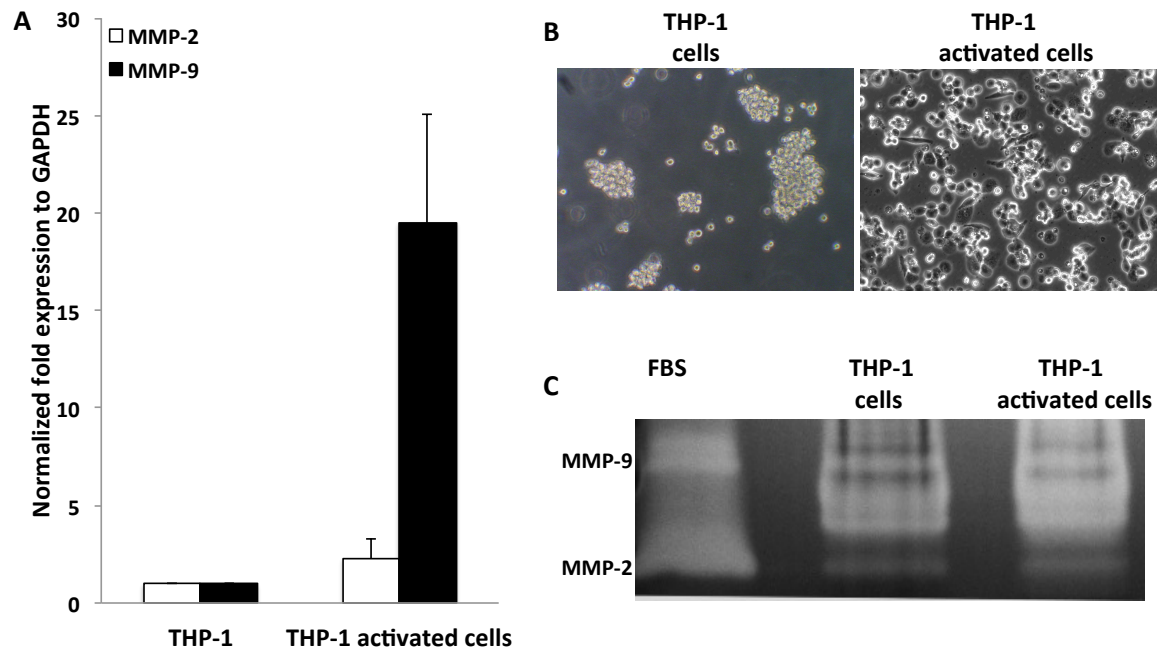

Figure 7: Expression and activity of MMPs in monocytes/macrophages THP-1 cell lines. (A) Histogram representing the normalized expression of MMP-2 and MMP-9 to GAPDH as assessed by qPCR. (B) Bright field images of THP-1 cells before and after activation with PMA and LPS. (C) Representative zymogram of enzymatic activity of THP-1 protein lysates in THP-1 and activated THP-1 cells.

3.4.2 Induction of matrix metalloproteinases in IECs under inflammatory conditions

One of the features of IBD is the activation of MMPs, and increased secretion of MMP-9, which is associated with proteolysis of the extracellular matrix (ECM). To assess the enzymatic activity of MMPs at both the cellular and secreted levels in IECs under inflammatory conditions,

gelatin zymography was performed. IECs were treated with conditioned media from activated

THP-1 cells for 24h, after which cells were washed and incubated with serum-free media for 48

h. We show that THP-1 supernatants (conditioned media contain a pool of inflammatory

cytokines) cause an increase in both the expression and the secretion of MMP-9, but not MMP-

2, as compared to control cells. A significant up regulation in protein expression of MMP-9 was

observed in both cells lines, a 1.7-fold and a 2.5-fold increase in Caco-2 and HT-29 treated cells,

respectively (Figure 8A). MMP-9 secreted levels were also up regulated by a 2.5-fold in Caco-2

treated cells and a substantial 5-fold increase was detected in treated HT-29 cells as compared

to untreated control cell (Figure 8B-D).
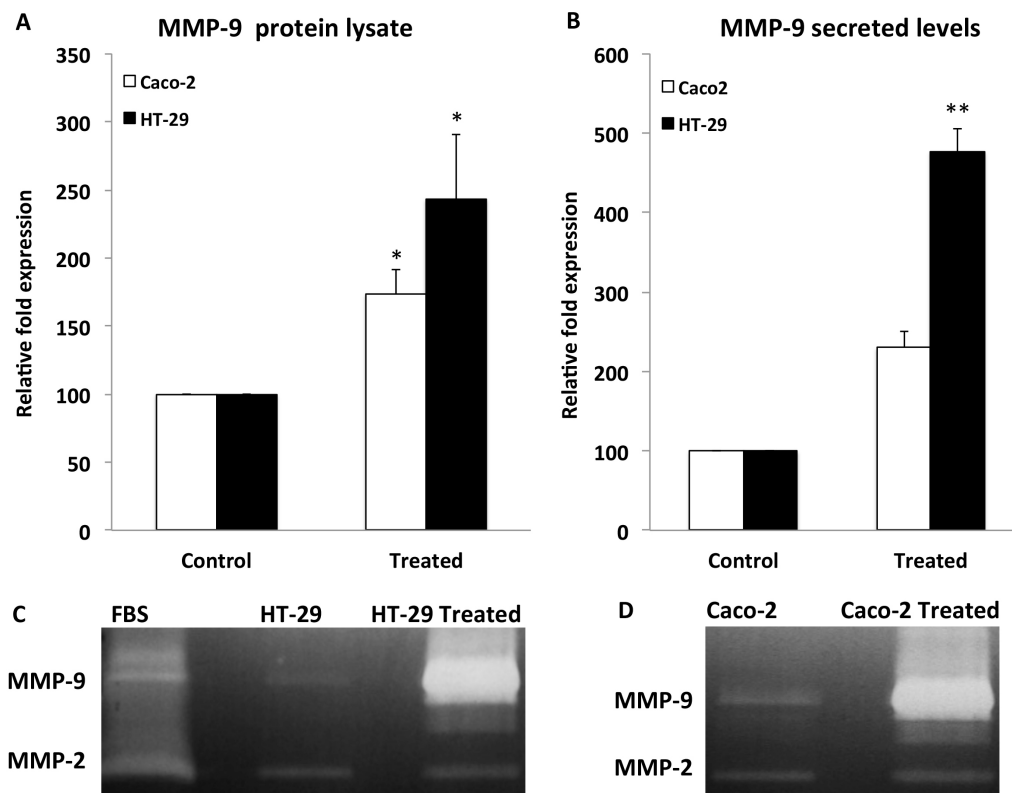

Figure 8: MMP-9 expression and secretion in IECs under inflammatory conditions. (A, B) Histogram analysis of zymogram gels of expressed and secreted MMP-9 in IECs. (C, D) Representative zymogram of secreted MMP-9 in IECs.

We also investigated the expression of TLR9 in IECs under inflammatory conditions. TLR9 is known to mediate inflammatory response to pathogenic bacteria. We demonstrated a significant 8-fold and 3.5-fold increase in TLR9 gene expression in Caco-2 and HT-29 cells treated with THP-1 supernatants, respectively, as compared to controls (Figure 9).
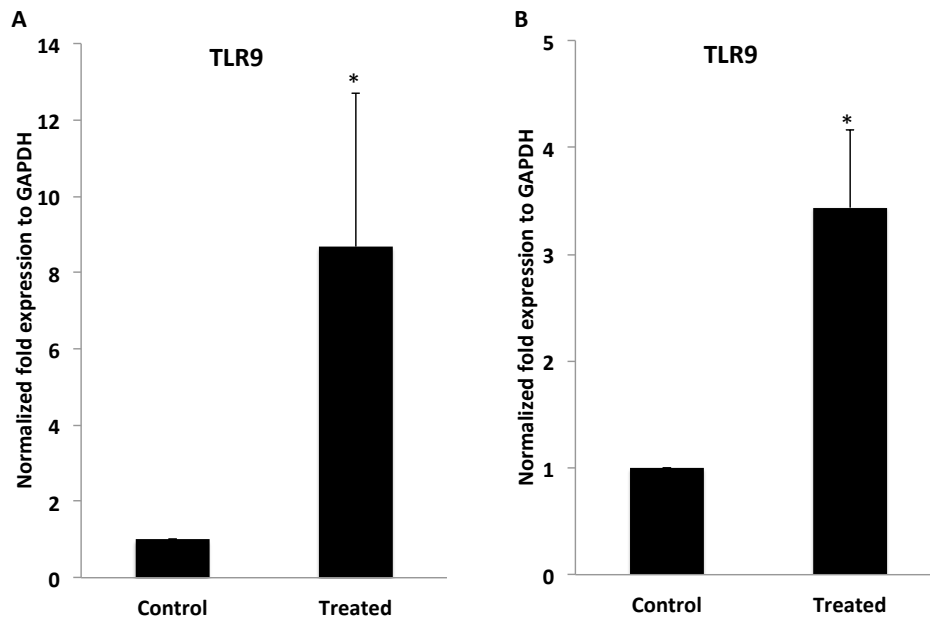

Figure 9: Expression of TLR9 in Caco-2 (A) and HT-29 (B) under inflammatory conditions assessed by qPCR.

3.4.3 Ahesion of IECs to activated THP-1 cells

Co-culture studies were performed between intestinal epithelial cells and macrophages to assess whether hetero-cellular GJIC exists between these cell populations. Dye transfer experiments were conducted between IECs and both non-activated (in suspension) THP-1 cells and activated THP-1 cells (seeded in six-well plates). IECs were seeded on top of activated THP-1 cells, to mimic the cyto-architecture observed in colon tissue. The co-cultures were incubated in complete media at 37 °C and 5% CO_2 for 1 h at a ratio of 1:2 (IECs: activated THP-1 cells). Dye

transfer assay was evaluated by measuring MFI and data was analyzed by dividing MFI over the percentage of adhered fluorescent cells after each co-culture. We show a 2-fold increase in fluorescence in Caco-2: activated THP-1 cells and a significant 10-fold increase in HT-29: activated THP-1 cells as compared to co-cultures with non-activated THP-1 cells (Figure 10B).
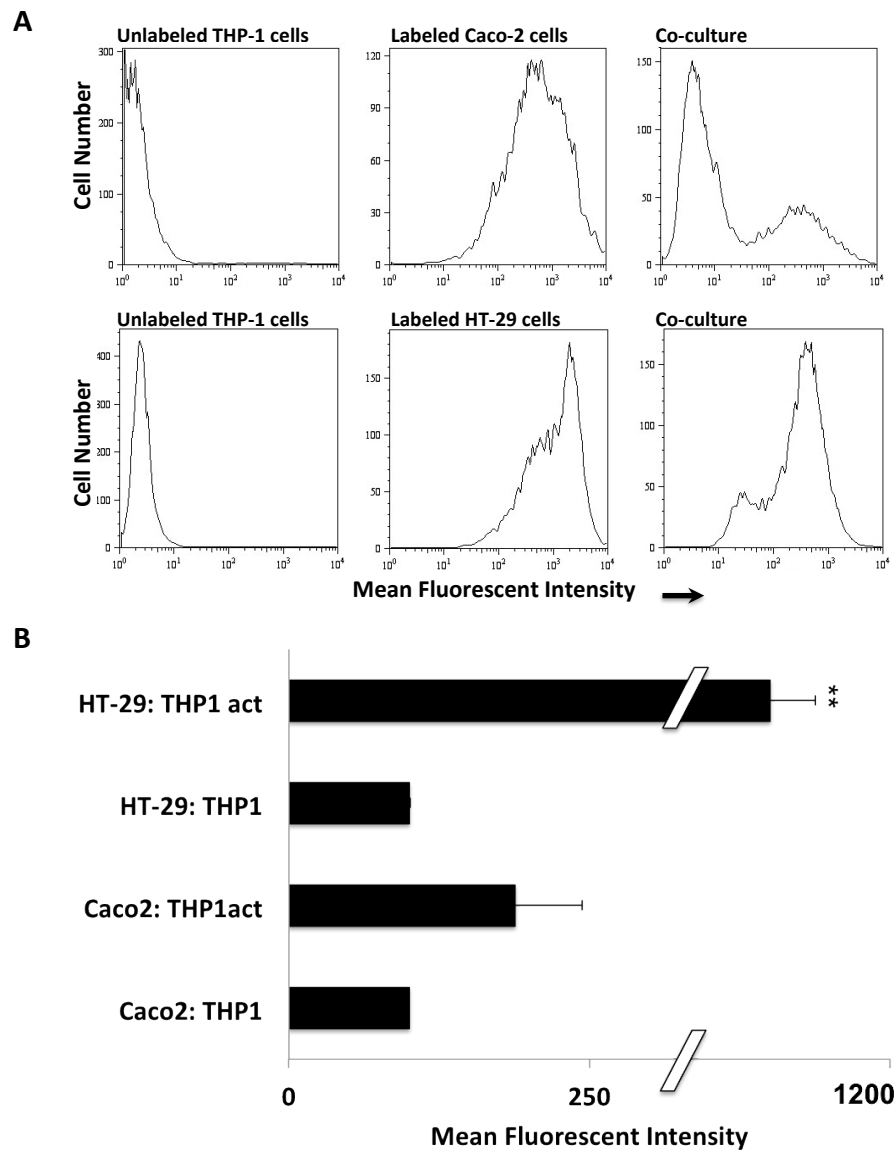

Figure 10: Hetero-cellular gap junction intercellular communication (GJIC) between IECs and THP-1 cells. (A) Dye transfer between IECs and activated THP-1 cells (THP1 act). (B) Histogram represents the flow cytometric analysis of three independent experiments.

3.4.4 Altered expression of connexins in IBD tissues

The data obtained from IECs-macrophages co-cultures *in vitro*, was supported by the expression and localization of Cxs in human tissues from IBD patients. Cx26 and Cx43 expression was diminished at the apical surface and their localization was redistributed to the basal surface of epithelial cells (Figure 11D, F) as compared to normal tissues (Figure 11C, E). We hypothesize that this re-localization of connexins in IBD tissue may facilitate the communication between IECs and infiltrating macrophages. The interaction between the two cell types is achieved through the degradation of the basement membrane mediated by proteolytic enzymes.
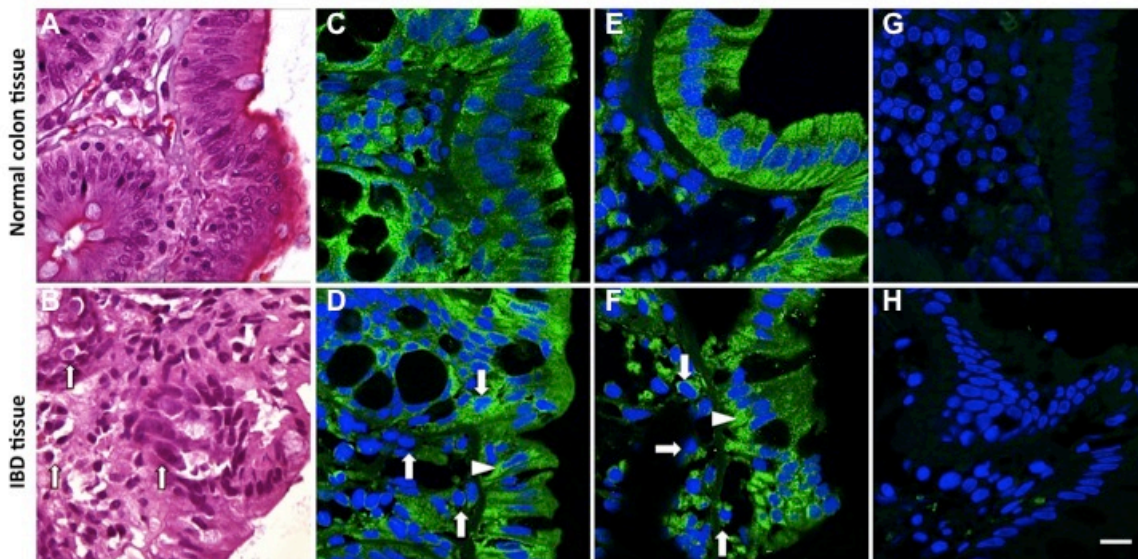

Figure 11: Connexin expression in human colon tissues. (A, B) H and E stain of normal and IBD tissues. Images were acquired with a 100x objective. (C, D) Cx26 expression. (E, F) Cx43 expression; DAPI is a nuclear stain (blue). Arrows indicate infiltration of inflammatory cells into mucosa and arrowheads indicate the expression of Cxs at the basolateral surface of epithelial cells. (G, H) Negative control tissues with no primary antibody, scale bar =10 µm.

To demonstrate the degradation of the basement membrane, we investigated the

expression of collagen IV as the major component of the extracellular matrix. Histological and immunofluorescence staining show that their expression is significantly decreased in IBD tissues as compared to normal tissues (Figure 12). Further, we investigated the expression of vimentin, an intermediate filament protein that play a role in the pathogenesis of IBD. We show that the expression and the distribution of vimentin are altered.
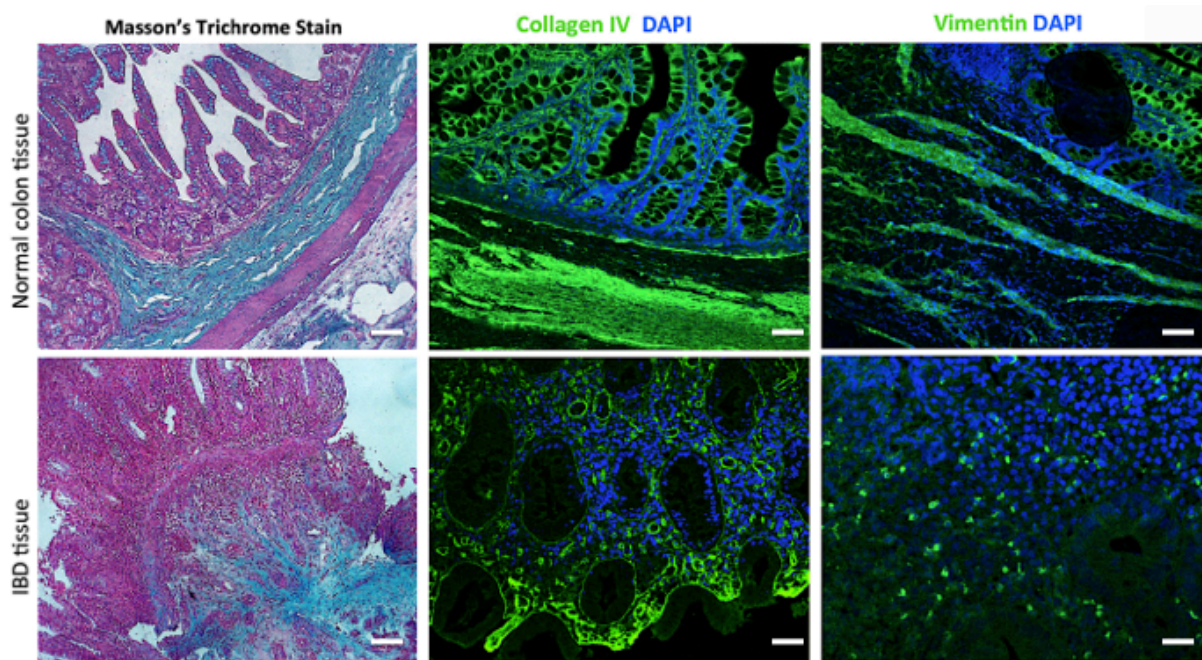

Figure 12: Expression of collagen IV and vimentin in human colon tissue. Sections were stained with Masson trichrome stain for collagen fibers (Blue: Collagen, scale bar = 100 µm). For immunofluorescence staining of collagen IV and vimentin, scale bar = 50 µm.

3.5 Expression and functionality of Cxs-Dendra2 chimeras

We have previously shown that Cx expression in IECs was below detection limits. To compensate for their expression and to study their localization with junctional complexes, we generated Cxs-Dendra2 lentiviral vectors.

3.5.1 Construction of Cx26-Dendra2 and Cx43-Dendra2

Bands corresponding to Cx26-cDNA (700bp) and Cx43-cDNA (1200bp) were excised from the gel, purified, digested with Hind III/BamH1, and ligated to the same digested pDendra2N vector (Figure 13). The clones were confirmed by multiple digests and sequencing with primers which span 5' and 3' joints (Figure 14).
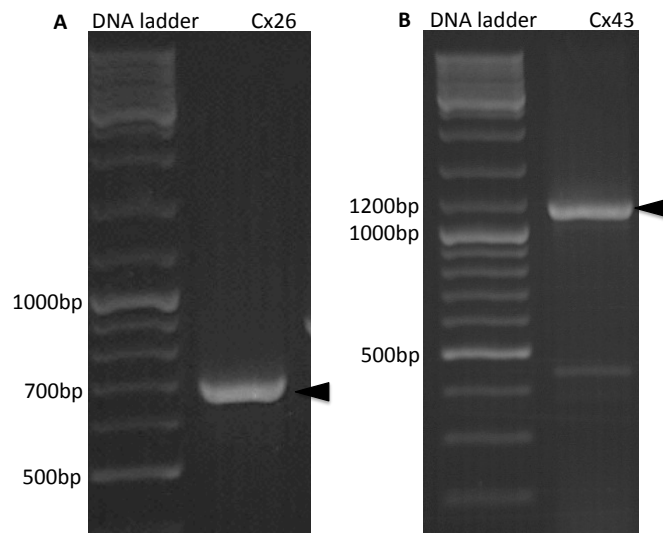

Figure 13: Connexins expression as revealed by PCR. Agarose gel of Cx26 cDNA (A) and Cx43 cDNA (B).
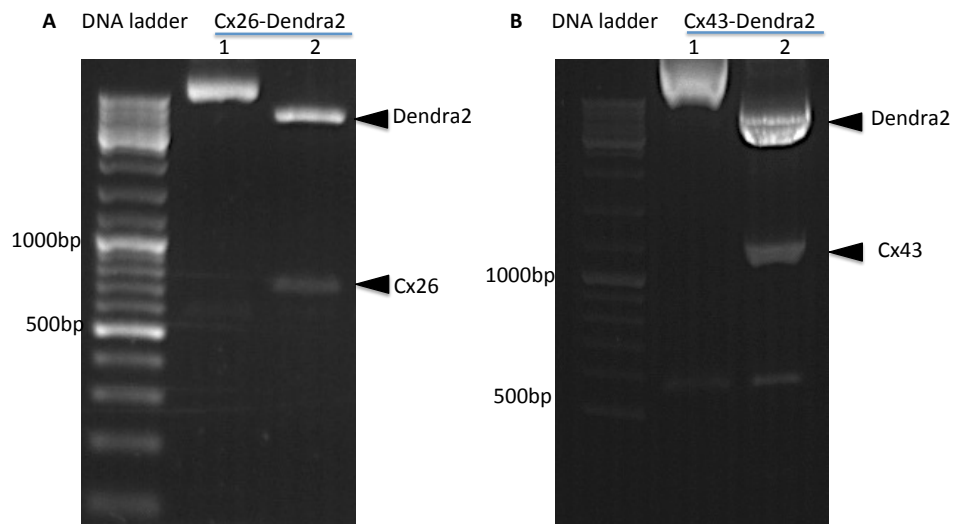

Figure 14: Restriction analyses of Cx-Dendra2 plasmids. Lane 1 represents the undigested Cx26-Dendra2 (A) and Cx43-Dendra2 (B) plasmids. Lane 2 represents the digested Cx-Dendra2 cDNA with restriction

endonucleases BamH1 and Hind III, the upper band corresponds to Dendra2, and the lower band is Cx 26 (A) and Cx43 (B).

To confirm the expression of Cx-Dendra2 constructs, we used communication-deficient cell line (HeLa). HeLa cells were transfected with either Cx26-Dendra2 or Cx43-Dendra2. Forty-eight hour post transfection, the efficiency of transfection was determined by flow cytometry and the cellular localization of connexins was visualized by fluorescent microscopy (Figure 15).
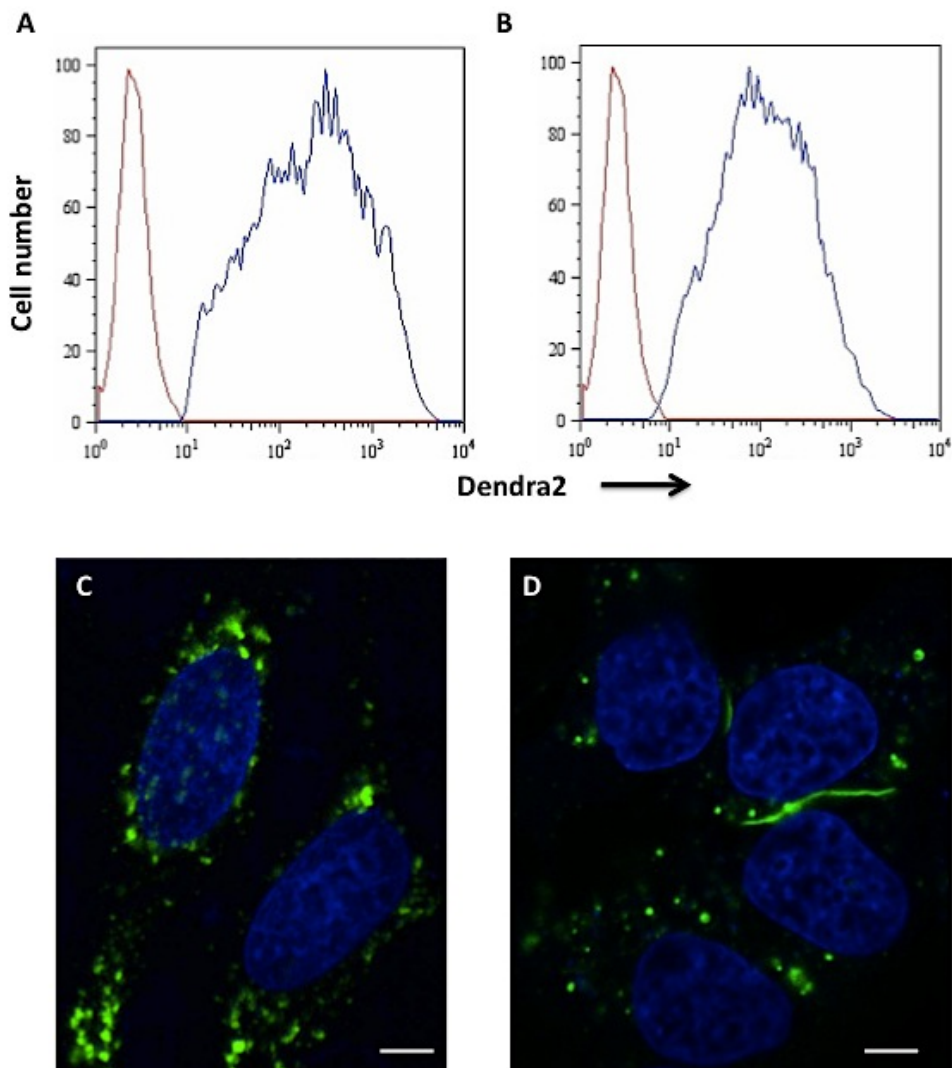

Figure 15: Representative flow cytometric analysis of transfected HeLa cells with Cx26-Dendra2 (A) and Cx43-Dendra2 (B). The red color represents un-transfected controls and blue color represents cells transfected with Cxs-Dendra plasmids. (C) HeLa cells transfected with Cx26-Dendra2 showing connexin

expression around the nucleus, scale bar = 5 μm. (D) HeLa cells transfected with Cx43-Dendra2 demonstrating gap junction plaques between two opposing cells, scale bar = 5 μm.

3.5.2 Construction of Cxs-Dendra2 lentiviral vectors

Bands corresponding to Cx26-Dendra2 cDNA and Cx43-Dendra2 cDNA were excised from the gel, purified, digested with NheI and XhoI, and ligated to the same digested pCSCW vector. As previously described in methods, all positive clones were verified by restriction analysis, and sequenced (Figure 16).

Lanes 1 and 2: Digested CSCW-Cx26Dendra2 Lentiviral vector with Nhe I and XhoI restriction endonucleases

Lanes 3 and 4: Digested CSCW-Cx43 Dendra2 Lentiviral vector with Nhe I and XhoI restriction endonucleases

Lane 5: Undigested CSCW-Cx26Dendra2 Lentiviral vector

Lane 6: Undigested CSCW-Cx43Dendra2 Lentiviral vector
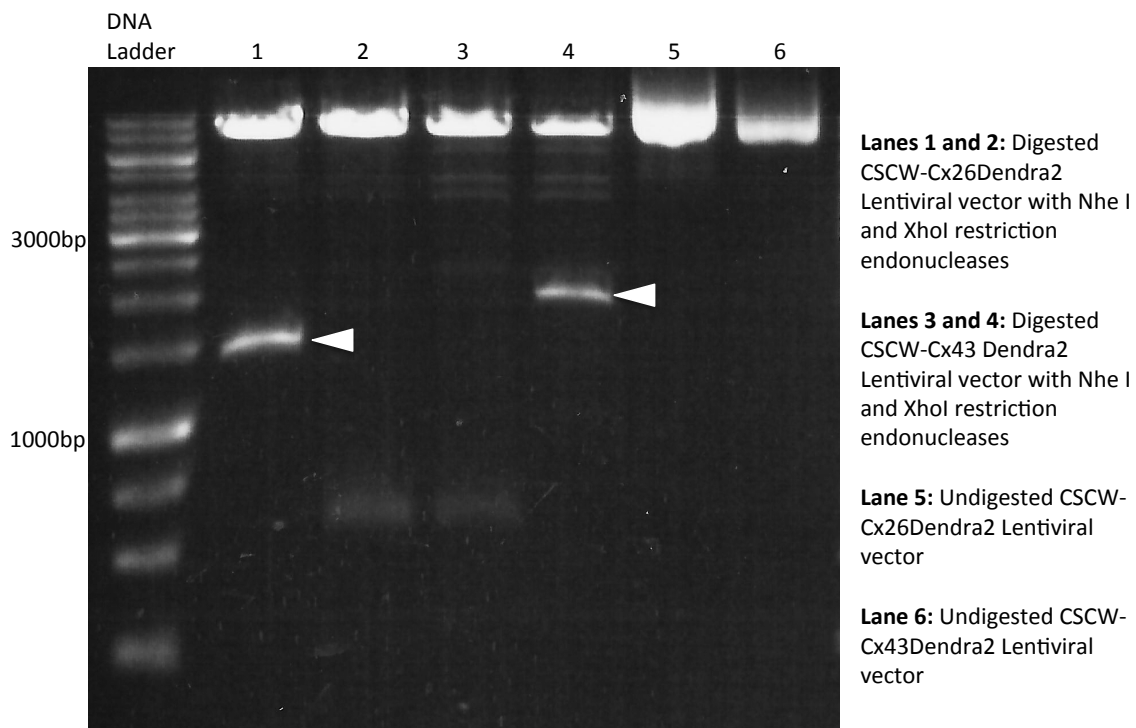
Figure 16: Restriction analysis of CSCW-Cx26Dendra2 Lentiviral vector. Lane 1 and 4 represents the positive colonies for CSCW-Cx26Dendra2 and CSCW-Cx43 Dendra2 Lentiviral vectors, respectively. The upper band corresponds to CSCW plasmid and the lower bands indicated by arrows are Cx26Dendra2 (Lane 1) and Cx43Dendra2 Chimeras (Lane 4). Lane 2 and 3 represent the negative colonies for CSCW-Cx26Dendra2 and CSCW-Cx43 Dendra2 Lentiviral vectors, respectively.

3.5.3 Expression of Cxs-Dendra2 chimeras in HeLa cells and in IECs

HeLa cells and IECs were transduced with either Cx26-Dendra2 or Cx43-Dendra2. Forty-eight hour later, the efficiency of transduction in Caco-2 and HT-29 cells was determined by flow cytometry (Figure 17). HeLa cells and IECs were screened for the presence of exogenous chimeras (Cx26-Dendra2 or Cx43-Dendra2) at both the transcriptional and the translational levels (Figure 18 A, D).
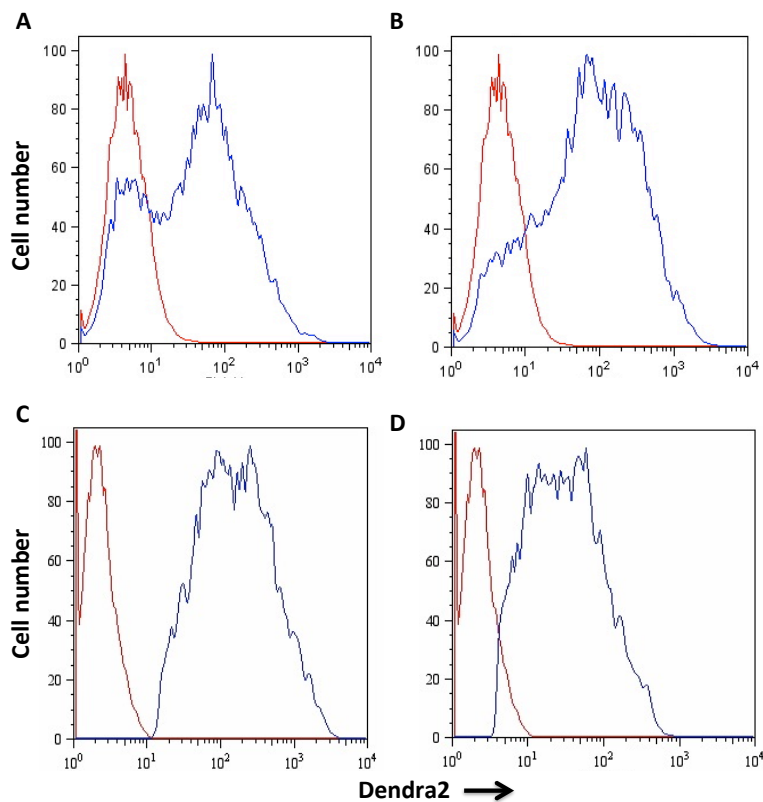
Figure 17: Representative flow cytometric analysis of Caco-2 cells transduced cells with either Cx26-Dendra2 (A) or Cx43-Dendra2 (B). Representative flow cytometric analysis of HT29 cells transduced with either Cx26-Dendra2 (C) or Cx43-Dendra2 (D). The red color represents un-transduced controls and blue color represents cells transduced with Cxs-Dendra2 plasmids.

In addition, we screened for the Cx26-Dendra2 or Cx43-Dendra2 transcripts in IECs at

different time points and revealed that their expression started as early as 6h in both Caco-2

and HT-29 cells (Figure 18 B, C).

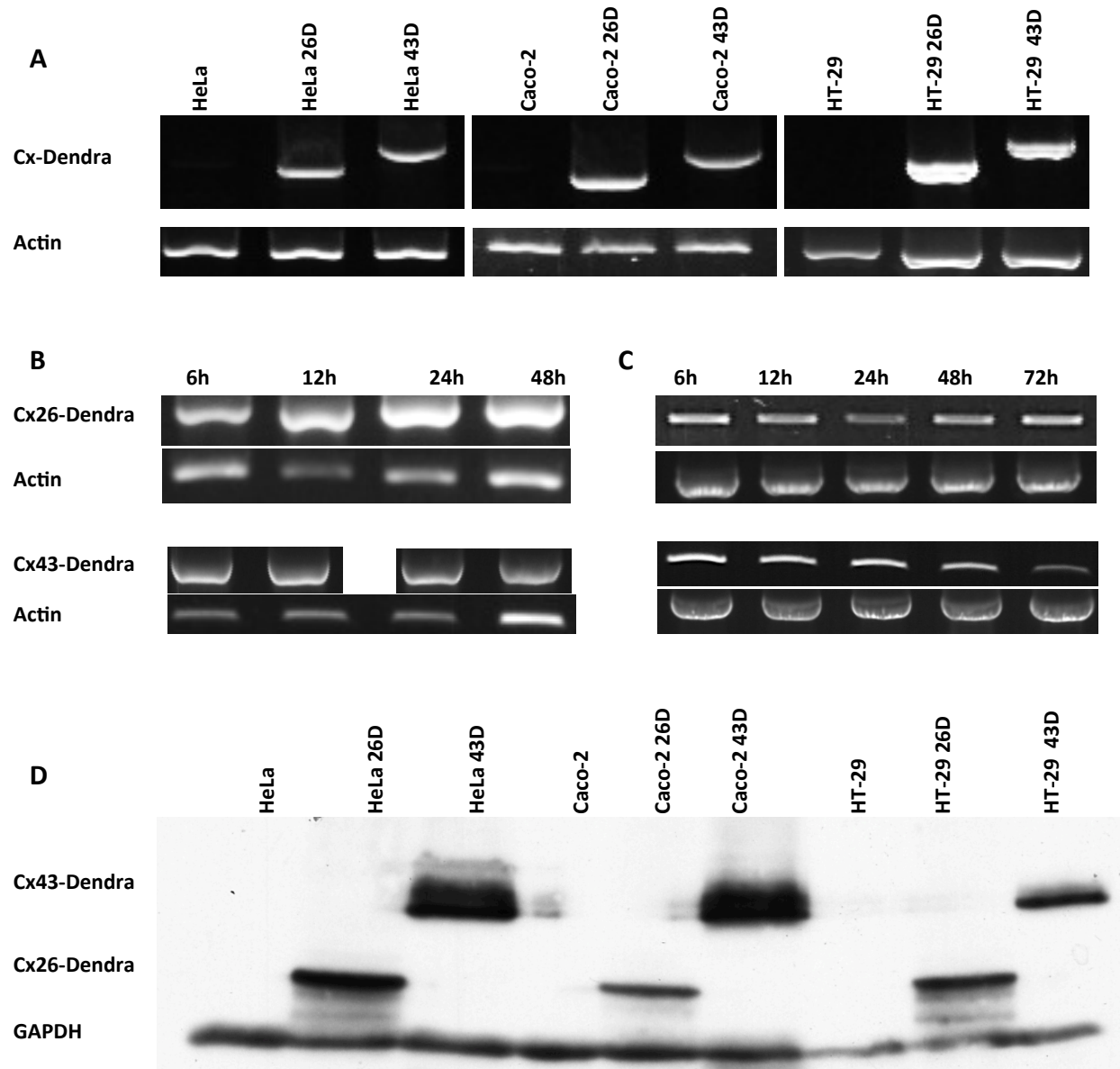**Figure 18:** Expression of Cx26-Dendra2 and Cx43-Dendra2 by PCR in HeLa cells and IECs (A), in Caco-2 cells (B) and HT-29 cells (C) at different time points. (D) Western Blot of Cxs-Dendra2 using Dendra2 antibody confirming the presence of Cx26 (43)-Dendra2 in HeLa cells and IECs, 48 h post transduction. Un-transduced cells are used as negative controls. Abbreviations: 26D, Cx26-Dendra2; Cx43D, Cx43-Dendra2.

3.5.4 Trafficking of Cx26-Dendra2 and Cx43-Dendra2 in Caco-2 cells

To study the intracellular trafficking of connexins and assembly into gap junction, we transduced Caco-2 cells with Cxs-Dendra2 lentiviral vectors. A selected region of Cx26-Dendra2 (Figure 19) or Cx43-Dendra2 protein accumulated at the ER was irreversibly photoconverted to red using a 405 nm laser. We monitored Cx26 (Figure 20) and Cx43 (Figure 21) trafficking from ER to the plasma membrane, where they formed gap junction plaques.
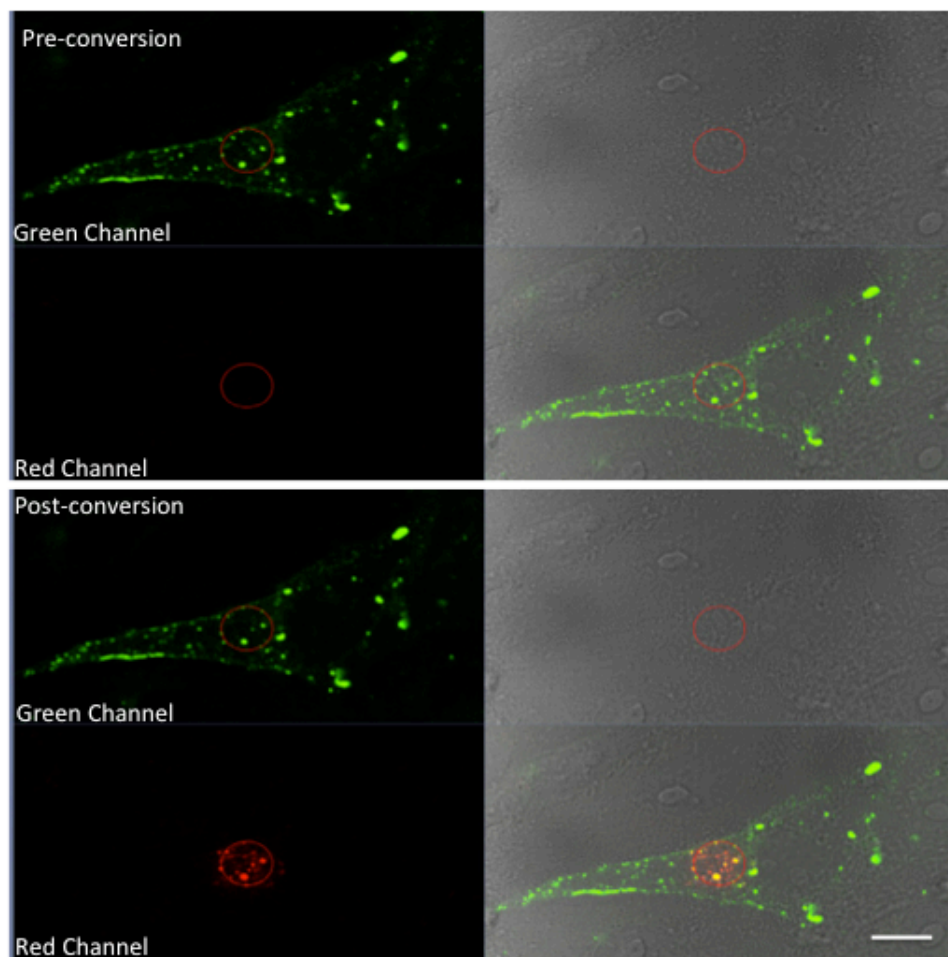

Figure 19: Pre- and post photo-conversion of Cx26-Dendra2 in Caco-2 transduced cells. Scale bar = 5µm.
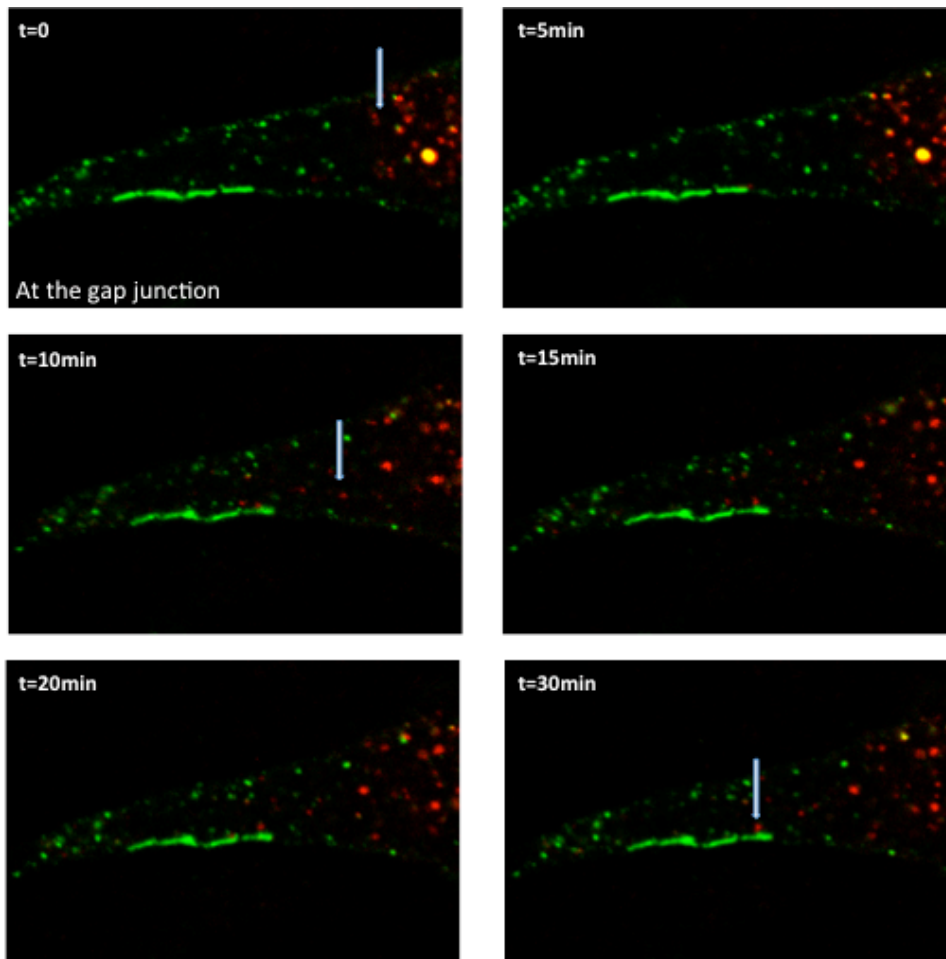
Figure 20: Trafficking of Cx26-Dendra2 from ER to plasma membrane. The arrow indicates a connexin protein.
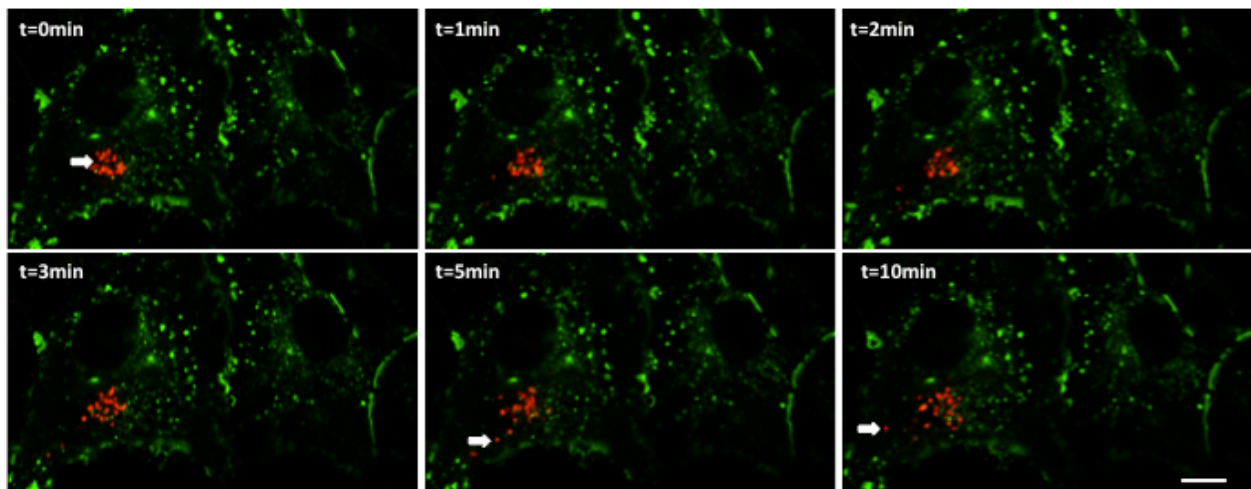

Figure 21: Trafficking of Cx43-Dendra2 from ER to plasma membrane. The arrow indicates a connexin protein. Scale bar = 5μm.

3.6 Regulation of Cxs-Dendra2 expression by treatment with conditioned media from activated THP-1 cells

IECs were transduced with either Cx26-Dendra2 or Cx43-Dendra2 for 24 h and then treated with conditioned media from activated THP-1 cells for an additional 24 h. The expression levels of Cxs-Dendra2 protein were studied by western blot. A significant increase in Cxs-Dendra2 expression was detected in both treated cell lines. A 2.5-fold and a substantial 5-fold increase in Cx26-Dendra and Cx43-Dendra expression was detected in Caco-2 treated cells, respectively (Figure 22A). A significant 10-fold increase of both chimeric proteins was determined in HT-29 transduced treated cells (Figure 22B).
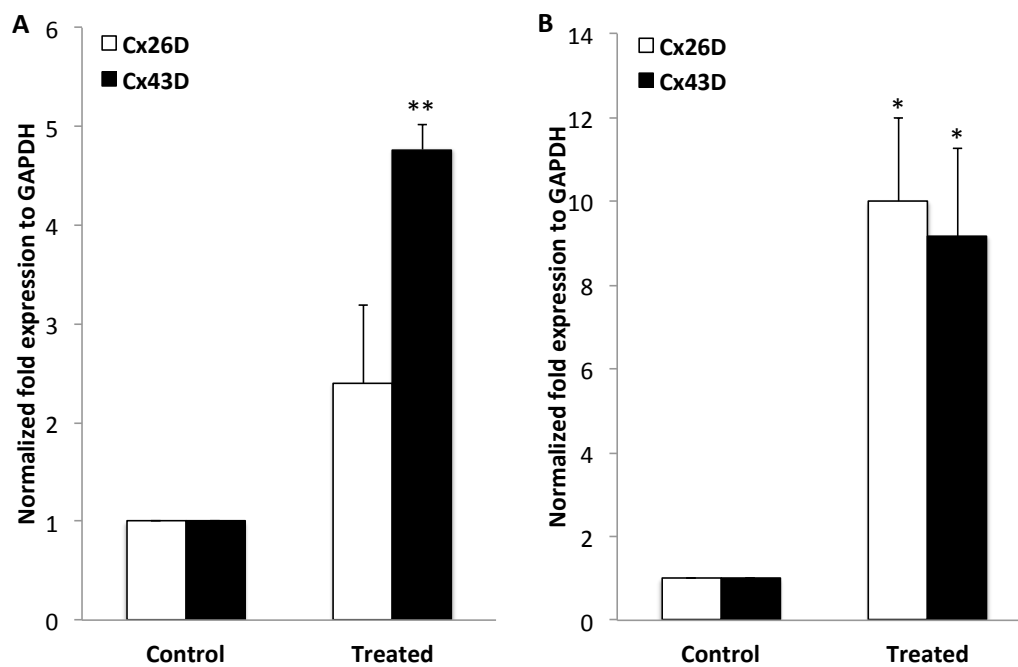

Figure 22: Expression of Cx26 (43)-Dendra at the protein level in (A) Caco-2 and (B) HT-29 transduced cells. Densitometry analysis of western blots of Cxs-Dendra expression normalized to GAPDH in IECs.

In addition, we performed an immunofluorescence assay to study the effect of inflammatory mediators on cellular localization of endogenous Cxs and exogenous Cxs-Dendra2

chimeras. Briefly, Cxs-Dendra2 transduced IECs were either untreated or treated with conditioned media from activated THP-1 cells for 24 h. The cells were then fixed and immunostained for Cx26 and Cx43. In figure 23A, Caco-2 cells were successfully transduced with Cx26-Dendra2 and Cx43-Dendra2, as shown by the punctate dots around the nucleus and by the gap junction plaques between adjacent cells (arrowheads). Treatment of transduced cells with conditioned media from activated THP-1 cells increased the expression of both endogenous Cx26 and Cx43 (red color) and exogenous Cx26 (43)-Dendra2 (green color). Likewise, in figure 23B, Cx26 (43)-Dendra2 chimeras were observed in HT29 transduced cells and treatment with conditioned media from activated THP-1 cells significantly increased the expression of both endogenous Cx26 (43) and exogenous Cx26 (43)-Dendra2.

It is worth noting that treatment of IECs with conditioned media from activated THP-1 cells affected the distribution of connexins (Figure 23A: lower right panel, B: lower left panel). This result supports our data where we have shown a re-localization of Cx to the basal surface of the epithelial cells in IBD tissues.
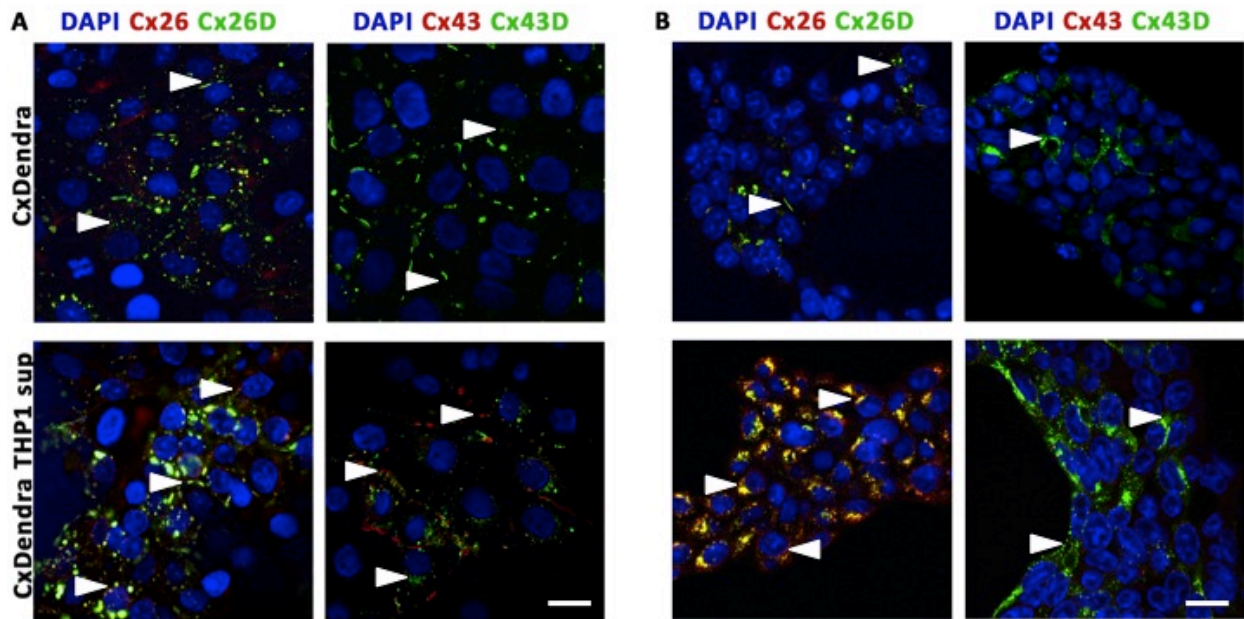
Figure 23: Cellular localization and expression of Cx26 (43) and Cx26 (43)-Dendra2 in (A) Caco-2 and (B) HT-29 cells, scale bar = 10µm.

3.7 Sorting of Cx43 overexpressing Caco-2 cells

Caco-2 cells transduced with Cx43-Dendra plasmids were isolated using a BD FACS Aria SORP cell sorter in the single cell mode. A negative control of non-fluorescent cells was used to determine the background fluorescence. After sorting, the cells were analyzed by flow cytometry for population purity. Approximately 90% of the sorted cells were fluorescent cells (Figure 24). The sorted cells were cultured, expanded and used to study junctional complexes in Caco-2 cells under inflammatory conditions. .
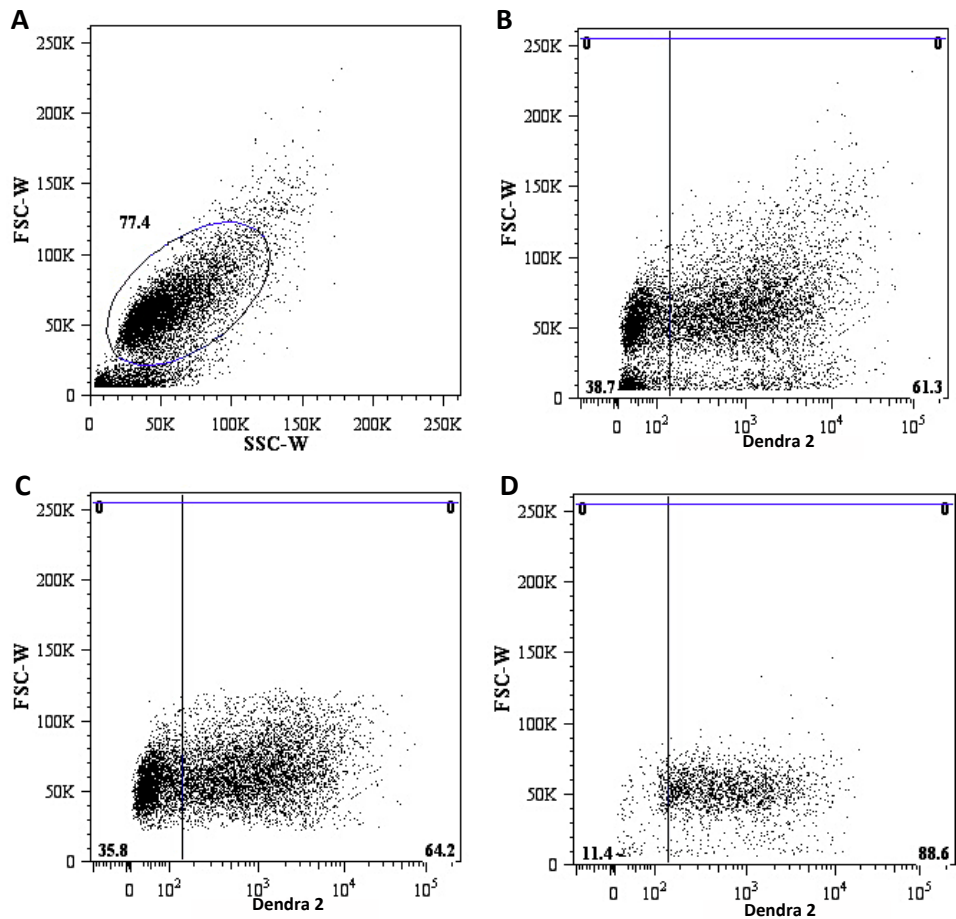
Figure 24: FACS analysis of Caco-2 cells transduced with Cx43-Dendra plasmid. (A) Dot blot of forward scatter (FSC-W) versus side scatter (SSC-W) of the cell population to be sorted. (B) Dot blots of Dendra2 versus FSC of the same population. (C) Selected pre-sorted cells. (D) Sorted cells.

3.8 Loss of junctional complex assembly in treated Cx43 overexpressing Caco-2 cells and IBD tissues

Alteration in the expression of adherens junction, α- and β-catenin, and tight junctions disrupts the epithelial barrier and increases paracellular permeability in IBD. To determine the effect of inflammatory mediators on junctional complexes assembly, immunostaining and western blot assays were performed. Cx43 overexpressing Caco-2 cells were treated with conditioned media form activated THP-1 cells for 24h. Cells were then immunostained for

junctional complexes. We show that Cx43 co-localized with E-cadherin, β-catenin, and ZO-1 at the intercellular junctions in Cx43 overexpressing Caco-2 cells (Figure 25). Expression and co-localization of E-cadherin and ZO-1 was reduced in Caco-2 cells treated with conditioned media from activated THP-1 cells (Figure 25). However, E-cadherin protein levels were not altered while ZO-1 expression was diminished in treated cells as compared to control cells (Figure 26C). β-catenin expression was not altered and no translocation to the nucleus was detected in treated cells, hence, we did not study its expression at the translational level (Figure 25). In parallel, we showed that the protein expression of E-cadherin and ZO-1 was decreased in Cx43 overexpressing Caco-2 cells upon direct co-culturing with activated THP-1 cells (Figure 26C).
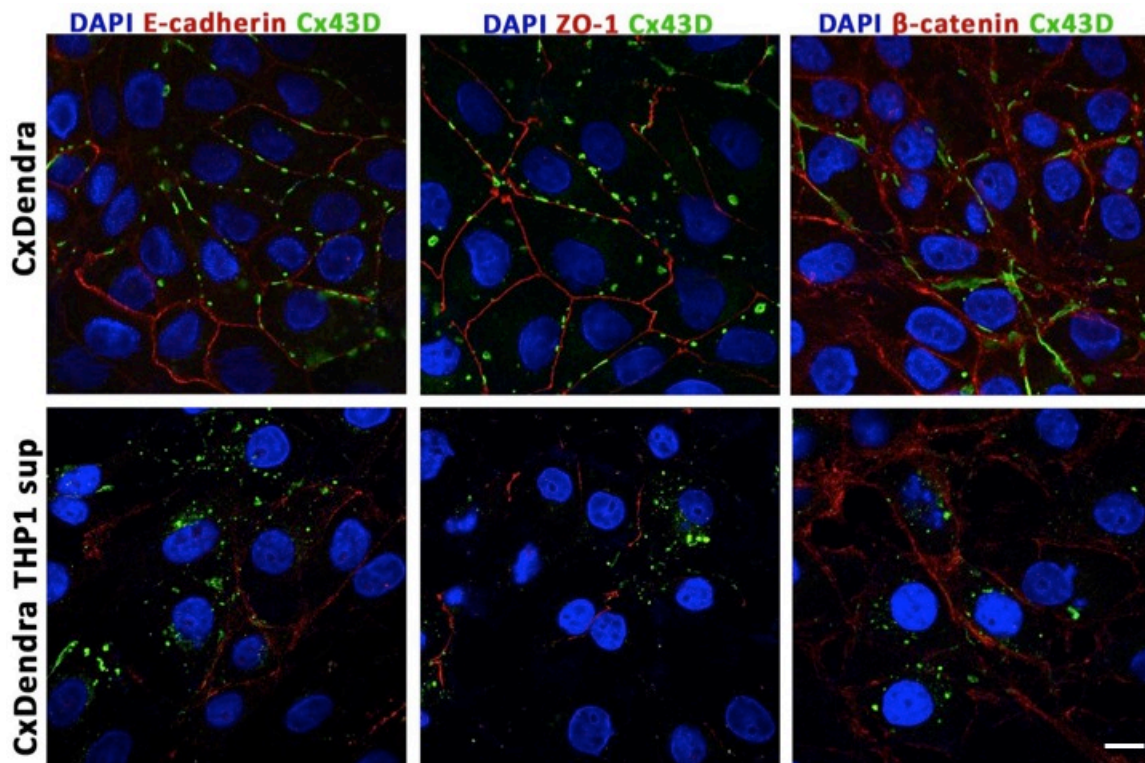
Figure 25: Co-localization images for E-cadherin, ZO-1, and β-catenin in Cx43 overexpressing Caco-2 cells. In treated cells, the expression E-cadherin, ZO-1, and β-catenin is decreased and their localization with Cx43 is lost. Scale bar = 10μm.

Further, we showed by immunofluorescence that E-cadherin (Figure 26A) and ZO-1 (Figure 26B) expression in IBD tissues was decreased and the localization on the apical surface was altered as compared to the normal colon tissues.
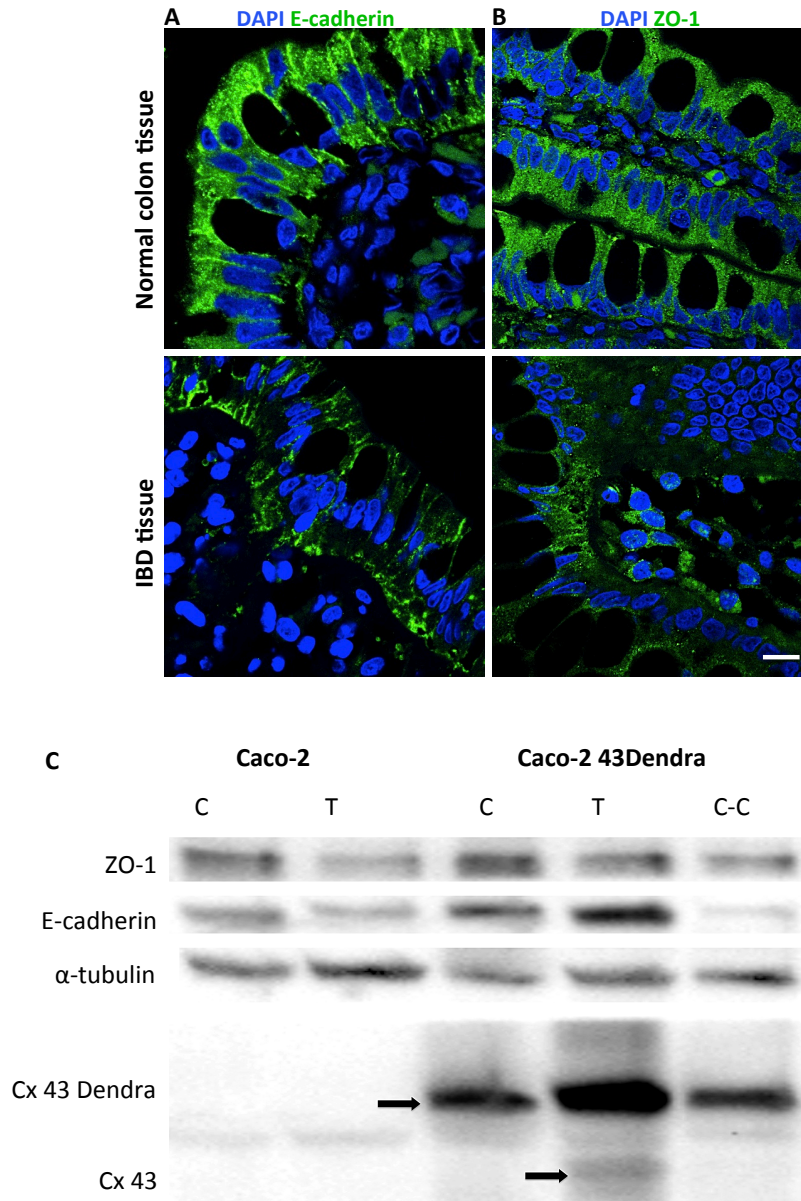
Figure 26: Expression of (A) E-cadherin and of (B) ZO-1 in colon tissues. DAPI as a nuclear stain (blue), scale bar = 10μm. (C) Protein expression of ZO-1, E-cadherin, Cx43 Dendra2, and Cx43 in Caco-2 and Cx43 overexpressing Caco-2 cells (C: Control; T: Treated; C-C: Co-cultured with activated THP-1 cells). α-tubulin used as loading control.

3.9 Regulation of Cxs-Dendra2 chimeras in IECs by exosomes

We have successfully isolated exosomes from culture supernatants of both non-activated and activated THP-1 cells. We characterized the exosomes by SEM and by Western Blot assays. Exosomes isolated from both cells were around 100nm in diameter (Figure 27A, B). Western blot data revealed the expression of the cell surface marker TSG-101 (Figure 27C). No change in endogenous Cx26 and Cx43 protein expression levels upon co-culturing of IECs with exosomes obtained both non-activated and activated THP-1 supernatants.
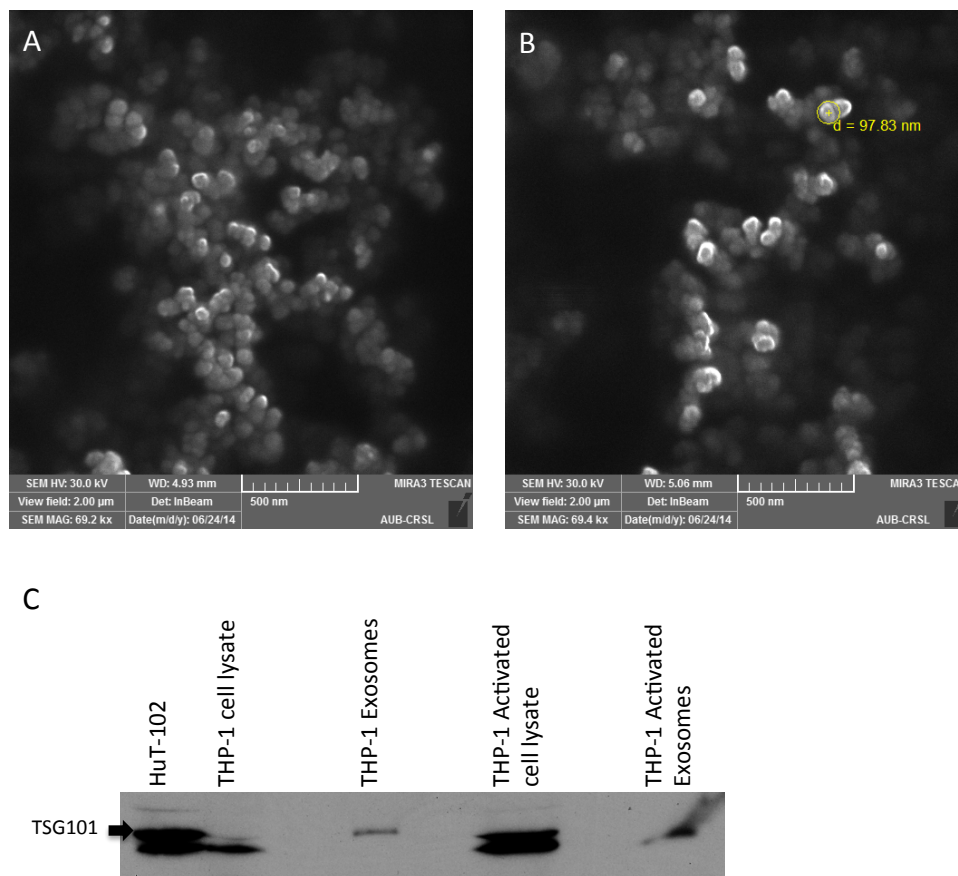
Figure 27: Characterization of exosomes derived from THP-1 cells. Scanning Electron microscope images of exosomes isolated from (A) non activated THP-1 cells and (B) activated THP-1 cells. (C) Western blot of cells and their purified exosomes probed for TSG101. HuT-102 cells are used as positive controls.

We further examined the effect of exosomes from activated THP-1 cells on the expression of intercellular junctional complexes at the transcriptional level in Cx43 overexpressing Caco-2 cells. We show that activated exosomes increase the expression of Cx26 and Cx43 with no change in the expression of either ZO-1 or E-cadherin as compared to control (Figure 28). However, cells treated with exosome free supernatants from activated THP-1 cells decreased the expression of Cxs, ZO-1 and E-cadherin as compared to the control (Figure 28).
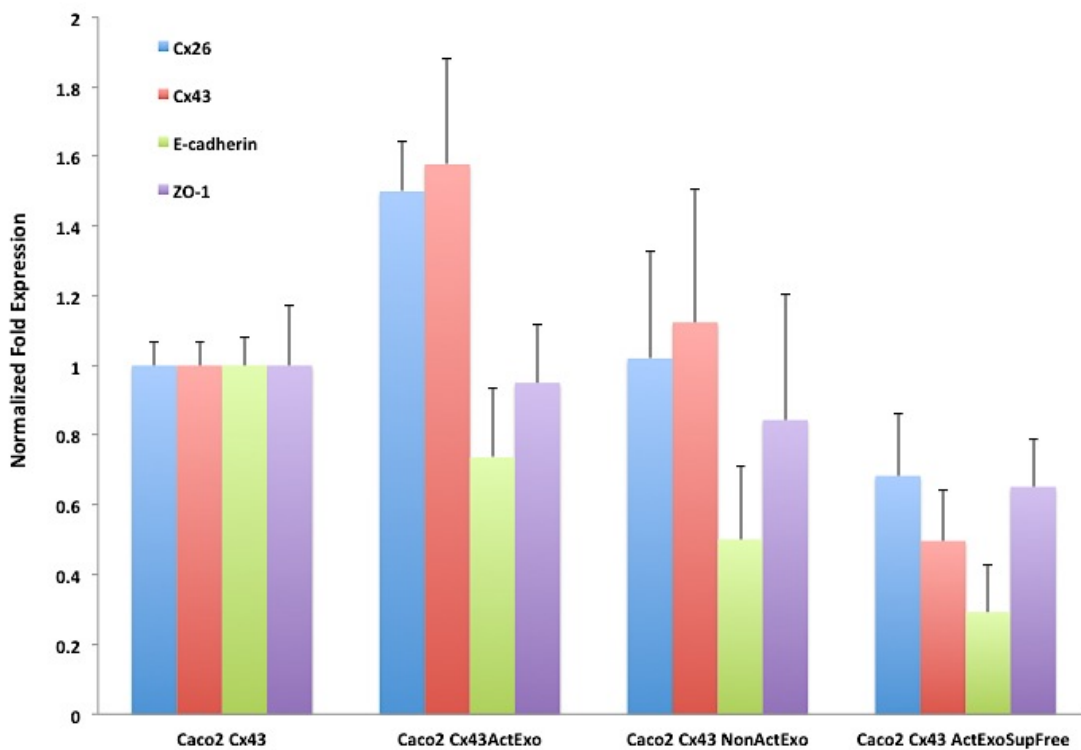
Figure 28: Expression of Cx26, Cx43, ZO-1, and E-cadherin in Cx43 overexpressing Caco-2 treated with exosomes. Histogram represents the normalized expression to GAPDH. Abbreviations: ActExo, Exosomes isolated from activated THP-1 cells; NonActExo, Exosomes isolated from non-activated THP-1 cells; ActExoSupFree, Supernatant exosomes free from activated THP-1 cells.

It is worth noting that treating cells with conditioned media from activated THP-1 cells increased the expression of ZO-1, E-cadherin, and Cxs as compared to untreated cells (Figure 29).

Figure 29: Expression of Cx26, Cx43, ZO-1, and E-cadherin in Cx43 overexpressing Caco-2 treated with conditioned media from activated THP-1 cells. Histogram represents the normalized expression to GAPDH.
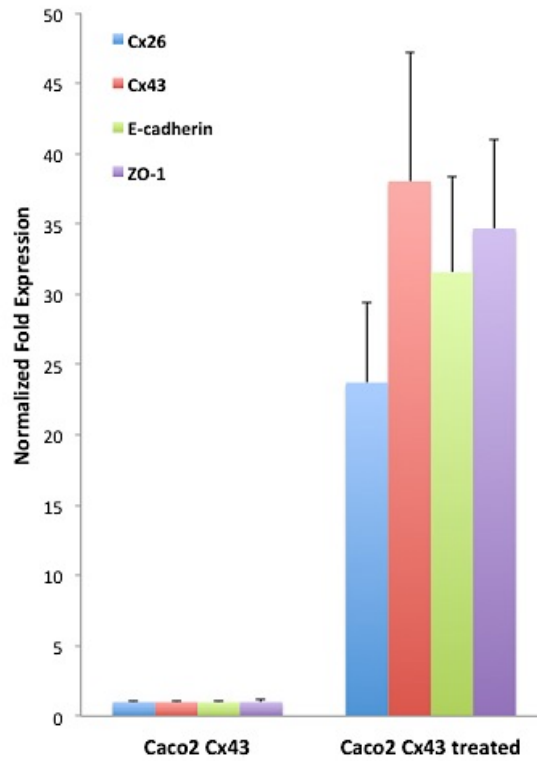
CHAPTER 4

Discussion

4. Discussion

Under normal conditions, the intestine displays a low-grade physiological inflammation, which is clinically silent. Inflammation, however, could be the product of either a large antigen load that overwhelms the immune system or an antigen that is resistant to the immune response or due to inappropriately prolonged, amplified or dysregulated immune response (1-3). Several studies have demonstrated the regulation of the epithelial layer by its immediate microenvironment (4-8). However, the ability and direct role of cells of the monocyte/macrophage lineage in regulating the epithelial physiology during the inflammatory state has not been elucidated yet. In the gastrointestinal mucosa, there are resident un-stimulated macrophages, which are strategically located in the sub-epithelium at sites of entry (9). Under pathological conditions such as IBD, immune cells infiltrate the submucosa, juxtaposed to the epithelial lining of the intestine (10). This close proximity of immune cells to epithelial cells suggests that a direct interaction between these two cell types could exist. Many studies have investigated this interaction in different tissues *in vitro* (11-15). Martin *et al.* showed that murine macrophages interact with intestinal epithelial cells through gap junctions, which provide means by which inflammatory cells might regulate IECs function (11-12). Sharma *et al.* demonstrated a direct interaction between alveolar macrophages and alveolar epithelial cells that contributes to the initiation of acute pulmonary injury *via* a pro-inflammatory cascade (13). Further, a study conducted by Khan *et al.* revealed that the direct interaction between HT-29 and tumor infiltrating leukocytes isolated from colorectal cancer increases the invasive properties of HT-29 (15).

In the present study, we hypothesized that a hetero-cellular interaction between human IECs and macrophages plays an essential role in the regulation of intestinal epithelial barrier. We screened for connexin expression in normal colon tissue, in two IECs (Caco-2 and HT-29) and in the monocyte/macrophage cell line (THP-1). We showed that the normal colon tissue expresses both Cx26 and Cx43 between epithelial columnar cells in the crypt and in the epithelium of colon mucosa. We demonstrated that IECs and THP-1 cells express Cx26, Cx30, Cx43, and Cx45; however, Cx32 is only expressed in IECs (Figure 1).
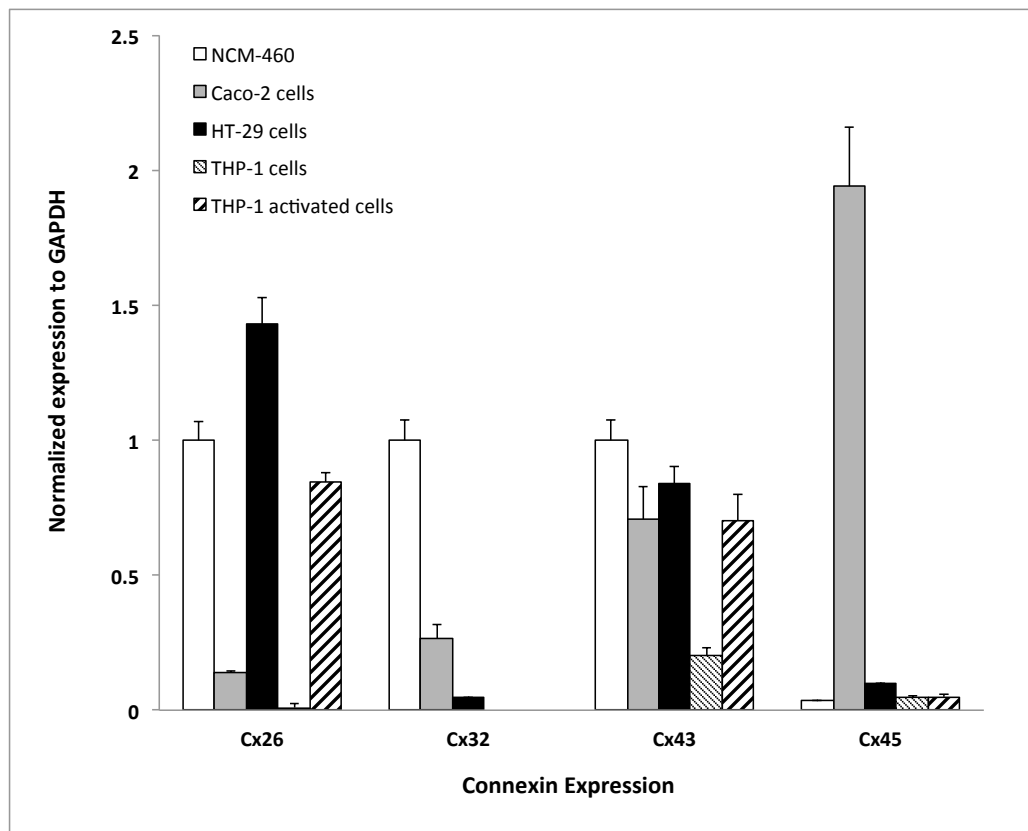

Figure 1: Connexin expression in cultured intestinal epithelial cells and macrophages. Connexin expression was assessed at the transcriptional levels in three human intestinal epithelial cell lines: NCM-460, Caco-2 and HT-29 and in the monocytes/ macrophages THP-1 cells.

We chose to focus our study on Cx26 and Cx43, for two main reasons: first, Cx26 and Cx43 have different trafficking pathways that allow for distinct interactions with connexin binding proteins, and second due to the demonstrated similarity between Cx43 and Cx45 channel characteristics. We compared the connexin expression in Caco-2 and HT-29 cells to a normal colon cell line NCM-460. We found that Cx26 expression level (both the transcriptional and translational) in Caco-2 is low as compared to NCM-460 and HT-29 cells. Connexin 43 transcript expression level is similar in all the three cell lines; however, Cx43 protein level is lower in Caco-2 cells as compared to both cell lines. We did not pursue working with NCM-460 cell line, because it is not well characterized and its use as *in vitro* model of IBD is not well established. Earlier studies report the lack of Cx43 expression in HT-29 cells, and low expression of Cx26 and Cx43 in Caco-2 cells (16-18). Studies have also shown the expression of Cx43 expression in monocytes (19). We then demonstrated that connexins expressed in Caco-2 and HT-29 cells form functional homo-cellular GJ, and this direct cell-cell communication was reduced in the presence of GJ inhibitor as shown in dye transfer and FRAP assays.

Inflammatory cytokines secreted by activated macrophages play a crucial role in the regulation of IBD. To study the effect of inflammatory mediators on cell-cell communication, we established an *in vitro* model for IBD using activated THP-1 cells. We showed that TLR2, and TLR4 gene expression as well as COX-2 and NF-κB p65 protein expression were up regulated in activated THP-1 cells (22-23). We also revealed that MMP-9 gene expression and enzymatic activity were increased in activated THP-1 cells emphasizing their role in inflammation. Conditioned media from activated THP-1 cells, which contain a pool of inflammatory cytokines induce IECs MMP-9 enzymatic activity presumably facilitating the breaching of the sub-

epithelial basement membrane and bringing activated THP-1 cells in close proximity with IECs. Our results on the increased activity of MMP-9 upon inflammatory stimulus are consistent with published data in IECs and colon tissues, implicating the role of MMPs in the pathogenesis of IBD (32-34). As a consequence, IECs adhere to THP-1 cells and a hetero-cellular communication is established. This communication was evident by dye transfer assays where a fluorescent calcein dye was transferred from labeled IECs to unlabeled THP-1 cells. Few studies have reported the establishment of functional GJs between macrophage and epithelial cells and highlighted their role in inflammation (20, 21).

It is well established that the expression of receptor/ligand pair that mediates adhesion between two cell types is required for the assembly of gap junction channels (24, 25). In this study, we revealed that the dye coupling between IECs (Caco-2 or HT-29) and THP-1 activated cells was increased as the adhesion between these two cell types increased. We supported our hypothesis of hetero-cellular communication between human IECs and macrophages by showing that connexin expression (Cx26 and Cx43) in IBD tissues is re-localized to the basolateral surface of epithelial cells as compared to normal tissue. We suggest that this redistribution of Cx expression facilitates the interaction of IECs with the infiltrated macrophages through formation of functional GJ.

We further investigated the effect of inflammatory mediators on the connexin expression and localization with junctional complexes by overexpressing connexins in IECs. We showed that Cx43 co-localize with E-cadherin, β-catenin, and ZO-1 at the intercellular junctions in Cx43 overexpressing Caco-2 cells. However, this association was lost under inflammatory conditions

as assessed by immunofluorescence and western blot assays. We further examined the localization of E-cadherin and ZO-1 in IBD tissues and showed an alteration in the expression of both proteins. These results are consistent with earlier reports describing the loss of junctional complexes under inflammatory conditions in IBD patients (21, 26, 27).

The widespread expression of gap junctions reflects the diversity of their function. They play a critical role in the development, differentiation, growth and repair of many tissues (28-31). In the present study, we provide evidence that macrophages form functional gap junction channels with IECs. Connexin 26 and Cx43 expression, and MMP-9 enzymatic activity is increased under inflammatory conditions. Collectively, we propose that the combination of paracrine and hetero-cellular communication between IECs and macrophages plays a pivotal role in the regulation of epithelial cell function by establishing junctional complexes between inflammatory cells and IECs that might contribute to the dysregulation of intestinal epithelial barrier as summarized by our model in figure 2. Further studies into the role of gap junctional communication in IBD can highlight the potential targeting of connexins as a therapeutic agent for this disease.
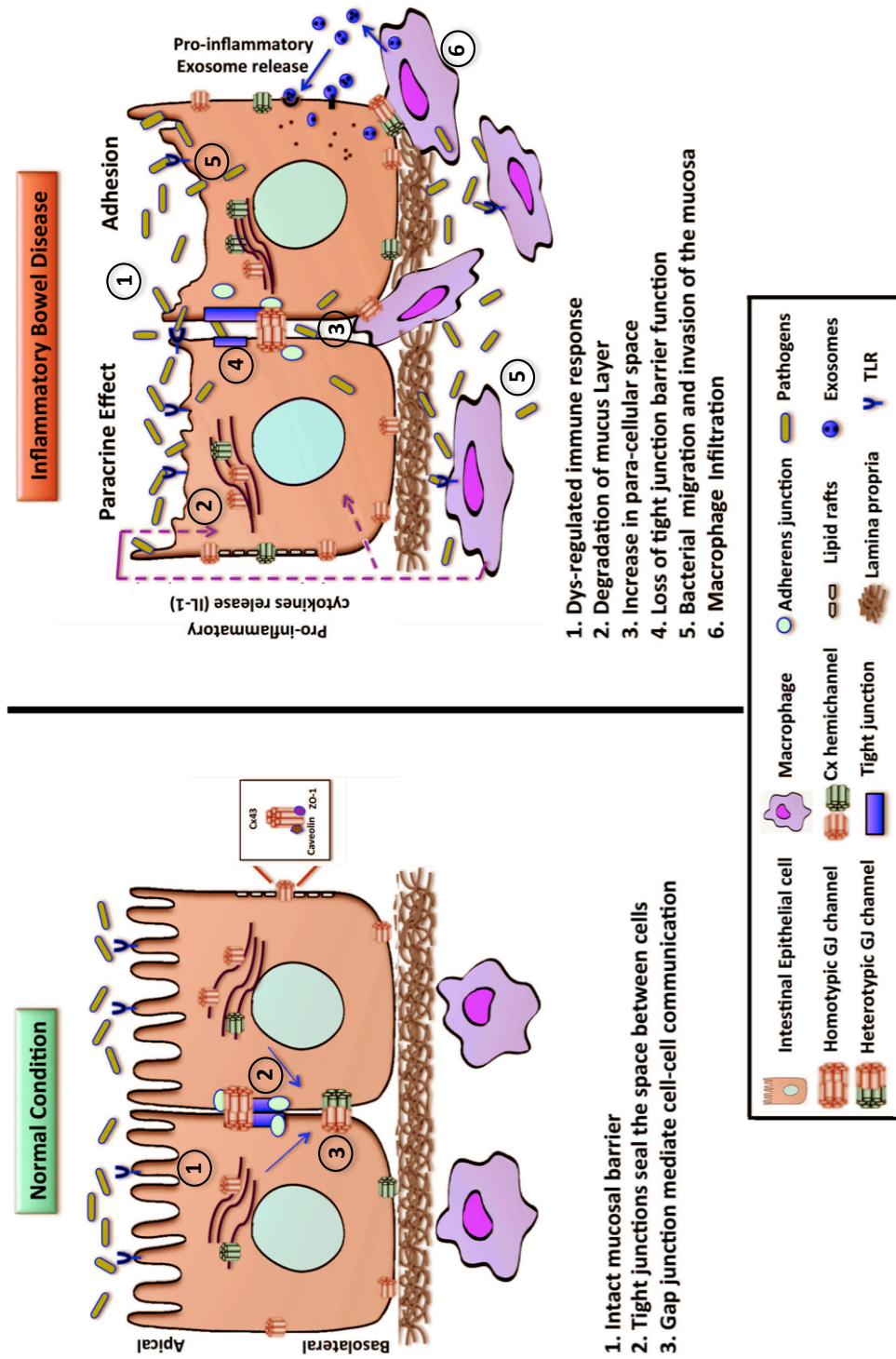
Figure 2: Proposed model for regulation of connexins in IBD.

References

1. Xu XR, Liu CQ, Feng BS, Liu ZJ. Dysregulation of mucosal immune response in pathogenesis of inflammatory bowel disease. World J Gastroenterol. 2014 Mar 28;20(12):3255-64.

2. Monteleone I, Vavassori P, Biancone L, Monteleone G, Pallone F. Immunoregulation in the gut: success and failures in human disease. Gut. 2002 May;50 Suppl 3:III60-4.

3. Abraham C, Medzhitov R. Interactions between the host innate immune system and microbes in inflammatory bowel disease. Gastroenterology. 2011 May;140(6):1729-37.

4. Yu LC, Perdue MH. Immunologically mediated transport of ions and macromolecules. Ann N Y Acad Sci. 2000;915:247-59.

5. Schreiber S, Raedler A, Stenson WF, MacDermott RP. The role of the mucosal immune system in inflammatory bowel disease. Gastroenterol Clin North Am. 1992 Jun;21(2):451-502.

6. Panja A, Goldberg S, Eckmann L, Krishen P, Mayer L. The regulation and functional consequence of proinflammatory cytokine binding on human intestinal epithelial cells. J Immunol. 1998 Oct 1;161(7):3675-84.

7. Kedinger M, Duluc I, Fritsch C, Lorentz O, Plateroti M, Freund JN. Intestinal epithelial-mesenchymal cell interactions. Ann N Y Acad Sci. 1998 Nov 17;859:1-17.

8. Homaidan FR, Tripodi J, Zhao L, Burakoff R. Regulation of ion transport by histamine in mouse cecum. Eur J Pharmacol. 1997 Jul 23;331(2-3):199-204.

9. Nagashima R, Maeda K, Imai Y, Takahashi T. Lamina propria macrophages in the human gastrointestinal mucosa: their distribution, immunohistological phenotype, and function. J Histochem Cytochem. 1996 Jul;44(7):721-31.

10. Burgio VL, Fais S, Boirivant M, Perrone A, Pallone F. Peripheral monocyte and naive T-cell recruitment and activation in Crohn's disease. Gastroenterology. 1995 Oct;109(4):1029-38.

11. Martin CA, Homaidan FR, Palaia T, Burakoff R, el-Sabban ME. Gap junctional communication between murine macrophages and intestinal epithelial cell lines. Cell Adhes Commun. 1998 Sep;5(6):437-49.

12. Martin CA, el-Sabban ME, Zhao L, Burakoff R, Homaidan FR. Adhesion and cytosolic dye transfer between macrophages and intestinal epithelial cells. Cell Adhes Commun. 1998 Mar;5(2):83-95.

13. Sharma AK, Fernandez LG, Awad AS, Kron IL, Laubach VE. Proinflammatory response of alveolar epithelial cells is enhanced by alveolar macrophage-produced TNF-alpha during pulmonary ischemia-reperfusion injury. Am J Physiol Lung Cell Mol Physiol. 2007 Jul;293(1):L105-13.

14. Shaykhiev R, Bals R. Interactions between epithelial cells and leukocytes in immunity and tissue homeostasis. J Leukoc Biol. 2007 Jul;82(1):1-15.

15. Khan MW, Keshavarzian A, Gounaris E, Melson JE, Cheon EC, Blatner NR, et al. PI3K/AKT signaling is essential for communication between tissue-infiltrating mast cells, macrophages, and epithelial cells in colitis-induced cancer. Clin Cancer Res. 2013 May 1;19(9):2342-54.

16. Sirnes S, Bruun J, Kolberg M, Kjenseth A, Lind GE, Svindland A, et al. Connexin43 acts as a colorectal cancer tumor suppressor and predicts disease outcome. Int J Cancer. 2012 Aug 1;131(3):570-81.

17. Morita H, Katsuno T, Hoshimoto A, Hirano N, Saito Y, Suzuki Y. Connexin 26-mediated gap junctional intercellular communication suppresses paracellular permeability of human intestinal epithelial cell monolayers. Exp Cell Res. 2004 Aug 1;298(1):1-8.

18. Ey B, Eyking A, Gerken G, Podolsky DK, Cario E. TLR2 mediates gap junctional intercellular communication through connexin-43 in intestinal epithelial barrier injury. J Biol Chem. 2009 Aug 14;284(33):22332-43.

19. Eugenin EA, Branes MC, Berman JW, Saez JC. TNF-alpha plus IFN-gamma induce connexin43 expression and formation of gap junctions between human monocytes/macrophages that enhance physiological responses. J Immunol. 2003 Feb 1;170(3):1320-8.

20. Saez PJ, Shoji KF, Aguirre A, Saez JC. Regulation of hemichannels and gap junction channels by cytokines in antigen-presenting cells. Mediators Inflamm. 2014;2014:742734.

21. Gassler N, Rohr C, Schneider A, Kartenbeck J, Bach A, Obermuller N, et al. Inflammatory bowel disease is associated with changes of enterocytic junctions. Am J Physiol Gastrointest Liver Physiol. 2001 Jul;281(1):G216-28.

22. Schildberger A, Rossmanith E, Eichhorn T, Strassl K, Weber V. Monocytes, peripheral blood mononuclear cells, and THP-1 cells exhibit different cytokine expression patterns following stimulation with lipopolysaccharide. Mediators Inflamm. 2013;2013:697972.

23. Daigneault M, Preston JA, Marriott HM, Whyte MK, Dockrell DH. The identification of markers of macrophage differentiation in PMA-stimulated THP-1 cells and monocyte-derived macrophages. PLoS One. 2010 Jan 13;5(1):e8668.

24. Meyer RA, Laird DW, Revel JP, Johnson RG. Inhibition of gap junction and adherens junction assembly by connexin and A-CAM antibodies. J Cell Biol. 1992 Oct;119(1):179-89.

25. el-Sabban ME, Pauli BU. Adhesion-mediated gap junctional communication between lung-metastatatic cancer cells and endothelium. Invasion Metastasis. 1994 -1995;14(1-6):164-76.

26. Kucharzik T, Walsh SV, Chen J, Parkos CA, Nusrat A. Neutrophil transmigration in inflammatory bowel disease is associated with differential expression of epithelial intercellular junction proteins. Am J Pathol. 2001 Dec;159(6):2001-9.

27. Ivanov AI, Parkos CA, Nusrat A. Cytoskeletal regulation of epithelial barrier function during inflammation. Am J Pathol. 2010 Aug;177(2):512-24.

28. De Maio A, Vega VL, Contreras JE. Gap junctions, homeostasis, and injury. J Cell Physiol. 2002 Jun;191(3):269-82.

29. Levin M. Gap junctional communication in morphogenesis. Prog Biophys Mol Biol. 2007 May-Jun;94(1-2):186-206.

30. Elias LA, Kriegstein AR. Gap junctions: multifaceted regulators of embryonic cortical development. Trends Neurosci. 2008 May;31(5):243-50.

31. Chanson M, Derouette JP, Roth I, Foglia B, Scerri I, Dudez T, et al. Gap junctional communication in tissue inflammation and repair. Biochim Biophys Acta. 2005 Jun 10;1711(2):197-207.

32. Medina C. and Radomski MW. Role of Matrix Metalloproteinases in Intestinal Inflammation. JPET. 2006; 318: 933–938.

33. Gan X, Wong B, Wright SD, Cai TQ. Production of Matrix Metalloproteinase-9 in CaCO-2 Cells in Response to Inflammatory Stimuli. J. Interferon. Cytokine Res. Abstract. 2001; 21: 93-98.

34. Pedersen G, Saermark T, Kirkegaard T, Brynskov J. Spontaneous and cytokine induced expression and activity of matrix metalloproteinases in human colonic epithelium. Clinical and Experimental Immunology. 2008; 155: 257–265.

SARA AL-GHADBAN

Date of Birth: 22-01-1980

Address: Beirut, Lebanon

Mobile Lebanon: +961 70803372

E-mail: sara.ghadban@gmail.com

EDUCATION

- **PhD candidate**, Cell Biology, Leibniz Universität Hannover, Germany   *2016*
- **Masters of Science**, Biochemistry, American University of Beirut, Lebanon   *2007*
- **Bachelor of Science**, Biology, Lebanese University, Lebanon   *2002*

EXPERIENCE

AMERICAN UNIVERSITY OF BEIRUT
Lebanon

PhD candidate   *2012– 2016*

- Dissertation title: "The inflammatory microenvironment in a model of Inflammatory Bowel Disease".

Research Associate

Department of Anatomy, Cell Biology, and Physiological Sciences, Faculty of Medicine

Supervisor: Dr. Marwan El-Sabban   *2010 – 2016*

- Technician in the project entitled: "Exploring Marine Resources for Bioactive Compounds: From Discovery to Sustainable Production and Industrial Applications".
- Contributed to ongoing research activity on cancer and cell-cell communication projects at the laboratory.
- Highly experienced in Cell culture and Molecular biology techniques (Cloning, protein, DNA, RNA analysis, Real-time PCR), xCELLigence Real-Time Cell Analyzer (RTCA), advanced microscopy techniques (Zeiss 710 Laser Scanning Confocal Microscope, Laser Microdissection Systems Leica LMD6500), and Flow cytometry.

- Represented AUB in two international conferences.
- Contributed to writing grant proposals and research papers.

Research Assistant

Department of Anatomy, Cell Biology, and Physiological Sciences, Faculty of Medicine

Supervisor: Dr. Marwan El-Sabban   *2008 – 2010*

- Technician in the project entitled: "Mechanisms of human skin cancer metastasis."

Master's student

Department of Biochemistry, Faculty of Medicine

Supervisor: Dr. Georges Nemer   *2005 – 2007*

- Thesis title: "*Hey 2*, a candidate gene for congenital heart disease."

LEBANESE UNIVERSITY
Lebanon

Supervisor   *2003 – 2007*

- Supervising senior year biology students working on projects in the field of functional genomics.

Signature: Sara Al Ghadban

List of publications (* = equal contribution)

1. Ahmad M Mansour*, **Sara Al-Ghadban***, Muhammad H Yunis, and Marwan E. El-Sabban. 2015. Ziv-aflibercept in macular disease. *Br J Ophthalmol., 0:1–5.*

2. Kazem Zibara, Zahraa Awada Leila Dib, Jamal El-Saghir, **Sara Al-Ghadban**, Aida Ibrik, Nabil El-Zein, and Marwan El-Sabban. 2015. Anti-angiogenesis therapy and gap junction inhibition reduce MDA-MB-231 breast cancer cell invasion and metastasis *in vitro* and *in vivo*. *Scientific Reports. In Press.*

3. **Sara Al-Ghadban**, Samira Kaissi, Fadia R. Homaidan, Hassan Y. Naim, and Marwan E. El-Sabban. 2015. Cross-talk between Human Intestinal Epithelial Cells and Immune Cells in Inflammatory Bowel Disease. *Under review.*

4. Maamoun Abdul Fattah*, **Sara Al-Ghadban***, Rafic Antonios, Marwan El-Sabban, and Rola N Hamam. 2015. Efficacy of Adalimumab Stored in Plastic Vials at Four Degrees Celsius. *Under review.*

5. Mohammad Sakr, Najeeb Halabi, Leen Kalash, **Sara Al-Ghadban**, Mayyasa Rammah, and Marwan El-Sabban, Kamal Bouhadir, Tarek Ghaddar. 2015. Synthesis and *In-Vitro* Cytotoxicity Evaluation of Ruthenium Polypyridyl-Sensitized Paramagnetic Titania Nanoparticles for Photodynamic Therapy. *Under review.*

6. Georges Khalil, Marwan El- Sabban, **Sara Al-Ghadban**, Sandy Azzi, Sara Shamra, Simon Khalifé, and Richard Maroun. 2008. Cytokines expression profile, by sensitized T human lymphocytes, after in vitro stimulation by amoxicillin. *Eur. Cytokine Netw., 19 (3):1-11.*

7. Inaam El-Rassy, Jad Bou-Abdallah, **Sara Al-Ghadban**, Fadi Bitar, and Georges Nemer. 2008. Absence of NOTCH2 and Hey2 Mutations in a Familial Alagille Syndrome Case with a Novel FrameShift Mutation in JAG1. *American Journal of Medical Genetics Part A. 146A: 937–939.*

Conferences (* = equal contribution)

1. Maamoun Abdul Fattah*, **Sara Al-Ghadban*,** Rafic Antonios, Marwan El-Sabban, and Rola N Hamam. American University of Beirut, Lebanon. February 2015.

Abstract: Efficacy of Adalimumab Stored in Plastic Vials at Four Degrees Celsius (Poster)

Award: Fifth Annual Basic Biomedical Research Day for outstanding poster presentation.

2. **Sara Al-Ghadban**, Samira Kaissi, Fadia R. Homaidan, Hassan Y. Naim, and Marwan E. El-Sabban. ASCB/IFCB Meeting, Philadelphia. December 2014.

Abstract: Expression and Regulation of Connexins under "Inflammatory" state: Communication between Human Intestinal Epithelial Cells and Immune Cells (Poster).

Award: The American Society for Cell Biology (ASCB) International Travel Award for Graduate Students.

3. Sawsan Sallouh, Marwan El-Sabban, and **Sara Al-Ghadban**. Advances in Cancer Research, From the Laboratory to the Clinic. Dead Sea, Jordan. 2010.

Abstract: Correlation between the expression of connexins in skin cancer cells and malignant phenotype (Poster).

Acknowledgments

I would like to thank my supervisor Professor Hassan Naim for providing me the opportunity to complete my PhD thesis at Leibniz Universität Hannover.

I would like to express my deepest appreciation and sincere gratitude to my mentor, Professor Marwan El-Sabban, whose motivation, guidance, and knowledge made my thesis work possible. Your continuous encouragement, thoughtful discussions and sharp ideas made me a research scientist and an independent thinker.

I would also like to thank my committee members for their time and effort spent to read my dissertation.

I would like to thank the present and past members of the MES lab: Jamal, Diana, Tala, Joyce, Remi, Farah, Sawsan, Najat, Jalal and Khaled. I extend my thanks to my colleagues at the American University of Beirut for their assistance and advice.

Completion of my doctoral dissertation would not have been possible without the help, invaluable support, sacrifices and encouragement of my family. I would like thank my parents, my brother, my sister and my lovely nieces: Laure and Leen, you are my joy in life. Special thanks go to my extended family: Samira and Sara Kaissi, the days we spent together are unforgettable.